10th International Symposium on Exploitation of Renewable Energy Sources and Efficiency
April 05-07, 2018, Subotica, Serbia

EXPRES 2018

Proceedings

10th International Symposium on Exploitation of Renewable Energy Sources and Efficiency

EXPRES 2018

10th International Symposium on Exploitation of Renewable Energy Sources and Efficiency

Subotica, Serbia

April 05-07, 2018

Proceedings

CIP - Каталогизација у публикацији , Библиотека Матице српске, Нови Сад , 620.91(082)
INTERNATIONAL Symposium on Exploitation of Renewable Energy Sources and Efficiency (10;2018;Subotica)
Proceedings [Elektronski izvori] / 8th International Symposium on Exploitation of Renewable Energy Sources and Efficiency, Subotica, April 05-07, 2018 ; [proceedings editor József Nyers]. - Subotica : Inženjersko-tehničko udruženje vojvođanskih Mađara, 2018. - 1 elektronski optički disk (CD-ROM) ; 12 cm
Tekst štampan dvostubačno. - Tiraž 50. - Bibliografija uz svaki rad.

ISBN 978-86-919769-3-4

а) Енергија - Обновљиви извори – Зборници

COBISS.SR-ID

http://Expres 2017 ISBN 978-86-919769-3-4

Table of contents

The following pipers accepted and published by journal IRASE (2018) (International Review of Applied Science and Engineering) indexed by Scopus:

1. **Energetic investigation of sausage-drying procedure with newly developed technique**
   M. KASSAI, P. ORBAN

2. **Energetic investigation of energy recovery technologies in air handling units**
   F. AL-HYARI, M. KASSAI

3. **Thermal comfort analyses in office buildings with different air-conditioning systems**
   J. SZABO, L. KAJTAR

4. **Transpired solar collectors in building service engineering: combined system operation and special applications**
   B. BOKOR, L. KAJTÁR

Committees

HONORARY COMMITTEE

Imre J. Rudas,	Óbuda University, Budapest
Branislav Todorović,	University of Beograd
Mihaly Reger,	Óbuda University, Budapest
Simeon Oka,	IJ of Thermal Science and Academy of Engineering Sciences of Serbia

GENERAL CHAIR

József Nyers,	Óbuda University, Budapest

INTERNATIONAL ADVISORY COMMITTEE

Wenxing Shi	University Tsinghua, Beijing, China
Bela Füri	University Bratislava, Slovakia
Zoltán Rajnai,	Óbuda University, Hungary
Felix Stachowicz,	University Rzesov, Poland
Mirko Ficko,	University Maribor, Slovenia
Petar Gvero	Univer. Banja Luka, Bosna and Herceg.
Ján Takacs	University Bratislava, Slovakia
Dušan Golubović,	University. East Sarajevo, Bosna and Hercegovina

ORGANIZING COMITTEE CHAIR

Slavica Tomić,	University, Novi Sad
Laszlo Kajtar,	BME, Budapest

ORGANIZING COMMITTEE

Zoltán Pék,	V3ME, Subotica**,**
László Veréb,	V3ME, Subotica

TECHNICA PROGRAM COMMITTE CHAIRS

Péter Láng,	BME, Budapest
Péter Kádár,	Óbuda University, Budapest
Péter Odry,	Subotica Tech
István Farkas,	Univ. SzIE,. Gödöllő, Hungary
Aleksandar Grubor	University of Novi Sad, Serbia

TECHNICAL PROGRAM COMMITTE

Milorad Bojić,	University of Kragujevac, Serbia
Marija Todorović,	University of Beograd, Serbia
Livia Cvetičanin,	University of Novi Sad, Serbia
Dragoslava Stojiljkovic,	University ofBeograd, Serbia
Velimir Stefanović,	University of Nis, Serbia
László Garbai,	University BME, Budapest¸ Hungary
Dušan Gvozdenac,	University of Novi Sad, Serbia
Jenő Kontra,	University BME, Budapest, Hungary
Miklós Kassai,	University BME, Budapest¸ Hungary
István Barótfi	University SzIE, Gödöllő, Hungary
Ferenc Kalmár,	University of Debrecen, Hungary
Stevan Firstner,	Polytechical College of Subotica, Serbia
László Sikolya,	University of Nyiregyhaza M I College, Hungary
Györgyi Petkovics	University of Novi Sad, Faculty of Economics, Subotica, Serbia
Laslo Seres	University of Novi Sad, Faculty of Economics, Subotica, Serbia
Arpad Nyers	University Pecs, Hungary
László Fülöp	University Pecs, Hungary
Zoltan Szantho,	University BME, Budapest¸ Hungary

PROCEEDINGS EDITOR

József Nyers, Óbuda University, Budapest

EXPRES 2018
ISBN: 978-86-919769-3-4

AIR DISTRIBUTION IN ACCORDANCE WITH FIRE REGULATION

Z. STRAKOVÁ, J. OLBŘÍMEK [2b]

[1]Slovak University of Technology in Bratislava, Faculty of Civil Engineering, Department of Building Services, Radlinského 11, 810 05 Bratislava, Slovak Republic
[2]Slovak University of Technology in Bratislava, Faculty of Civil Engineering, Department of Building Construction, Radlinského 11, 810 05 Bratislava, Slovak Republic
[a]zuzana.strakova@stuba.sk
[b]juraj.olbrimek@stuba.sk

The article deals with the basic issue of the total reconstruction of prefabricated buildings in Slovakia. Solved area is the concept of ventilation's design for living rooms. The case study covers a flat's ventilation system in a specific prefabricated building. The study focuses on the appliance of legal requirements to the ventilation system, as well as to cutting edge of technical methods. The study covers the concept, design and optimization of ventilation channel positioning, the selection of fire safety requirements, as well as from the operational and maintenance point of view. The exchange of windows and doors for such as with low infiltration and insulation of the building by an external thermal insulation composite system (ETICS) leads to increased need of ventilation system of rooms and flats. Air handling systems open an option for spreading of fire and smoke in buildings. The application of central ventilation system triggers higher demands on fulfillment of fire safety requirements. In order to minimize the necessity of many fire dampers, as it was required according to previous technical standards, we design a ventilation system within one fire area in first place. New findings enable to design ventilation systems which reduce the fire spreading in shafts and false ceilings. Correct design of fire shafts, fire false ceilings, and ventilation channel passage between two fire areas determine non-fumigation and suppression of fire in ventilated or unventilated spaces.

Keywords: *mechanical ventilation, block of flats, air distribution, fire regulation*

1. Introduction

Over the past decades, revitalization of residential buildings has resulted in significant improvement in their thermal and service characteristics.

Figure 1a. Residential building with an insulated part of the envelope [6]

Houses with originally unpleasant look but sophisticated reconstruction are rapidly being transformed into aesthetic residential buildings. This has ultimately a positive impact on the general appearance of the locality as well as on the people having a pleasant place to live. (Figure 1a., Figure 1b.). There is no doubt that reconstruction of the peripheral and roof envelope of the house in the form of insulation and replacement of building envelope openings (windows, skylights entrance and patio doors) help reduce operating costs for heating in winter. Even the so called additional heating in cold transition seasons becomes completely unnecessary.

Figure 1b. Residential building with uninsulated part of the envelope [6]

Top quality materials, advanced technology and technological processes enable a significant increase in life span of a residential building as a whole. However, the question is whether such an intervention resulting in changed properties in the peripheral building structures will ensure the optimum indoor environment microclimate in individual apartments.

2. Ventilation requirements of residential buildings - legislation

It is not possible to rely solely on natural ventilation in case of reconstructed residential buildings that have undergone thermal insulation. After reconstruction, this method of ventilation is already insufficient.
The only technical solution is to build a system of *controlled forced ventilation*. This affirmation is moreover supported by Slovak legal regulations, which are binding. The most important documents are following:

- *Health Ministry Decree no. 259/2008 Coll.* on the details of the requirements for indoor climate environment and the minimum requirements for apartments and accommodations of lower standards
- *Ministry of Regional Development Decree no. 311/2009 Coll.*, stating the details of the calculation of energy efficiency of buildings and the content of the certificate,

Technical standards - non-binding but recommended by professionals:
STN EN 15251:2008 + STN EN 15251 / OA 2012 input data on indoor environment for design and assessment of energy performance of buildings - air quality, thermal condition of environment, lighting and acoustics.

- *STN EN 13779:2007* Ventilation of non-residential buildings. General requirements for ventilation and air conditioning equipment.

Since the formation of the internal environment by central adjusted air requires large air ducts and has relatively high energy requirements, in the vast majority of cases it is common to design the strength of the ventilation device to so called sanitary minimum, which, according to the legislation, means ensuring enough fresh outdoor air for people. [8], [9]
In each of the documents above you can find references why, how and when to ventilate. The binding Ministry Decree no. 259/2008 Coll. is the most important among them. It refers to the STN EN 15251: 2008. It clearly defines how to ventilate living spaces (Table 1). Quote: (Table A.2, Table B.5):

Table 1a. Table A.2 - Examples of recommended design values of operational temperatures for designing of buildings and systems of Environmental Engineering

Building type (area)	Category	Operative temperature [°C]	
		Minimum for heating (winter period) ~ 1,0 clo	Maximum for cooling (summer period) ~ 0,5 clo
Residential buildings living rooms (bedroom, kitchen) sedentary activities 1.2 met	II	20.0	26.0
Residential buildings other areas (hall, warehouse) standing/walking 1.6 met	II	16.0	no requirements

Note: In accordance with STN EN 15251: 2008 Table 2 - Description of the applicability of the various categories - the revitalized residential buildings belong to the category II - normal level of expectation and should be used for new and renovated building.

Table 1b. Table B.5 - Examples of ventilation intensity in residential buildings. Continuous operation during the occupancy of the building. Complete mixing

Category	Air exchange rate		Outdoor air volume (living room, bedroom)		Exhaust air volume [l/s]		
	[l/(s.m²)]	[1/h]	[l/(s person)]	[l/(s.m²)]	Kitchen	Bathroom	WC
II	0.42	0.6	7	1.0	20	15	10

The designer often works with volumetric airflow measured in units (m^3/h). The conversion Table B.5 is as follows:

Table 1. The conversion Table B.5 from (l/s) to (m^3/h)

Category	Air exchange rate		Outdoor air volume (living room, bedroom)		Exhaust air volume [m³/h]		
	[m³/(h.m²)]	[1/h]	[m³/(h.person)]	[m³/(h.m²)]	Kitchen	Bathroom	WC
II	1.512	0.6	25.2	3.6	72	54	36

For comparison - see the following tables (Table 2. And Table 3.) of the hygiene requirements for indoor environment climate in selected foreign regulations:

Table 2. Requirements for ventilation of residential areas – foreign regulations

Cross-border regulation	Air exchange rate [1/h]	Exhaust air volume
DIN 4701	0.5	-
VDI 2088	0.4 – 0.8	-
NKB Publication	≥ 0.5	30 m³/h
BSF 1998:38	0.4	1.26 m³/(h.m²)
ASHRAE	-	27 m³/h
ČSN 73 0540	0.1 – 0.5	-
ČSN EN 15251	0.07 – 0.7	15; 25; 36 m³/h 2.16 – 5 m³/(h.m²)
ČSN EN 15665/Z1	0.5	25 m³/(h.person)

Table 3. Ventilation requirements for kitchens and sanitary rooms – foreign regulations

Cross-border regulation	Kitchen [m³/h]	Bathroom [m³/h]	WC [m³/h]
DIN 18017/3	40 – 60	-	20 – 30
DIN 1946/6	40 – 60	40 – 60	20 – 30
ECE Compendium	36 – 180	36 – 180	-
BSF 1998:38	36 – 54	36 – 108	36
ČSN EN 15251	50 - 72	36 – 54	25 – 36
ČSN EN 15665/Z1	150	90	50

An additional binding technical parameter mentioned in Ministry Decree No. 259/2008 Coll. is the maximum allowable concentration of CO_2 in residential areas. The limit value is 1500 ppm. It is clearly stated to what extent to ventilate so that the internal environment for users is comfortable and healthy, however, on the other hand, there are owners or tenants, who are concerned about the poor quality of indoor climate and who in many cases inhabit areas that are not compliant with the requirements on the quality of environment. [1]

3. Controlled ventilation with partial adjustments to the outdoor air

The necessity of designing and building in a new way is based on the requirements defined in the Decree of Ministry of Regional Development No. 364/2012 Coll., which stipulates that residential buildings built after 1 January 2015 must achieve energy class A1 and energy class A0 as of 31 December 2020 in primary energy consumption. That means that no building inspection will be performed after 1 January 2016, unless the new residential buildings have the energy certificate of energy class A1.
The controlled forced ventilation system with partial adjustment to outdoor air using recovery HVAC unit, is one of the several solutions building equipment as a whole can offer in order to achieve energy class A1. [2]

a) Ventilation with recovery unit – Central System
The central ventilation consists of one or more separate units that are placed on the roof of an apartment house or in its technical areas, providing a common ventilation of dwellings situated above one another, connected by a common vertical shaft with HVAC ducts for inlet and outlet air. In order to provide individual ventilation of these apartments according to user's requirements, the entry and the exit of each apartment is equipped with volumetric air flow controllers. Living rooms, bedrooms and children's rooms are provided by modified intake of outdoor air. The air is exhausted from kitchens, bathrooms, toilets, or wardrobes. Volumetric flow regulator provides power control of ventilation in the apartment. It can be controlled either manually, automatically in combination with air quality sensors or CO_2 sensor.
The capacity of central air unit is thus continuously adjusted to achieve the optimum environmental conditions for the people in the indoor environment, but at the same time at the lowest operating costs. [3], [5]
A significant advantage of this system is the possibility of controlled ventilation using heat recovery - using heat from the exhaust air, which in winter is used to preheat the cold outside air and in the summer to precool the hot outdoor air. This separation of two outer exhaust air streams in air heat exchanger creates favourable quality of supply air with sufficient air temperature and humidity, dust free indoor environment and reduced odour in the rooms. Thanks to recovery system we can save up to 7 GJ per year for heating of one apartment 3 + 1 kitchen, occupied by four users.
The main benefit, however, remains a healthy indoor environment and the related reduction in morbidity and last but not least the increase in the value of the dwelling and its preparation for future use by next generations. [4], [7]

b) Ventilation with recovery unit – Decentralised system
A small ventilation unit is located in each apartment (Figure 2.). This unit provides controlled ventilation with heat recovery. The location is typically under the ceiling of the entrance hall, where the supply air is distributed by ducts under ceiling into residential areas through nozzles with long-range air flow, air valves or rectangular two-tier diffusers.

Figure 2. Example of decentralised system of ventilation [10]

Exhausting air from the sanitary rooms and kitchens. Supply and exhaust of outside air is solved according to the actual situation, in case of one or a group of apartments, but all with regard to fire protection requirements.
The airflow calculation is based on sanitary dose of external (fresh) air per person. Based on this calculation, the HVAC units in residential buildings are designed with air flow rate from 60 to120 m^3/h, depending on the number of rooms in the apartment.
The ceiling mount HVAC units itself is usually equipped with supply and exhaust EC-fan, rotary recovery heat exchanger with a maximum recovery efficiency of 88 %, an electric heater used for additional heating of the outside air and air filters of class F7.

4. Air distribution in accordance with fire regulation

In terms of fire safety of building the design of the HVAC system must be based on the classes of characteristics and risk analysis from harmonized standards of construction products as a requirement for class reaction on fire, including smoke production and fall off and dripping of burning parts and drops and fire risk analysis of HVAC units. Standard STN 73 0872 Fire safety of buildings. Protection of buildings against fire through HVAC units is no more of issue in some areas as for its design. It is preferable to process the design according to the standard STN EN 15423, which is more compliant with the new

requirements for products as for the fire safety of buildings.
In the past, the air-exhausting devices were used in apartments and buildings. Fire dampers were not used on these wirings in the installation shaft and sanitary cabins but fire insulated steel pipes with fire resistance led out to the flat roof of the building. This principle should be retained for the future. Sanitary cabins placed on each floor were used in place of shafts as a key fire fighting measure. The replacement of the wirings leads to the rupture of the seals and the new building products do not have the original technical parameters for fire fighting system. Even the use of fire dampers according to STN 73 0834 is not suggested [11], [12].
New fire dampers with diameter 100 mm, placed closer together according to the test conditions as required by STN 73 0872 are designed in buildings in the HVAC systems. The choice depends on the structure through which the damper (e.g. a fire damper in a sandwich construction, the wooden structure etc.) is designed, the orientation of the structure and the proper fire fighting damper seal is a very significant feature. It is also crucial whether the valve is mounted on the pipe, whether in case of fire the damper is not broken by the pipeline expansion and lastly if there has to be a pipeline knotted to the damper. New dampers and pipelines are categorized in grading classes that do not have established national criteria but are useful in the fire engineering approach based on these characteristics. Of course, according to the test standards, the conventional dampers in the fume-hood exhaust systems are functionless. Fire ventilation grilles by ETA are used as well but these are not suitable for cold smoke.
In the central distribution, it is necessary to design the fire pipelines or shafts (or a combination with fire integrity of HVAC distribution). The most important thing, however, is the separation of the escape ways. Expansion elements with fire resistance should be included. Fire valves by ETA can be placed at the end of these wirings. Ventilation of escape routes (staircases) as a variant of the fire ventilation is included in a separate chapter where recovery is not normally designed [13], [14], [15].
As for smoke management in buildings, it is necessary to have a design of measurements and control, to ensure safe movement and stay of residents of the buildings. For example the local smoke alarms according to EN 14064 [16].

5. Summary

Systems for ventilation, or rather systems for controlled ventilation with heat recovery are nothing new on the world market. In the area of construction of residential buildings with low energy consumption they have well established themselves on the Slovak market. Their offer, variability and efficiency is increasing in certain aspects, in particular their recovery efficiency, which is very high. It is a system that owners or tenants can benefit from at all levels.
Meeting the requirements for residential buildings to achieve energy class A1 and A0 time will significantly influence the choice of a HVAC system. Evaluation of systems in terms of space requirements for installation, the investment costs, the costs of primary energy, energy cost savings using reverse heat gain (or humidity), energy cost savings of fans - all this will be reflected in the final and determining value of the return on investment costs.

Acknowledgement

This work was supported by the Slovak Research and Development Agency under the Contract No. DS-2016-0030 and by the Ministry of Education, Science, Research and Sport under VEGA Grant 1/0807/17.

References

[1] M.Bažant, Vetranie s rekuperáciou tepla v bytových (panelových) domoch. (Ventilation with recovery unit in residential buildings). 2015. www.tzb-info.cz
[2] B. Füri, M. Kurčová, Termomechanika. Cvičenia. (Thermodynamics. Exercises). Bratislava : Vydavateľstvo STU, 2014. 350 s. ISBN 978-80-227-4132-3.
[3] M. Kassai – L. Kajtar, Cooling energy saved investigation of air-to-air heat-and energy exchangers. Proceedings EXPRES 2016. 8th International Symposium, Subotica, Szerbia, 03.31-04.02. 2016. pp.6-10. ISBN:978-86-919769-0-3.
[4] K. Malinová, Nový zdroj tepla v 12-podlažnom bytovom dome. (A new heat source in a 12-levels apartment building). In Správa budov. Roč. 6, č. 1. s. 40-42., 2012. ISSN 1337-6233.
[5] Koudelková, D. "Meranie a regulácia v TZB. 1. časť – Vykurovanie" (M&R in HVAC. Part 1 - Heating). Bratislava: STU, 182 p. 2014. ISBN 978-80-227-4291-7.
[6] https://sk.wikipedia.org/wiki/Panelov%C3%BD_dom
[7] www.allworks.sk
[8] www.istavebnictvo.sk
[9] www.abcweb.cz
[10] http://www.zeleneatrium.sk/smf-marko
[11] Gy. Homonnay at el. Épületgépészet 2000 - Fűtéstechnika II. (Building Automation 2000 - Heating Technology II). Budapest : Épületgépészet kiadó Kft., 2001
[12] Masaryk M: Exergy and V entropy – useful efficiency parameters, Conference proceedings Heat engines and enviromental protection 2013, June 5-7 2013, Balatonfured, Hungary, Budapest university of Technology and Economy BME, ISBN 978-963-313-091-9.
[13] Koudelková D., Regulace větrání podle kvality vnitřního vzduchu. (Ventilation control by indoor air quality). In TZB Haustechnik. ISSN1803-4802, 2011, vol.4, issue.1, p. 46-49
[14] Hirš, J. Vzduchotechnika v příkladech. (Ventilation in the examples). Brno : CERM, 2006. 230 ISBN 80-7204-486-9.
[15] Nyers J., 2016, COP and Economic Analysis of the Heat Recovery from Waste Water using Heat Pumps, I. J. Acta Polytechnica Hungarica Vol. 13, No. 5, pp. 135-154.
[16] Ferstl, K., Masaryk, M. Prenos tepla. (Heat Transfer). Bratislava: STU. 360 p. 2011. ISBN 972-80-227-3534-6.

EXPRES 2018
ISBN: 978-86-919769-3-4

THE CARS NEED LIGHTWEIGHT COMPOSITES TO REDUCE THE CO_2 EMISSIONS TO IMPROVE THE FUEL EFFICIENCY

L. SZABÓ[a], R. SZABÓ[b]

[a] Institute of Environmental Protection Engineering, Rejtő Sándor Faculty of Light Industry and Environmental Protection
Engineering, Óbuda University, H-1034 Budapest, Doberdó u. 6, Hungary
E-mail: szabo.lorant@rkk.uni-obuda.hu

[b] Ingtex Bt - Rejtő Sándor Foundation H-1056 Budapest Nyáry Pál u. 5, Hungary
E-mail: ingtex@t-online.hu

This paper will explore a series of current trends in the automotive composite sector. With tremendous pressures to improve fuel economy, CO_2 emissions reduced and lower production costs, of market pressures and industry trends that make composites more attractive for automakers than ever before. Although there are many challenges facing the carbon fibre industry, all the elements are in place to promote the more widespread use of CFRP. Paradigm change occurs in the assessment and use of structural materials.

Keywords: *auto industry, carbon fibers, composite materials, fuel efficiency*

1. Introduction

In recent years, nearly 100 million/year vehicles (cars, light commercial vehicles, heavy trucks and buses) have been produced worldwide.
The market continues to grow, due to market globalization and the huge demand worldwide. The 2014 vehicle ownership rate per 1,000 inhabitants in India was only 20, and in China 91. Compare to 167 in Latin America, 565 in Europe, or 649 in North America.
Globally, composites currently account 1-2% of the total weight of an average mass-produced car. The penetration rate of composites continuous increase can be seen in Fig. 1.

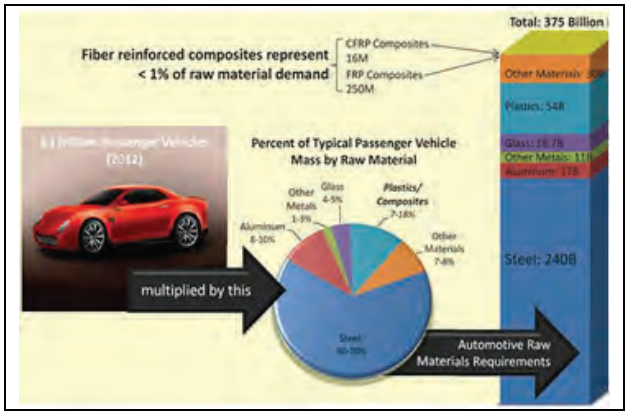

Fig. 1. Global passenger automobile raw materials Demand in 2012

A paradigm shift in the use of materials and energy, the use of strong, rigid and lightweight materials are more important (Fig. 2).

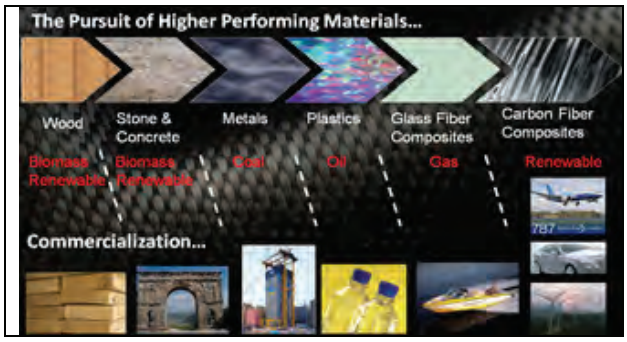

Fig. 2. Evolution of materials

Carbon fiber composite materials offer high strength-to-weight ratios compared to metals and are critical in meeting national goals of energy efficiency by reducing weight in automobiles, aircraft and other transportation vehicles Fig. 3.

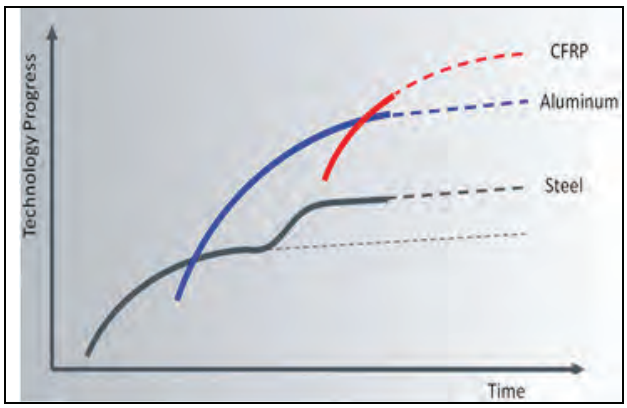

Fig. 3. Cycles of technology developments

In the European Union (EU), the European Commission, which develops and promulgates most of the regulations that govern EU industry, is focusing on direct reduction of emissions in cars and trucks. The current emissions limit in passenger cars is 130 g of CO_2/km, but by 2020 that figure will drop to 95 g CO_2/km. Lowering the weight of vehicles is one of the most effective ways to comply with these standards, so it is not surprising that the use of composites is included among the solutions. To reach this new goal, about 200 kg per vehicle will have to be eliminated. The 100 kg weight reduction results in an 8.5-10 g/km reduction in CO_2 emission. Carbon composites are also being more and more widely adopted in alternative vehicles such as electric/hybrid and fuel cell vehicles Fig. 4.

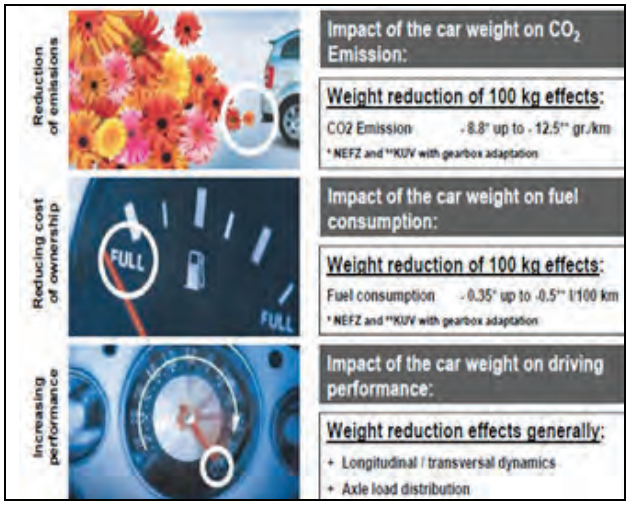

Fig. 4. Importance of lightweight in vehicle construction

However, initially the high costs of carbon fibre and existing production techniques results in higher manufacturing cycle times, which leads to low-volume production. Later, CFRP was applied in structural components in special edition models and luxury sports vehicles produced in small numbers. Although the carbon fiber reinforced composite is more expensive than the metal – in addition to the beneficial properties of CFRP – even in the case of smaller series production, the cost per piece is cheaper. By reducing the cost of carbon fiber and the manufacturing cycle and cost of structural parts, CFRP is rapidly and widely used in automotive manufacturing (Fig. 5).

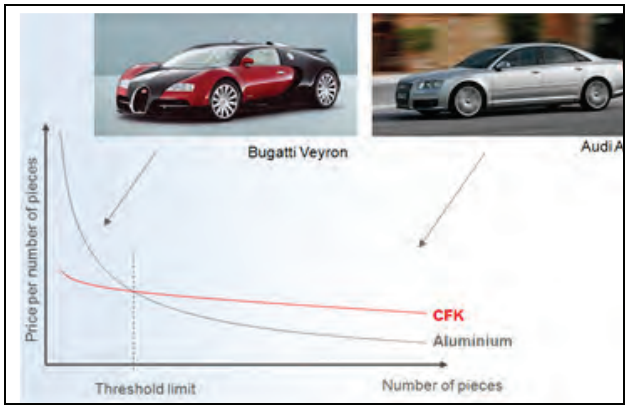

Fig. 5. Composite use in car manufacturing

2. Carbon fiber (CF) and carbon fiber reinforced polymers (CFRP)

The carbon fibre demand is estimated to be of 72 ktons (metric) in 2017 and could reach 120 ktons in 2022. The investments required for growth are huge (billions of euros), both for fibre producers and part manufacturers. Global carbon fiber reinforced market is expected to expand at CAGR in range of 8%-10% over the forecast period. Automotive industry is expected to exhibit the largest market share coupled with highest growth during the forecast period. Some of the key players in automobile industry are expanding their carbon fiber manufacturing partnership Fig. 6.

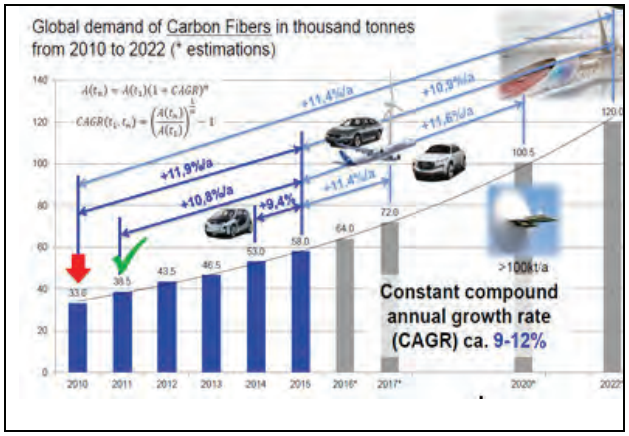

Fig. 6. The global carbon fibre market

The three main factors that help mold the end composite material are the matrix, reinforcement and manufacturing process. As matrix, many composites use resins, which are thermosetting or thermo softening plastics (hence the name 'reinforced plastics' often given to them). These are polymers that hold the reinforcement together and help determine the physical properties of the end composite Fig. 7.

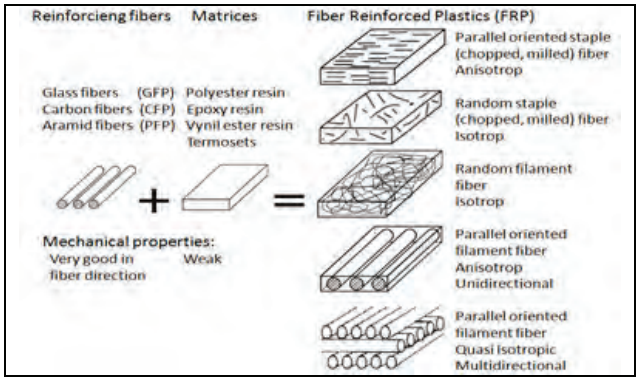

Fig. 7. The characteristic features of fibre reinforced plastics (FRP)

3. The CFRP properties

Carbon fibre / epoxy composites are best suited for automotive applications, the report states, given their high tensile strength, high stiffness (Fig. 8.) fire retardant properties, high energy absorption and fatigue

resistance. These advantages have created increasing awareness of CFRP among automotive with regard to crashworthiness, styling and parts consolidation.

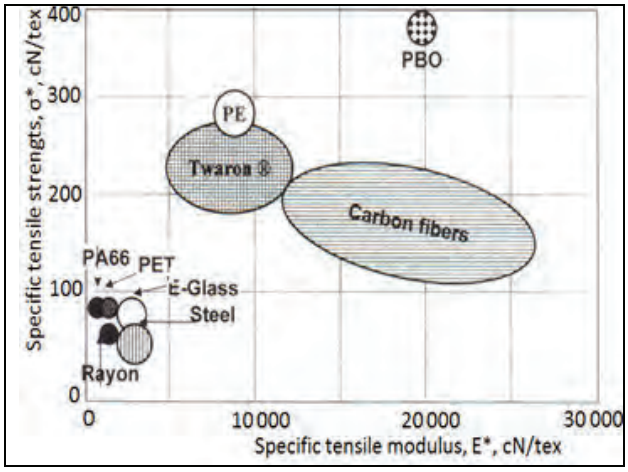

Fig. 8. Specific tensile strength comparison

Generally, one can achieve 60 percent weight saving with respect to steel and 40 percent for aluminum alloys with carbon fiber composites (Fig. 9).

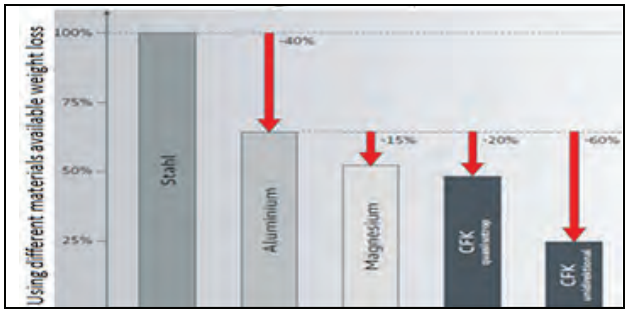

Fig. 9. The available weight loss compared to steel

Composite materials offer good vibrational damping (Fig. 10.) and low coefficient of thermal expansion (CTE), characteristics that can be engineered for specialized applications.

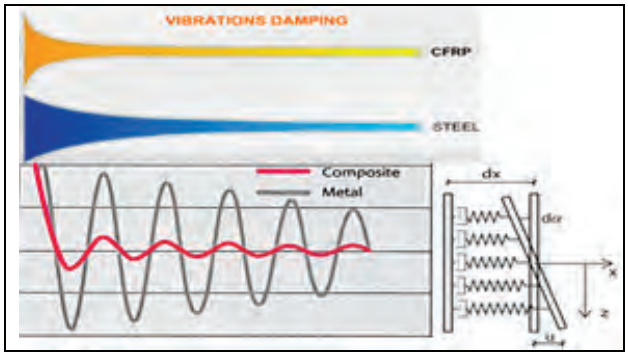

Fig. 10. Vibration damping properties

Composites are resistant to fatigue (Fig. 11.) and provide design/fabrication flexibility that can significantly decrease the number of parts needed for specific applications — which translates into a finished product that requires less raw material, fewer joints and fasteners and shorter assembly time.

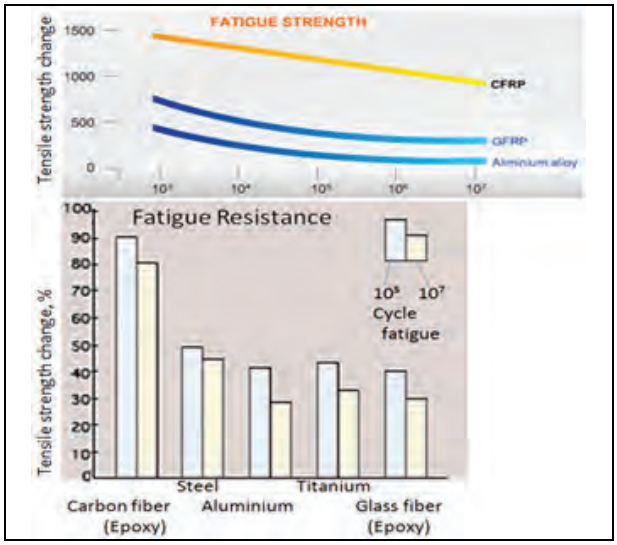

Fig. 11. Tensile strength change depending on the fatigue cycles

Composites have proven resistance to temperature extremes, corrosion and wear, especially in industrial settings, where these properties do much to reduce product lifecycle costs. These characteristics have propelled composites into wide use.

4. Auto evolution

Vehicle technology is rapidly changing on a variety of fronts: Power train, fuel type, safety features, sensor technology, interior amenities and — near and dear to our composite hearts — light weighting. But the most radical change ahead could be vehicle autonomy — the prospect that everyone in a car is a passenger — no driver.

Composites have generally benefitted from the growth in hybrid vehicles, because lightweight materials are used to help offset heavy batteries and extend driving range on a single charge. In the near future, a rapid increase in the proportion of hybrid cars is expected (Fig. 12.).

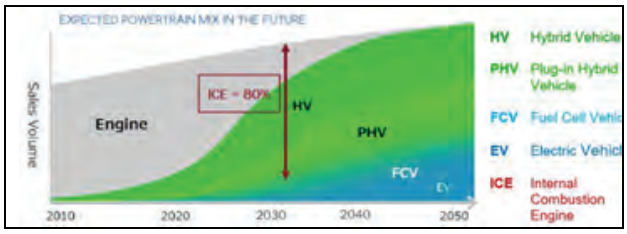

Fig. 12. Hybrid vehicles

A vehicle is a hybrid if it uses two or more power sources to achieve propulsion. Typically, the primary power comes from fossil fuel — gasoline or diesel — with supplemental power coming from batteries and/or energy recaptured during braking (regenerative braking) using a generator and electric motor. This reduces the power demand on the engine, which in turn lowers fuel consumption and emissions.

Top automotive companies are collaborating with carbon fibre suppliers to ensure long-term supply and rein in price fluctuations. The number of automakers turning to carbon fibre composites to save weight

continues to rise.

According to reduce the overall system cost of automotive components, suppliers of automotive carbon fibre reinforced plastic (CFRP) parts should implement new fabrication techniques such as **Resin Transfer Molding (RTM)** in Fig. 13.

Fig. 13. Resin Transfer Molding (RTM)

Various **core materials** (honeycomb, foam) can be manufactured with lightweight components with high bending stiffness Fig. 14.

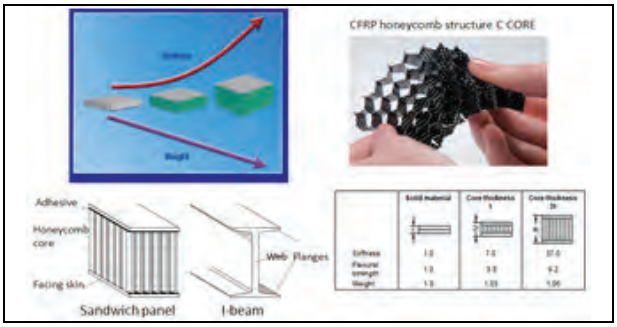

Fig. 14. Benefits of honeycomb sandwich constructions

The **BMW i3** (Megacity Vehicle), to roll off the assembly line in 2013, will be the first high-volume production vehicle with extensive CFRP components, including the passenger cell. The battery-powered vehicle built in Germany at the rate of 40, 000 units per year. The BMW i8, a CRFP-intensive sports car with electric-hybrid drive

Carbon fiber wheels bring a wealth of advantages over traditional aluminum wheels, including weight savings, improved vehicle dynamics and ride quality - making the innovative material the perfect complement for the all-new Ford GT.

Beyond simply reducing overall vehicle weight for improved acceleration, braking and dynamic performance, carbon fiber's incredibly strong, light nature means a reduction in unsprung weight and rotational inertia, which benefits suspension action, ride quality and dynamic performance Fig. 15.

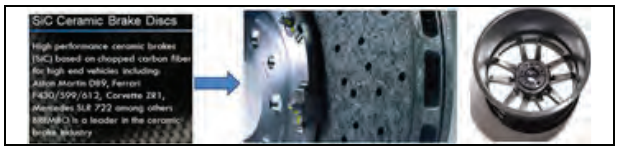

Fig. 15. Carbon Ceramic matrix composite wheel

Electric engines are four times more efficient than internal combustion engines. Electric engines use braking energy, normally wasted due to heat dissipation and friction, to improve traditional vehicles efficiency. This feature turns them into the ideal choice for urban distances. Since they have got less mechanical components, their operation costs are lower. Electric vehicles costs per km, for the first time in history, are equal or lower than those from conventional gasoline or diesel vehicles. An electric car currently requires between 10 and 20 kWh to cover 100 km, which represents a 2 Euros cost, versus the 8 Euros required by a gasoline or diesel car covering the same distance. The lower variable cost compensates the battery higher fixed cost. New commercial formulas have been suggested, like selling the car with no battery and charge for the covered km. This system is similar to those applied in the cellular phone sector, which uses leasing formulas.

Batteries can be upload in several ways powered by electricity. They can be recharged during off-peak hours (lower demand hours) and in the future they might even be able to deliver electricity into the network during peak hours (**Vehicles to Grid - V2G**) (Fig. 16). Road transport electrification is nowadays much more than a mere possibility.

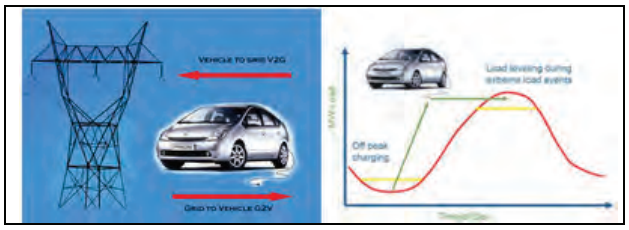

Fig. 16. Vehicle to grid (V2G)

Fuel pressure vessel sales are driving a 10 percent annual growth sales the lower fuel costs and escalating emissions standards Fig 17. Low prices for compressed natural gas (CNG) are fueling orders for natural gas-powered buses, a commercial trucks high-pressure storage tanks that hold the hydrogen in developed economies them could be in great demand.

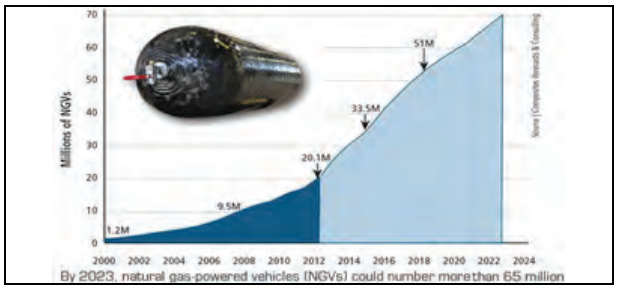

Fig. 16. Global natural gas vehicle (NGV) population

In the coming years deliver increasing numbers of zero-emission technologies, such as full battery electric cars, newly emerging plug-in hybrid electric vehicles and hydrogen fuel cell cars. Hydrogen is a colorless, odorless gas that accounts for 75 percent of the entire universe's mass. Hydrogen is found on Earth only in

combination with other elements such as oxygen, carbon and nitrogen. To use hydrogen, it must be separated from these other elements.

The widespread use of these fuels is largely explained by their energy density and ease of onboard storage, as no other fuels provide more energy within a given unit of volume. Compared to gasoline and diesel, other options may have more energy per unit weight, but none have more energy per unit volume Fig. 17.

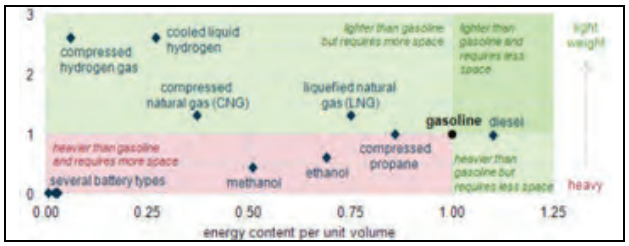

Fig. 17. Energy density comparisons

A **fuel cell** harnesses the chemical energy of hydrogen and oxygen to generate electricity without combustion or pollution. Fuel cell technology is not new, NASA has used fuel cells for many years to provide power for space shuttles' electrical systems Fig. 18.

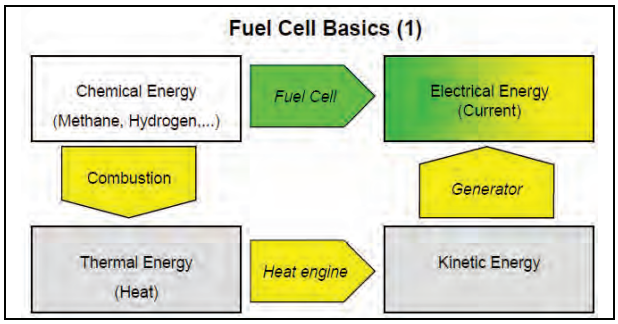

Fig. 18. Fuel cells Basics (1)

In the near future, your vehicle may also be powered by fuel cells. The type of fuel cell typically used in automobiles is a Proton Exchange Membrane (PEM), also called a Polymer Electrolyte Membrane fuel cell (Fig. 19).

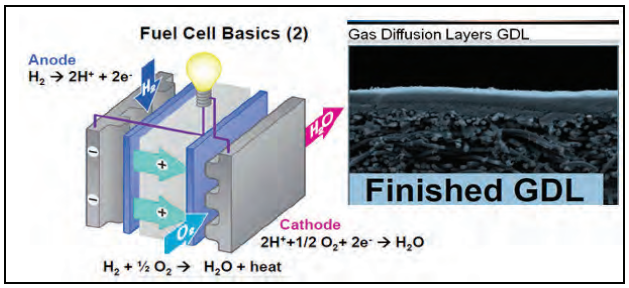

Fig. 19. Fuel cell basics (2)

Some experts think that hydrogen will form the basic energy infrastructure that will power future societies, replacing today's natural gas, oil, coal, and electricity infrastructures.

The widespread use of these fuels is largely explained by their energy density and ease of onboard storage, as no other fuels provide more energy within a given unit of volume. Compared to gasoline and diesel, other options may have more energy per unit weight, but none have more energy per unit volume.

The **flywheel** is designed for short-term storage of electrical energy produced by the two electric motors mounted on the front axle of the vehicle. They provide power to the front wheels but double as generators when the car brakes. The produced electricity is fed into the flywheel, causing an increase in the rpm of the rotor. In effect, the flywheel acts as a battery, storing energy in the rotational inertia of the rotor. The electricity generated by the flywheel is fed back to the motors on the driveline during times of high power demand, helping to reduce the overall power demand placed on the vehicle's internal combustion engine.

The glass-fiber/epoxy, magnetically loaded composite rotor is housed inside an air-cooled, aluminum containment structure. The rotor, which also includes a outer carbon-fiber composite layer for reinforcement and mass, rotates at speeds up to 40,000 rpm, creating an electrical current in the copper-coil wound stator at the flywheel's core. Power is fed to the drivetrain at moments of high demand on the engine Fig. 20.

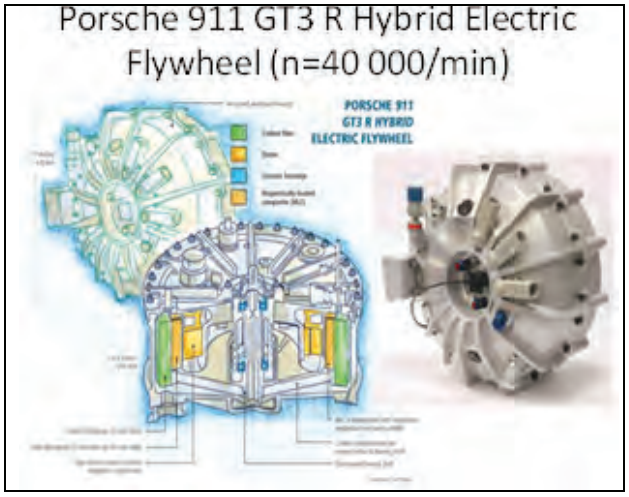

Fig. 20. Porsche hybrid electric flywheel

Design a highly efficient, mobile electric flywheel capable of high-density energy storage that can supplement the power of internal combustion engines in hybrid electric vehicles during acceleration or other periods of high energy demand, resulting in fuel savings. The weight of the flywheel is approximately one-seventh in relation to the weight of the battery when storing the same energy.

Hydraulic hybrid systems are efficient, compact and affordable, reusing braking energy to provide power for acceleration, which reduces vehicle fuel use and emissions (Fig. 21).

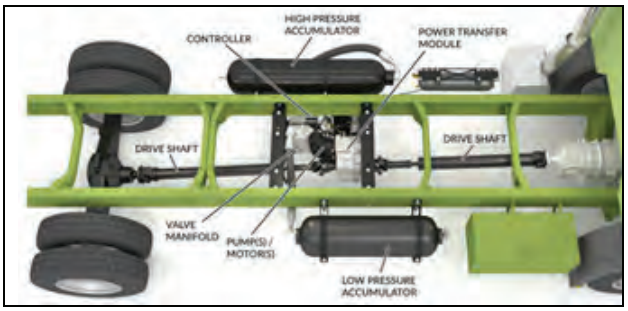

Fig. 21. Hydraulic hybrid delivery trucks

Vehicles with hydraulic hybrid delivery trucks which use carbon fiber composite wrapped accumulators, offer a 15-55% reduction in fuel usage and CO_2 emissions and cut NOx (nitrogen oxides) emissions in half.

Different uses of carbon fibers are illustrated by the bar graph in Fig. 22.

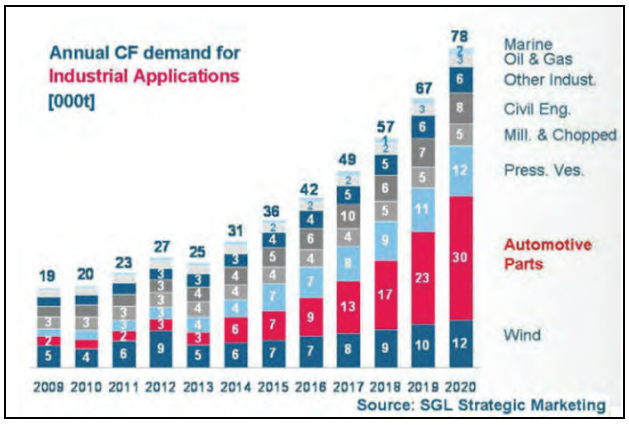

Fig. 22. Different uses of carbon

From the chart, it is clear that the automotive industry of CFRP is ahead of a bright future.

5. Conclusions

The vehicles including passenger cars increasingly important in everyday use. These large-scale mass production requirements of the car manufacturers of safety, economy and environmental protection requirements must be taken into account to solve. To meet this challenge car chassis and bodywork of the increasing importance of carbon fiber reinforced plastics to a growing area of application.

References

[1] K. Dreschler: CFK – Technologie im Automobilbau Was man von anderen Märken lernen kann? C.C.e.V. Automotive Symposium, Neckarsulm, 2010

[2] T. Gries, Dipl. B.: Veihelmann: Kombinierte Faserverbundstrukturen zum Aufprallschutz Institut für Textiltechnik der RWTH Aachen (ITA)

[3] K. Durst: Faserverbunde im Automobilbau: Warum „leicht“ schwer ist Materialica 13. Oktober 2009, München

[4] Szabó R.: A könnyű a jövő XVII. ENELKO 2016. Kolozsvár, 2016. október 6-9. p.146-151.

[5] Czvikovszkiy T., Nagy P., Gaál J.: A polimertechnika alapjai Műegyetemi Kiadó 2000. 455 p.

[6] R. Szabó, L. Szabó: New textile technologies, challenges and solutions XXIII Congress of IFATCC, Budapest, 2013. 05. 08. 10. 11 p.

[7] Composite flywheel: HEV racing dynamo

[8] Is the BMW 7 Series the future of autocomposites?

[9] Hydraulic hybrids: Boosting fuel economy without batteries

EXPRES 2018
ISBN: 978-86-919769-3-4

OPEN GEOTHERMAL ENERGY SYSTEM FOR THE HEAT SUPPLY IN VEĽKÝ MEDER

J. TAKÁCS[a], *S. GAŽIKOVÁ*[b]

Slovak University of Technology in Bratislava, Faculty of Civil Engineering,
Department of Building Services, Radlinského 11, 810 05 Bratislava, Slovak Republic
[a] E-mail: jan.takacs@stuba.sk
[b] E-mail: sonka.gazikova@gmail.com

Abstract

In Slovakia, there are approximately 170 geothermal sources with geothermal water (GTW) with temperature on the borehole head from θ_O = 15,7 to 126,0 °C The majority of GTW has a temperature suitable for preparation of hot water and heating for flats, civil amenities, agriculture and industrial areas.
In this paper, we would like to show out an example for a solution for the heat source reconstruction, which is using geothermal energy. Then cooled water from GTW is using for heating polyclinic and the thermal spa.
Modern elements have been used as a solution for the heating supply for the residential district: peak heat sources, which using natural gas, that are also used as stand-by heat sources, two demountable plate heat exchangers and cooled GTW is using for needs of thermal spa. The connection between the heat source and this spa is solved by using pre-insulated pipes with minimal heat losses.
With this solution, we will contribute to meeting the obligations of EU Directive 31/2010 on energy efficiency in the use of renewable energy sources and reducing greenhouse gas emissions and increasing energy efficiency.
The open geothermal energy system in Veľký Meder is a great example of how to optimally solved the supply of heat to the residential district using geothermal energy with subsequent use this energy for the thermal spa.

Keywords: *district heating, circulation pump, heating network, pressure diagram, geothermal energy*

1. Geothermal energy source

Geothermal drill VM-1 was realized in Veľký Meder in 2015, directly on the courtyard of the original heat source - hot-water boiler house, which is called Stred. This heat source is no longer suitable for the current requirements and needs. Therefore, its reconstruction was carried out, with the dominant position for the renewable heat source - geothermal drill VM-1. Energy parameters of this drill are shown in tab. 1. Mineralization of GTW is 3600 mg / l. Borehole head is shown in Fig. 1.
The expected cooling of GTW is on 25 ° C. However, real cooling of GTW is different (between 15 - 50 °C). Heat output in kW is shown in Fig. 2. The first column (green) showing GTW with free overflow and the second (blue) showing GTW which is pumping.

Fig.1. Borehole of drill VM-1 in Veľký Meder

Table 1. Energy parameters of the geothermal drill VM-1

Locality	Mark of borehole	Flow rate		Borehole temperature	Temperature of cooled GTW	Useful energy potential
		Free overflow	pump			
		(l/s)	(l/s)	(°C)	(°C)	(kW)
Veľký Meder	VM-1	10		93	25	2 847,2
Veľký Meder	VM-1		15	93	25	4 270,7
		10		93	40	2 219,1
			15	93	40	3 328,7

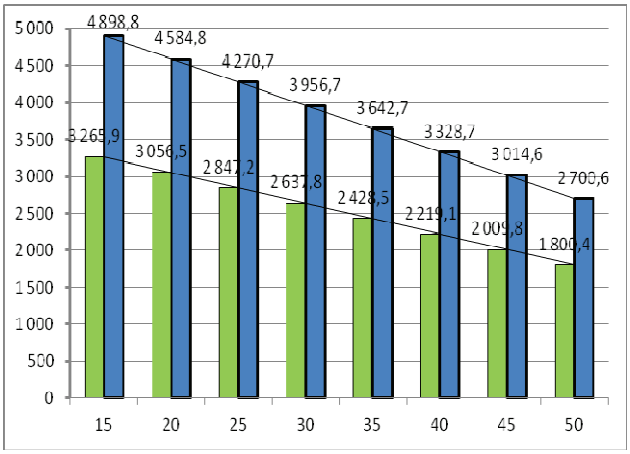

Fig. 2. Useful energy potentialpotential, which is depending from cooling of GTW

Technical solution

The geothermal water from the borehole is transporting by free overflow to the accumulation and degassing tank with volume 10 m^3, where is degassing and then transporting into two G-MART plate heat exchangers with heat output Q = 1 549 kW. GTW transfer its energy from heat exchangers HEX1 and HEX2 to the heating medium - the heating water, which is supplying the distributor and the collector by heat, from which the pass-outpoints are connected, according to Fig. 3.

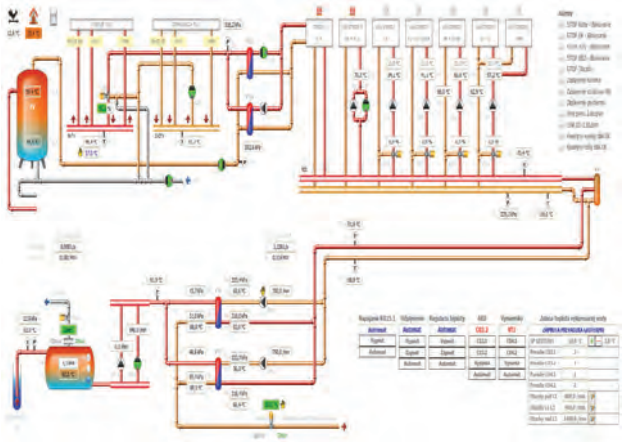

Fig. 3 – Circuit scheme of GTW from drill VM-1 to the heat exchangers HEX1 and HEX2 and pass-outpoints.

The secondary heat transferring medium stands out from the heat exchangers HEX1 and HEX2 and ensuring distributor and collector with heat, from which are connected pass-out points - 1 600 flats, kindergarten, elementary school, children's home, cultural center and polyclinic. The preheating of hot water running in two plate heat exchangers HEX1a and HEX1b with heat output Q = 400 kW according to Fig. 4.

Fig. 4 – Lying accumulation and degassing tank with volume 10 m^3

Then the hot water is accumulating in a standing accumulation tank with volume 4000 liters. From this tank, the residential district is supplied with hot water. The lying accumulation and degassing tank is located at the lowest floor and is shown in Fig. 4. View to heat exchangers HEX1 and HEX2 is shown in Fig. 5.

Fig. 5 – View on the plate heat exchangers HEX1 and HEX2, in foreground are circulating pumps

Aftercooling, the GTW in the plate heat exchangers HEX1 and HEX2 enter to the plate heat exchangers HEX1a and HEX1b which are located on the other floor and serve for preheating of hot water. The cooled GTW is transporting through a pipeline into the thermal spa. Before the entrance to the spa area, the pipeline is divided and a pipeline that supplying a near polyclinic with heat is connected to it. In the thermal spa, GTW is using in two pools.

Concept of heat source design

The heat source for a residential district is a hot-water boiler house on natural gas which is located on a two-story building. Its function is to ensure the need for heat for heating and hot water preparation. Both the original heat source and the heating system were dimension at a thermal gradient of 90/70 ° C. However, practical experience confirms, that after reconstruction for ensuring the need for heat, lower thermal gradients been enough, with a temperature of the water for heat supply to the heating system between 70 - 75 ° C.
After reconstruction, three hot-water boilers on natural gas with a pressure burner and a heat output of 1,000 kW and two modern boilers on natural gas with a pressure burner and a heat output of 1,600 kW are installed in the boiler house. The view for the boilers is shown in Fig.6.

Fig. 6 - View to the reconstructed hot-water boiler house on natural gas

2

Two boilers with a heat output of 1600 kW are fitted with flue gas heat exchangers, which increase the degree of usage of these boilers. View of the building of boiler house itself or the energy center is shown in Fig. 7.

Fig. 7 – View to the reconstructed heat source – hot-water boiler house on natural gas.

Production of heat in the boiler house

The reconstructed hot-water boiler house on natural gas was put on the operation on October 15, 2015. Since then, natural gas consumption, respectively the amount of heat produced has been recorded, which shown tab. 2. The graphical representation is on Fig. 8.

Amount of heat and consumption of natural gas during the heating season 2015/2016 Table no.2

Natural gas			
Date	**(MWh)**	**(m^3)**	**(eur)**
10.2015	1 196,60	111 043	47 539
11.2015	1 590,64	148 104	60 242
12.2015	1 979,64	183 776	72 759
1.2016	2 236,17	208 016	72 898
2.2016	1 660,56	154 370	56 977
3.2016	1 713,64	159 068	58 445
4.2016	1 104,05	102 236	41 584
5.2016	610,16	56 288	27 923
6.2016	364,78	33 451	21 136
7.2016	358,35	32 952	20 958
8.2016	354,23	32 714	20 844
9.2016	328,35	30 313	20 128
Sum	**13 497,17**	**1 252 331**	**521 433**

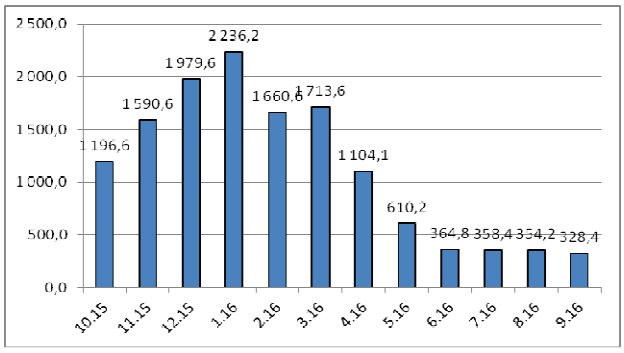

Fig. 8 - Amount of produced heat (MWh) in the heating season 2015/2016

From table 2 and Fig. 8 is clear that in the heating season 2015/2016 the residential area was most supplied with heat from the reconstructed boiler house. For the monitored heating season 2015-2016, heat consumption was 12 091.45 MWh (43 529.2 GJ – measured data), respectively 1 122 901 m^3 of natural gas. For further analysis, this value represents the comparable base.

In the autumn of 2016, the geothermal source VM-1 was successfully put into operation, resulting in some of the heat energy is producing by the geothermal source. The recorded values of the produced heat from geothermal water are in tab. 3 and the graphical representation is on Fig. 9. Due to the use of GTW, a reduced demand for natural gas has been achieved, thus fulfilling the prerequisites for the use of a renewable source of heat based on geothermal energy. GTW was using in plate heat exchangers HEX1 and HEX2 and subsequently in plate heat exchangers HEX1a and HEX1b for hot water preparation for a residential set of 1,600 flats. Partially cooled GTW is using in the polyclinic and ends on the area of the thermal spa, where it provides the operation of two swimming pools. Waste water from spa is disposing of in the Ižop canal.

Amount of heat and consumption of natural gas during the heating season 2016/2017 Table no.3

Energy source with geothermal energy			
date	(MWh)	(m^3)	(eur)
10.16	284,15	26 455	18 906
11.16	564,85	52 588	26 670
12.16	1 030,08	95 982	35 594
1.17	1 479,19	137 766	38 514
2.17	634,64	59 108	19 556
3.17	154,76	14 396	10 025
4.17	44,57	4 128	7 655
5.17	0,00	0	6 696
6.17	22,11	2 048	7 172
7.17	0,00	0	6 696
8.17	0,00	0	6 696
9.17	0,00	0	6 696
Sum	**4 214,35**	**392 471**	**190 874**

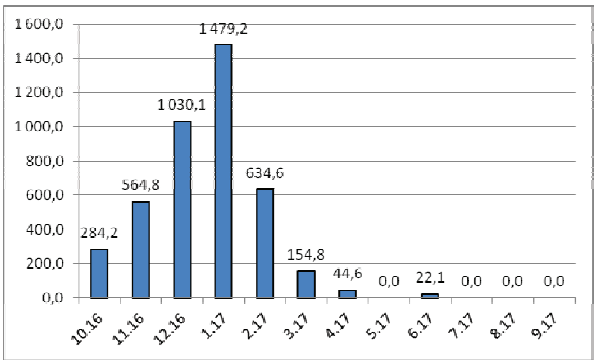

Fig. 9 – Amount of produced heat (MWh) between October 2016 – May 2017

From table 3 and Fig. 9, is clear that the largest production, respectively the heat consumption supplying from the reconstructed boiler house was in January 2017 in heating season 2016/2017 for the residential complex. During the monitored heating season 2016/2017, was

measured reduced heat consumption 4 214,35 MWh (15 171,66 GJ) from natural gas, which corresponds to 392,471 m^3 of natural gas, (31.22% of the consumption in the previous year).
Comparison of boiler house operation during the heating season 2015/2016 and 2016/2017 is shown in tab. 5, the graphical representation is in Fig. 10.

The difference in natural gas consumption during the heating season 2015/2016 and 2016/2017. Table no.4

Difference			
month	(MWh)	(m^3)	(eur)
10.	912,45	84 588	28 633
11.	1 025,79	95 516	33 573
12.	949,56	87 794	37 165
1.	756,98	70 250	34 385
2.	1 025,92	95 262	37 421
3.	**1 558,88**	**144 672**	**48 420**
4.	1 059,48	98 108	33 929
5.	610,16	56 288	21 227
6.	342,67	31 403	13 964
7.	358,35	32 952	14 262
8.	354,23	32 714	14 148
9.	328,35	30 313	13 432
sum	**9 282,82**	**859 860**	**330 559**

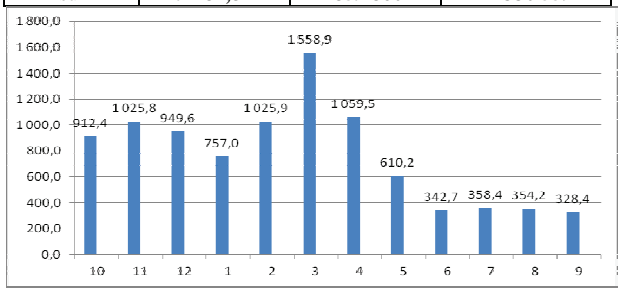

Fig. 10 – Saved natural gas during the heating season 2015/2016 and 2016/2017.

From tab. 4 and Fig. 10, is clear that the greatest savings, respectively the heat consumption for the residential complex supplied from the reconstructed boiler house was in March 2017 when we comparised heating season 2015/2016 and 2016/2017. We can say that we also saved 859 860 m^3 of natural gas per year. From an environmental viewpoint, this situation is equivalent for the emissions reduction as shown in tab. 5.

Quantification of unreleased emissions Table no. 5

Emission		Saved amount of NG	Emission
	($kg/10^6$ m^3)	(10^6 m^3)	(kg)
CO_2	1 920	0,85986	1 650,9
NO_2	320	0,85986	275,2
Sum			**1 956,2**

From tab. 5 is clear, that by saving 859 860 m^3 of natural gas, were not released 1650,9 kg of CO_2 and 275,2 kg of NOx per year into the environment, which together represented 1 956,2 kg emissions per year.

Summary

In Veľký Meder, there was drilled the geothermal drill in the courtyard of the local hot-water boiler house. The heat source was reconstructed and the basic load on the source took up a renewable energy source which is based on geothermal energy. By comparing the heating seasons 2015/2016 and 2016/2017, I can say that the designed heating supply solution for flats is right. Consumption of the natural gas has decreased, renewable energy source is using, and pollutant production in the form of CO_2 is reduced. This solution can be an example for how to carry out the obligations of the European Parliament and Council Directive 2010/31 / EU of 19 May 2010 about the energy performance of buildings.

This work was supported by the Ministry of Education, Science, Research and Sport of the Slovak Republic under VEGA Grant 1/0807/17.

References

[1] Petraš D. at all.: Renewable energy sources for low-temperature systems. JAGA, Bratislava 2009, 223 pp., ISBN 978-80-8076-075-5

[2] Fričovský B., Marcin D., Černák R., Benková K.: Renewability and sustainable usage and use of geothermal energy resources: needs and principles in conditions in Slovakia. In: Renewable energy sources. 2017 [electronic source]: Collection of papers from the 17th scientific-technical conference with foreign participation on theme: "Buildings with nearly zero needs of energy". Štrbské Pleso, SR, 9. - 10 5. 2017. 1. vyd. Bratislava: SSTP, 2017, CD-ROM, pp. 61-66. ISBN 978-80-89878-10-9

[3] Halás O.: Utilization of geothermal energy for heating in Veľký Meder. In Renewable energy sources. 2017 [electronic source]: Collection of papers from the 17th scientific- technical conference with foreign participation on theme: "Buildings with nearly zero needs of energy". Štrbské Pleso, SR, 9. - 10 5. 2017. 1. Bratislava: SSTP, 2017, CD-ROM, s. 73-76. ISBN 978-80-89878-10-9.

[4] Koščo J., Kudelas D., Tauš P., Antolíková S., Possibilities of using thermal water from drill G-4 in Košice/Ján Koščo: [et al.], 2015. In: SGEM 2015., Sofia: STEF92 Technology, 2015 P. 517-522, ISBN 978-619-7105-36-0, ISSN 1314-2704

[5] Kontra J.: Usage of the geothermal energy. Műegyetemi könyvkiadó, Budapest 2004

[6] Halász Gy-né. - Kalmár F.: Energy comparison of heating systems with different heat sources I.-II. part, Magyar Épületgépészet, vol. L VI. 12 sz. vol. L VII. 1-2 sz., 2007

[7] Malinová K.: The decisive factor on the reconstruction of the heat source, TZB Haustechnik, annual volume VII, č.4/2014, str. 38-39, ISSN 1803-4802

[8] Documents from operation of the boiler house Stred in Veľký Meder MPBH spol. s r. o.

[9] Nyers J., Pek Z., 2014, Mathematical Model of Heat Pumps' Coaxial Evaporator with Distributed Parameters. Acta Polytechnica Hungarica, Vol.11, No.10, pp. 41-54.

[10] Nyers J. (2016), A new analytical method for defining the pump's power optimum of a water-to-water heat pump heating system using COP, Thermal Science, doi: https://doi.org/10.2298/TSCI161110324N.

EXPRES 2018
ISBN: 978-86-919769-3-4

EFFECTIVENESS COMPARISON OF THE GROUND-WATER AND AIR-WATER HEAT PUMP FOR DOMESTIC HEAT WATER PRODUCTION

B. B. FÜRI [a] , *L. ŽIVNER* [b], *I. SKALÍKOVÁ* [c]

Department of Building Services, Faculty of Civil Engineering, Slovak University of Technology in Bratislava SK-810 05 Bratislava, Radlinského 11, Slovakia
[a]E-mail: belo.furi@stuba.sk
[b]E-mail: lukas.zivner@gmail.com
[c]E-mail: ingrid.niko@gmail.com

This contribution is focused on reviewing the effectiveness of domestic hot water (DHW) preparation, using the renewable energy source (RES) of the environment – ground/water versus air/ water heat pumps. In both cases the evaluation was based on measurements taken in family houses belonging to a nearly Zero Energy Buildings (nZEBs) group. The realistic assessment of the heat pumps effectiveness is represented by experimental measurements, which take into effectiveness of all components within the actual operating condition in the buildings. The experimental measurements, described in this article, were performed for a critical summer period from 18th July 2015 to 24th July, 2015.

Keywords: *heat pump (HP), effectiveness, domestic hot water (DHW)*

1. Introduction

The heat pump measurements were performed during the summer season, within the weekly period from 07/18/2015 to 07/24/2015. Data recording has been set on the minute basis. Measurements are performed within the family house "A" and family house "B". The heat source is a heat pump air/water in family house "A" and ground/water in family house "B". Properly designed heat pump should be one of the energy saving systems. Global indicator of primary energy is the performance factor – SPF [1, 2].

1.1 Identification of object „A"

The house is located in Bratislava - Devín. The house was built in 2009. The construction of a family house consists of materials that allow achieving optimal thermal insulation properties. The house belonging to the category of Low Energy House. House has two floors with a total floor area of 175 m^2 and is occupied by 3 inhabitants during the entire year. The primary energy source is the air / water heat pump. For a given location, the use of this type of HP is the most advantageous, even with regard to the acquisition costs. The thermal loss of the building was set at 8 kW.

Fig. 1 Outdoor unit of Air/Water HP

Fig. 2. Indoor Unit of HP system object A

1.2 Identification of object „B“

The object is a single-storey house belonging to Low Energy House standard Figure 3 and Figure 4. This house is occupied by 4 inhabitants during the entire year. Ground surface has 106 m^2. Primary energy source is the ground collector situated in the backyard at a depth of 1.2 meters in two circle area with 2x 150 m size. Pipelines are separated by a minimum 0.9 m and the material is PE 100 RC diameter 32x 3.0 mm. At the given depth is the black soil with an estimated thermal energy drain of 35 - 40 W/m^2. Heat loss of the building according to EN 12831 is 5.5 kW.

Fig. 3 Outdoor unit of Ground/Water HP

Fig. 4 Indoor unit of HP system

2. The heat source parameters and heating system parameters

2.1 Technical parameters of object “A”

For the object was designed an outdoor unit heat pump (monobloc), with a rated output of 14 kW, which was situated at the boundary of the land Figure 1. The indoor unit is located in the technical room of the family house Figure 2. The indoor unit includes an electric boiler, circulation pumps for the primary and secondary side, a stainless steel 500 litre hot water tank and regulation

2.2 Technical parameters of object “B”

The heat source is heat pump ground / water placed in the maintenance room Figure 4. Rated power is 5 kW. The unit has an integrated reservoir of hot water of volume 180 litres and an additional source of hot water with the power of 2 - 9 kW. Water heating is designed by storage water heater with the temperature gradient 55/50 °C.

Heating output (at B0 / W55 ° C): 3.56 kW
Electric power (at B0 / W55 ° C): 1.28 kW
Coefficient of Performance (COP): 2.78

3. Experimental measurements

The heat pump measurements were performed during the summer season, within the weekly period from 07/18/2015 to 0/24/2015. Data recording has been set on the minute basis. The indicator is a seasonal performance factor – SPF [4, 5].

Measured parameters of the experiment:
Outside temperature: θ_e (° C)
The internal reference temperature: θ_i (°C)
The temperature of the heating flow: θ_i (°C)
Temperature of return heating water: θ_o (°C)
Temperature of the water tank at the top of the container: $\theta_{tan\text{-}Top}$ (°C)
The temperature of the mixture in the collector to the heat pump: $\theta_{col\text{-}P}$ (°C)
The temperature of the mixture in the collector output temperature: θ_{col} (°C)
The flow on the secondary side: M_{SEK} (l / m)
Electric current - compressor: I_{comp} (A)
Electric current - circulation pumps, electric boiler: I_{ost} (A)

The calculated parameters of the experiment:
Electric power HP: P_{HP} (kW)
Electric power circulation pumps, regulation, additional resources: P_{OST} (kW)
Φ heat pump (kW)
SPF - seasonal performance factor determined on a weekly basis for the entire system (-)
SPF_{HDW} - seasonal performance factor determined on a weekly basis for the preparation of the hot domestic water (-)

3.1 Experimental measurements of object “A”

During the experimental measurement, individual parameters were evaluated to determine the SPF_{DHW} value. The system during the measurement was operated in monovalent mode as shown in Figure 5 and Figure 6.

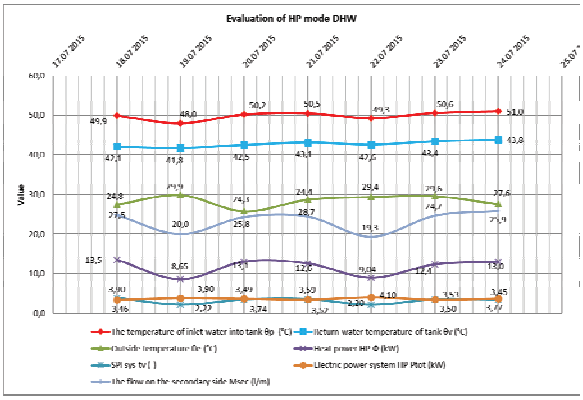

Fig. 5 Evaluation of the heat pump in DHW mode „Object A“

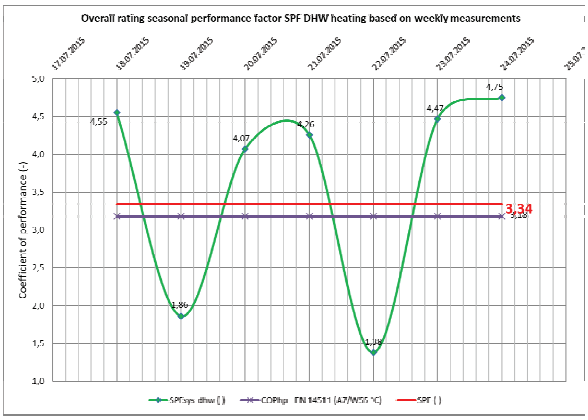

Fig. 6 SPF overall rating based on weekly measurements for DHW „Object A“

3.2 Experimental measurements of object “B”

During the experimental measurement, individual parameters were evaluated to determine the SPF_{DHW} value. The system during the measurement was operated in “monovalent” mode as shown in Figure 7.

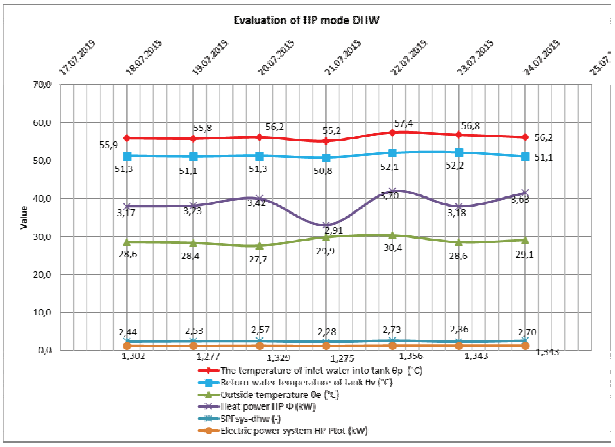

Fig. 7 Evaluation of the heat pump in DHW mode „Object B“

In Figure 8 is the SPF_{DHW} of the object "B". The average value of SPF_{DHW} for the given preparation period of the DHW heat pump system Ground/Water is 2.52.

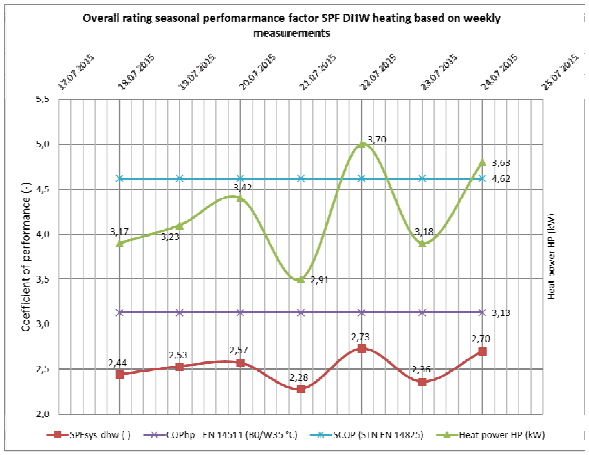

Fig. 8 SPF overall rating based on weekly measurements for DHW “Object B”

With the Air/Water heat pump system, the SPF_{DHW} value is increased more quickly due to the primary influence of the outdoor air temperature. Finally, it is important to note that the user of the house has a great influence on the operating conditions and its own set-up of the DHW heating system.

4. Conclusion

The SPF_{DHW} value of the object "A" is determined for each day where the weighted arithmetic mean is the total SPF for the whole week, and for comparison the COP calculation values according to STN EN 14511 are calculated.

The total SPF value from the experimental measurement for the given period preparation of the DHW heat pump system Air / Water is 3.34. Based on this value, we can say that HP works very efficiently in the preparation of DHW under given climatic and operational conditions.

The SPF_{DHW} value of the object "B" is determined for each day where the weighted arithmetic mean is the total SPF for the whole week and for comparison the COP calculation values.

The total SPF_{DHW} value from the experimental measurement for the given period preparation of the DHW heat pump system Ground / Water is only 2.52. In case of heat pump system Air/Water values o SPF_{DHW} are raising expressively from reason of direct influence of outdoor air temperature. In ending necessary remind, that great influence for operation conditions of DHW preparation, has users of building readjusting of heat pump system.

Acknowledgment

This work was supported by the Ministry of Education, Science, Research and Sport of the Slovak Republic under VEGA Grant 1/0847/1.

REFERENCES

[1] Petráš D., Lulkovičová O., Takács J., Füri B., Obnoviteľné zdroje energie pre nízkoteplotné systémy,(Renewable energy sources for low temperature systems,) Bratislava, 2009, ISBN 978-80-8076-075-5

[2] Füri B., Niková I., Živner L., Evaluation of heat pump system effectiveness for domestic heat water preparation extracted renewable energy from environment. In.: TOP 2016 22nd Annual International Scientific Conference Engineering for Environment Protection, Častá Papiernička, SR, 7. - 9. 6. 2016. 1. ed. Slovenská technická univerzita v Bratislave, 2016, ISBN 978-80-227-4568-5

[3] STN EN 15450, Vykurovacie systémy v budovách. Navrhovanie vykurovacích systémov s s tepelnými čerpadlami (Heating systems in buildings. Design of heat pump systems), 2007

[4] STN EN 14825 , Klimatizačné jednotky, na chladenie kvapalín a tepelné čerpadlá s elektricky poháňanými kompresormi na vykurovanie a chladenie – skúšanie a hodnotenie pri podmienkach čiastočnej záťaže a výpočet sezónnej účinnosti (Air conditioners, liquid chilling packages an heat pumps with electrically driven compressors, for space heating and cooling – Testing and rating at part load conditions), 2016

[5] ST EN 15316 4-2 , Vykurovacie sústavy v budovách. Metóda výpočtu energetických požiadaviek systému a účinnosti systému - Časť 4-2: Priestorové systémy výroby tepla, systémy tepelného čerpadla (Heating systems in buildings – Method of system energy requirements and system efficiencies- Part4-2: Space heating generation systems, heat pumps systems), 2008

[6] Nyers J., Pek Z., 2014, Mathematical Model of Heat Pumps' Coaxial Evaporator with Distributed Parameters. Acta Polytechnica Hungarica, Vol.11, No.10, pp. 41-54.

[7] Nyers J. (2016), A new analytical method for defining the pump's power optimum of a water-to-water heat pump heating system using COP, Thermal Science, doi: https://doi.org/10.2298/TSCI161110324N.

[8] Kalmár T., Kalmár F. (2010), Comfort and energy analysis of heating up, International Review of Applied Sciences and Engineering, 1-2, 35-43.

[9] Kajtár L., Kassai M., A new calculation method to analyse the energy consumption of air handling units. 4th International Symposium on Exploitation of Renewable Energy Sources: EXPRES 2012. Subotica, Serbia, pp. 10

ISBN:978-8685409-70-7

[10] Szabo J, Kajtar L, Expected thermal comfort in underground Spaces. EXPRES 2016, Subotica, Serbia. pp. 76-80. ISBN:978-86-919769-0-3

[11] Takács J., Bukoviansky M., Utilization of Geothermal Energy for Residential Sector of the City District Galanta North. EXPRES 2014, pp.82-85, ISBN 978-86-85409-96-7, 2014.

[12] Takács J. (2015), Enhance of the efficiency of exploitation of geothermal energy, EXPRES 2015 Proceedings, ISBN 978-86-82621-15-7, Subotica, pp. 46-49.

[13] Nyers, J., Garbai, L., Nyers, A. (2015), A modified mathematical model of heat pump's condenser for analytical optimization, International J. Energy, Vol. 80, pp. 706-714, 1 February 2015. DOI:10.1016/j.energy.2014.12.028

[14] Nyers, J., Nyers, A. (2013), Hydraulic Analysis of Heat Pump's Heating Circuit using Mathematical Model, 9th ICCC International Conferenc, Proceedings-USB, ISBN 978-1-4799-0061-9, pp. 349-353, Tihany, Hungary, 2013

[15] Füri B., Practical experiences with multi-compressor refrigeration systems, Proceedings of 6th International Conference on Compressors and Coolants – Compressors 2006, 27. - 29. 9. 2006, Častá – Papiernička, p. 158– 161. ISBN 80-968986-5-5

[16] Kalmár F., Csomós Gy., Lakatos Á. (2013), Focus on renewable energy (energy policy) — Editorial, International Review of Applied Sciences and Engineering, 4 (1), 95-95 (2013)

[17] Šereš L., Grljević O., Bošnjak S., IT Support of Buildings Energy Efficiency Improvement, International Conference on Energy Efficiency and Environmental Sustainability, EEES 2012, Conference proceedings, ISBN: 978-86-7233-320-6, pp. 55-62.

EXPRES 2018
ISBN: 978-86-919769-3-4

POSSIBILITIES OF ENERGY SAVINGS AT REPLACEMENT BOILER FOR GAS FUEL INTO RENEWABLE ENERGY SOURCE

M. KURČOVÁ

Slovak University of Technology in Bratislava, Faculty of Civil Engineering, Department of Building Services
SK – 810 05 Bratislava, Radlinského 11, Slovakia
E-mail: maria.kurcova@stuba.sk

This contribution deals with possibilities of energy savings in case of gas fuel plug in combined with sources on the basis of renewable energy sources. In this case of plug in, put the accent on necessary of accurate operating to reach maximally measure of energy savings. In present time, put the accent on exploration of renewable energy sources for energy production of heating. Sources of heating with gas fuel basis in heat economy, will be in retire and step by step will be replaced with equipment's, whose utilize renewable energy sources. Exertion these sources in heat production have though Influence on heat distribution network parameters and on the method of heat transfer. Renewable energy sources (RES) works with lower operation temperatures, which for distribution network are not enough. Hence sources of heat on gas fuels in possible totally replace with renewable energy sources. The operation character of distribution network, request combination of RES with source of heat on gas fuels, so that reach parameters of heat transfer material. The economy of operation such combined heat source, have be care the control system.
The contribution deals with possibilities of energy savings in case of gas fuel plug in combined with sources on the basis of renewable energy sources what is a solar collector system. Comparison of energy savings are compare for three of alternative onto solar collector surfaces. Further comparison of energy saving comparison is with supplement of combined energy source of other renewable energy source, with a heat pump.

Keywords: *renewable energy source (RES), solar collector, heat pump (HP)*

1. Introduction

Currently attached great importance to the production of heat, using heat sources based on renewable energy sources. Therefore, we often deal with the production of heat, which is the classical gas boilers assigned to another - a renewable source of energy, whether solar collector or heat pump. The priority of managing such multi-valent heat sources is to maximize the use of renewable energy.

2. Management of heat production with multiple heat sources

Systems with one heat source (most often a gas boiler) are equipped with a controller from heat producer, which is part of the boiler. Their control is quite simple, it is about switching on and off the source, respectively. To increase boiler output to achieve the desired heating water temperature. These regulators can easily manage a cascade of multiple identical sources. Heat source management becomes more complicated if a renewable source of heat - a solar collector or a heat pump - is placed in the system. The task of management is to ensure the priority of heat production from a renewable energy source.

2.1 Bivalent system – solar collector and gas boiler

The most commonly used combination of bivalent system involvement solar collectors in combination with a gas boiler. The main source of heat in this case is a solar collector, which can only serve for the preparation of domestic hot water or as a support for heating.
The gas boiler serves as an additional top heat source. Bivalent control system is based on sensing the temperature in the system. Therefore, the correct positioning of heat sensors is important. A schematic diagram of a heating system consisting of two heat sources - a solar collector and a gas boiler with the location of temperature sensors and actuators required for control is shown in Figure 1.

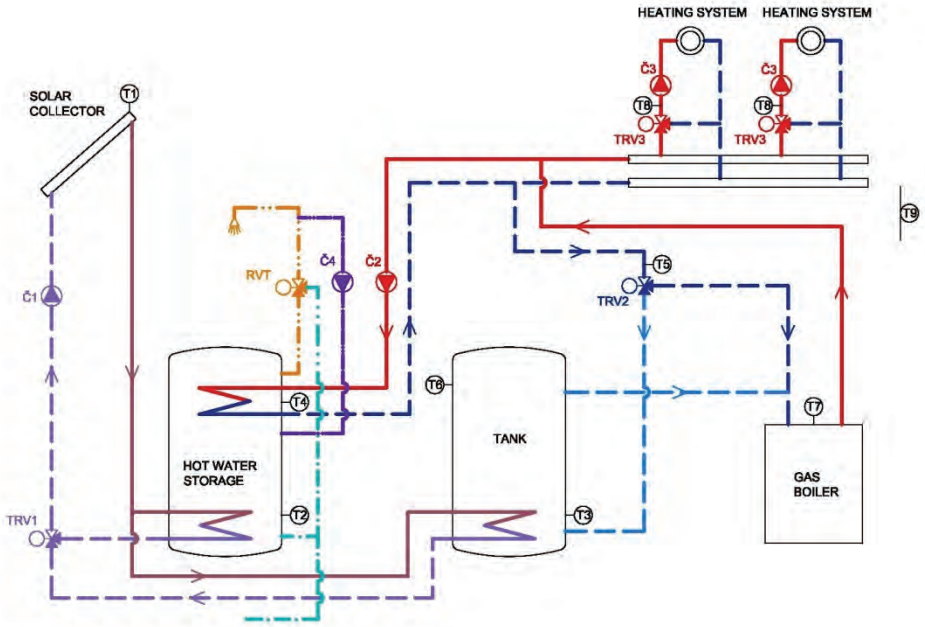

Fig. 1. Bivalent system – solar collector and gas boiler
T – temperature sensor, TRV – three-way control valve, RVT – thermostat control valve, Č – pump

2.2 Multivalent heat source – solar collector, heat pump and gas boiler

Due to low space requirements, a heat pump, especially an air/water type, is a suitable renewable energy source. This renewable energy source can be used in combination with a solar collector. The main source of heat is the solar energy used by the solar collector for warm water heating in the storage heater and consequently for the support of heating. The heat pump is used for the preparation of domestic hot water (DHW) and for space heating.

In regions with extremely low outside temperatures, only a renewable energy source is not enough. A top heat source with primary energy independent of climatic conditions is also needed. Then a connection is made to the three heat sources - the solar collector, the heat pump and the gas boiler (Figure 2).

The task of regulation is the use of solar energy to the maximum extent of both hot water heating in the storage heater and heating through a storage tank.

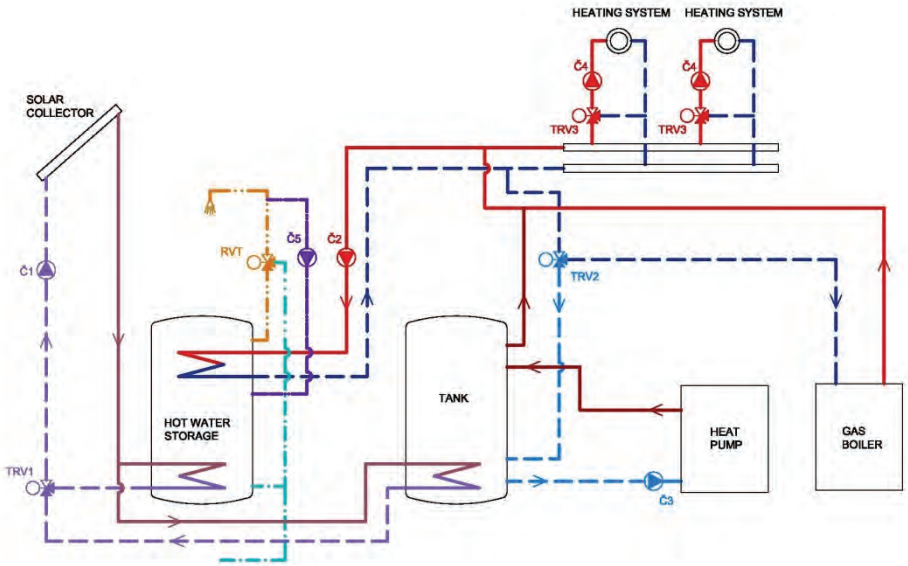

Fig. 2. Multivalent heat source – solar collector, heat pump and gas boiler
T – temperature sensor, TRV – three-way control valve, RVT – thermostat control valve, Č – pump

3. Savings options in connection solar collector and gas boiler

The inclusion of a solar collector as a renewable energy source for a heat source for a gaseous fuel, leaving one gas boiler as the peak source can save a significant part of the operating costs for fuel (gas). The amount of fuel savings will affect how much of the heat produced will be covered by the renewable source.

The fuel savings comparison is combined for the heating system (heaters 70/55 °C and underfloor heating 45/35 °C) with a total heat input of 400 kW and for DHW heating for 60 apartments (140 persons) with 1000 litre storage heater (heating time 5 hours per day for space heating water temperature 70 °C and hot water 60 °C) with thermal input of spiral 120 kW.

The estimated annual heat demand is:

- for heating: 2 550 GJ/year = 706 350 kWh/year,
- for DHW: 740 GJ/year = 204 980 kWh/year,
- total: 3 290 GJ/year = 911 330 kWh/year.

The calculation of the area of the solar collectors is made for three variants and the results are Table 1:

A. Area calculations are based on 80 % coverage of the daily energy demand for hot water heating in the summer months,
B. Area calculation is based on 100 % coverage of the daily energy demand for hot water heating in the summer months,
C. Area calculations are based on 100 % annual energy demand for hot water heating.

In the case of a gas boiler without a renewable energy source, an estimated annual gas demand is 109 120 m³, which at the gas price of 0.55 €/m^3 represents the annual gas operating costs. The annual savings in operating costs of gas using solar collectors are shown in Table 2.

Table 1. Design of solar collectors

Variant	Surface (m^2)	The amount of heat transferred by the collectors (kWh/year)	Coverage of annual heat demand (%)
A	80	75 000	40
B	110	103 000	50
C	220	206 000	100

Table 2. Annual savings in operating costs for gas with solar collectors

Variant	Gas savings (m^3)	Saving gas costs (€)	Percentage savings (%)
A	8 948	4 920	8.2
B	12 330	6 780	11.3
C	24 660	13 560	22.6

4. Possible savings for connection of solar collectors, heat pumps and gas boilers

The heat sources combined solar collector, heat pump and gas boiler is to maximize the use of solar energy for the preparation of DHW and heating support. The gas boiler in this case is a top resource that has to cover 100 kW of heat output. The other heat demand comes from renewable energy sources. The gas saving results are shown in Table 3 for all three variants of the solar collector design.

For heat pump operation, electricity is needed to enter the savings calculation as an item of operating load. The need for electric power for the heat pump operation reduces the cost savings of gas operating costs when replacing the gas boiler with the heat pump. Calculation of the annual electricity demand for the heat pump is in Table 4.

The calculation of the heat pump operation costs is considered at the electricity price of 0.13 €/kWh_{el} and is also accounted for by saving the gas costs in Table 5. The annual savings in running costs for the combination of solar collectors, heat pump and gas boiler are in Table 6.

Table 3. Annual gas savings with the combination of solar collectors and heat pumps

Variant	Annual gas savings				
	Solar collector		Heat pump		Total
	(m^3)	(%)	(m^3)	(%)	(m^3) / (%)
A	8 948	8.2	79 042	71.8	87 990 / 80
B	12 330	11.3	75 660	68.7	
C	24 660	22.6	63 330	57.4	

Table 4. Annual electricity demand for the heat pump

Variant	Quantity of heat produced (kWh)	Annual electricity demand (kWh_{el})
A	659 850	212 855
B	631 850	203 823
C	206 043	170 583

Table 5. Operating costs and annual heat pump savings

Variant	Cost of heat pump operation (€)	Cost of operation of gas boiler (€)	Annual savings on gas operating costs (€)
A	27 670	43 470	15 800
B	26 500	41 610	15 110
C	22 180	34 830	12 650

Table 6. Annual savings on gas operating costs when combined with solar collectors, heat pump and gas boiler

Variant	Solar collector (€)	Heat pump (€)	Solar collector + heat pump (€)	Percentage of savings (%)
A	4 920	15 800	20 720	34.5
B	6 780	15 110	21 890	36.5
C	13 560	12 650	26 210	43.7

5. Conclusion

Renewable energy sources are often promoted as resource-efficient, with minimal operating costs. Often, this requires people to provide some of the heat demand with a renewable resource, without thinking more about the system's input data. When replacing conventional sources - gas boiler renewable energy is essential to energy needs, in what quantities and at what temperature gradient system, it will cover, to achieve the desired savings.

Acknowledgment

This work was supported by the Ministry of Education, Science, Research and Sport of the Slovak Republic through the grant VEGA 1/0807/17.

References

[1] Takács J., Rácz, L., Možnosti využívání obnovitelných energií v soustavách centralizovaného zásobování teplem. In TZB Haustechnik. Roč. 9, č. 4 (2016), s. 32-33. ISSN 1803-4802.

[2] Kurčová M., The effect of thermal insulation of an apartment building on the thermo-hydraulic stability of its heating system. In Slovak Journal of Civil Engineering. Vol. 23, no. 4 (2015), s. 8-18. ISSN 1210-3896. Database WOS: 000217748500002

[3] Kurčová M., Ehrenwald P., 2016, Possibility Cooperation of Space Heating System with Heat Pump. Proceedings EXPRES 2016 Symposium, Subotica, Serbia, 31. 3. - 2. 4. 2016, CD-ROM, pp. 52-54. ISBN 978-86-919769-0-3.

[4] Živner L., Niková, I., Füri B., 2016, Efficiency of the Heat Pump System for Domestic Hot Water Preparation in The Winter Season. In Magyar Épületgépészet. Vol. 65, no. 7-8 (2016), pp. 12-15. ISSN 1215-9913.

[5] Skalík L., 2016, Variation of Solar Energy System Components According to its Efficiency. Proceedings EXPRES 2016, Symposium Subotica, Serbia, 31. 3. - 2. 4. 2016, Subotica : CD-ROM, pp. 119-122. ISBN 978-86-919769-0-3.

[6] Nyers J., Pek, Z., 2014, Mathematical Model of Heat Pumps' Coaxial Evaporator with Distributed Parameters, Acta Polytechnica Hungarica, vol.11, no.10, pp. 41-54.

[7] Nyers J., 2016, COP and Economic Analysis of the Heat Recovery from Waste Water using Heat Pumps, International J. Acta Polytechnica Hungarica Vol. 13, No. 5, pp. 135-154.

[8] Kajtár L., Kassai M., 2010, A new calculation procedure to analyse the energy consumption of air handling units, Periodica polytechnica-mechanical engineering 54:(1) pp. 21-26.

[9] Takács J., 2015, Enhance of the efficiency of exploitation of geothermal energy, International symposium, Subotica, Serbia, Proceedings EXPRES 2015, pp. 46-49.

[10] Füri B. , 2006, Practical experiences with multi-compressor refrigeration systems, Proceedings of 6th International Conference on Compressors and Coolants Compressors 2006, Častá – Papiernička, pp. 158–61, ISBN 80-968986-5-5.

EXPRES 2018
ISBN: 978-86-919769-3-4

APPLICATION OF ADIABATIC COOLING IN OUR CLIMATIC CONDITIONS

Belo B. FÜRI [a], *Mária FRŤALOVÁ* [b]

Department of Building Services, Faculty of Civil Engineering, Slovak University of Technology in Bratislava
SK-810 05 Bratislava, Radlinského 11, Slovakia
[a]E-mail: belo.furi@stuba.sk
[b]Email: maja.frtalova@gmail.com

Abstract: This article is about direct and indirect evaporative equipment, air washers, and their associated equipment used for air cooling, humidification, dehumidification and air cleaning. The use of water evaporation for decreasing air temperature is a well-known cooling technology and an environmental friendly application. Due to increase in the awareness of environmental problems resulting from greenhouse gas emissions, various applications of evaporative cooling have been extensively studied and used for industrial and residential sectors, such as, humidifier and evaporative cooler.

Keywords*: adiabatic cooling,*

[1] Introduction

Evaporative cooling process is commonly used in cooling water tower, air washes, evaporative condensers, fluid cooling and also to soothe the temperature in places where several heat sources are present. However, it is seldom utilized for human thermal comfort. Evaporative cooling equipment can be direct evaporative cooler (DEC) or indirect evaporative cooler (IEC). Direct evaporative cooling equipment decrease air temperature by direct contact with a liquid surface or a wet solid surface or else with the use of spray systems [4, 5].
Principal advantages of evaporative air conditioning include:

1. Reduced pollution emissions
2. Improved indoor air quality,
3. Substantial energy and cost savings,
4. Reduced peak power demand,
5. Easy to use with direct digital control
6. Wide variety of packages available
7. Provides humidification and dehumidification when needed,
8. For same amount of cooling, less water is evaporated than with conventional air conditioning.

Figure 1 shows a schematic direct evaporative cooling system. In a DEC, water is vaporized inside the air streams and heat and mass transferred between air and water decreases the air dry bulb temperature (DTB) and increases its humidity, keeping the enthalpy constant (adiabatic cooling); the minimum temperature that can be reached is the wet bulb temperature (WBT) of the incoming air.

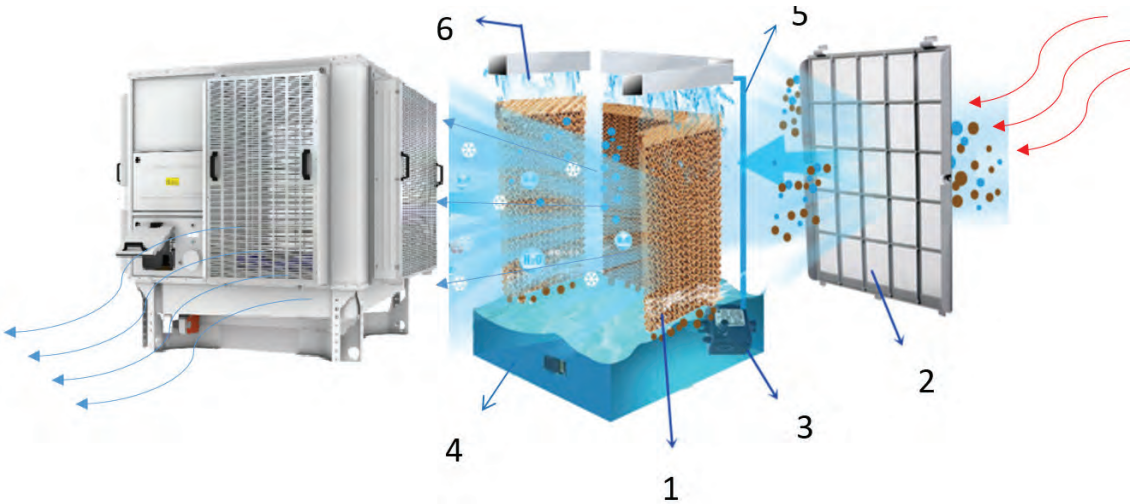

Fig.1 The function of the evaporator cooler
1 – Cooling pad, 2 - Dust filter, 3 – Water pump, 4 – Water tank, 5 – Water distribution lines, 6 - Water spray

Direct evaporative air coolers, air washers, indirect evaporative air coolers, evaporative condensers, vacuum cooling apparatus and cooling towers exchange sensible heat to latent heat.
This equipment falls into two general categories: those for 1 - air cooling and 2 - heat rejection. In direct evaporative cooling, water evaporates directly into the air stream, reducing the air´s dry-bulb temperature and raising its humidity level. Direct evaporative equipment cools air by direct contact with water, either by an extended wetted-surface material. In indirect evaporative cooling, secondary air removes heat from primary air using a heat exchanger. In indirect evaporative cooling, secondary air removes heat primary air using a heat exchanger. In one indirect method, water is evaporative cooled by cooling tower and circulates through one side of a heat exchanger. Supply air to the space passes over the other side of the heat exchanger. In another common method, one side of an air – to –air heat exchanger is wetted and removes heat from the conditioned supply air stream on the dry side. Supply air to the space passes over the other side of the exchanger. In another common method, one side of air – to – air heat exchanger is wetted and removes heat from the conditioned supply air stream on dry side. Even in regions with high wet-bulb temperatures, indirect evaporative cooling can be economically feasible. This is especially true if building return air from an air – conditioned build is used on the wet side of an air – to – air heat exchanger.

The return air´s lower wet-bulb temperature, which derives from mechanical refrigeration, may be used to extend indirect evaporative cooling performance in more humid climates. It is often desirable to combine the effects of direct and indirect evaporative processes (indirect /direct). Direct evaporative coolers for residence in low – wet – bulb regions typically require 70 % less energy than direct – expansion air conditioners. Depending on climatic conditions, many buildings can use indirect/direct evaporative air conditioning to provide comfort cooling. Indirect/direct systems achieve a 40 to 50 % energy saving in moderate humidity zone [1].

If clean and well-maintained evaporators with about 80% efficiency, can reduce the indoor air temperature around 4 - 10 °C. In some units, supplementary filters are added to reduce the particle count of delivered air when the unit is operating with or without water circulation. Evaporative pads may be chemically treated to increase wet ability. An additive may be included in the fibres to help them resist attack by bacteria, fungi, and other micro organisms.

Methods to evaluate evaporative cooling systems - Feasibility Index (FI)

This section presents method that may be used to verify the viability of using evaporative cooling equipment of air conditioning for human thermal comfort and their application. A fast method to evaluate approximately the potential of the evaporative cooling is based on the Feasibility Index, defined by: FI = WBT – ΔT where ΔT = (DBT – WBT) is the wet bulb depression. DBT and WBT are, respectively the dry bulb temperature and wet bulb temperature of the outside air. This index decreases as the difference between dry bulb and wet bulb temperature increases, i.e. as air relative humidity decreases. It shows that, the smaller FI is more efficient the evaporative cooling will be. Thus, this number indicates the evaporative cooling potential to give thermal comfort. From these limits it can be stated that to achieve the recommended thermal comfort it is necessary to decrease the temperature and increase the relative humidity.

It corresponds, e.g. to a temperature of 1; $\theta_e = 34°C$ with relative humidity $\varphi_e = 35\,\%$ to decrease temperature to state 2; $\theta_i = 22°C$ with relative humidity $\varphi_i = 70\,\%$.

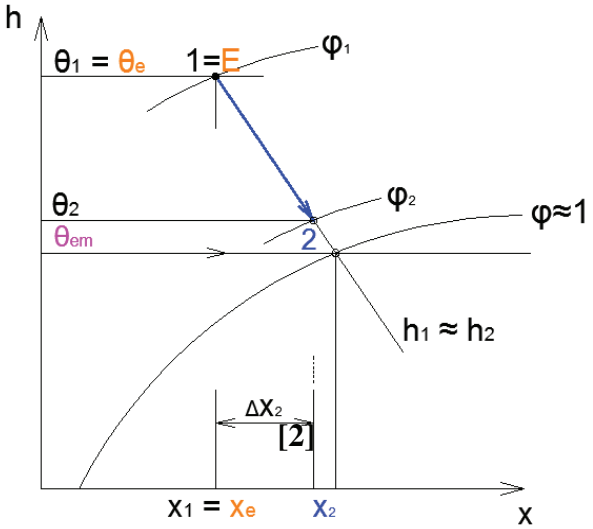

Fig. 2 Mollier's chart, which shows air treatment at direct adiabatic cooling

Comfort conditions are not defined by state values; slightly warm air is comfortable at low humidity, while cold air at low humidity is not comfortable. Most people feel comfortable at a outdoor temperature $\theta_i = 20 \; to \; 27\,°C$ with a relative humidity of $\varphi_i = 30 \; to \; 65\%$. These conditions define a "comfort zone" that is delineated in the Mollier´s diagram [1, 2].

[3] Direct evaporative cooling saturation efficiency

When relative humidity is too low it can be increased with evaporative cooling. And when it is too high it can be decreased with the use of desiccants. In direct evaporative air cooling, air is drawn through porous wetted pads or a spray and its sensible heat energy evaporates some water. Heat and mass transfer between the air and water lowers the air dry – bulb temperature and increases the humidity at a constant enthalpy (wet – bulb temperature remains nearly constant). The dry bulb temperature of the nearly saturated air, approaches the ambient air´s wet – bulb temperature. Saturation effectiveness is key factor in determining evaporative cooler performance. The extent to which the leaving air temperature from a direct evaporative cooler approaches the thermodynamic wet – bulb temperature of the entering air defines the direct saturation efficiency ε_e expressed as [5]:

$$\varepsilon_e = 100.\frac{\theta_1 - \theta_2}{\theta_1 - \theta_{em}} \quad (\%)$$

where:

ε_e is a direct evaporative cooling saturation efficiency (%)

θ_1 - dry bulb temperature of entering air (°C)

θ_2 - dry bulb temperature of leaving air (°C)

θ_{em} - wet bulb temperature of entering air (°C)

An efficient wetted pad (with high saturation efficiency) can reduce the air dry-bulb temperature by as much as 95% of the wet – bulb depression (ambient dry – bulb temperature less wet – bulb temperature), although an inefficient and poorly designed pad may only reduce this by 50 % or less.
Although direct evaporative cooling is simple and inexpensive, its cooling effect is insufficient for indoor comfort when the ambient wet – bulb temperature is higher than about 21 °C; however, cooling is still sufficient for relief cooling applications (e.g., greenhouses, industrial cooling). Direct evaporative coolers should not recalculated indoor air; exhaust should equal incoming conditioned air.

[4] Methodology of experimental measurement of direct evaporative cooling in industry hall

The objective of experimental measurement of the inlet and outlet parameters of the indoor air was to determine the efficiency of adiabatic evaporation cooling in the industrial hall. Inside the hall were 5 measuring devices - programmable temperature and relative humidity sensors. Within the building, five measuring points were selected and the *TESTO 175 H1* data loggers were installed [6]. The installation height was about 170 cm - the residence zone. Values were recorded in a time interval every 30 minutes. Deduction of values was done every 7 days during the summer period. For reasons of objectivity, one data logger was mounted on the roof of the object (SSV, azimuth 30 °). When installing an external sensor, it is important to install it so that it is not exposed to direct sunlight. Ideal if protected from external weather effects, which could distort the measured values. Due to the installation in the outdoor environment, IP54 data loggers have been selected. Data from data loggers were processed in the TESTO Comfort Software Basic 5.0 in the form of graphs and spreadsheets in the reference period (1.8.2017 to 19.8.2017).

Outputs from measurements in space were compared with the temperature and humidity in the exterior (*Figure 4 and Figure 5)*. It is important to say that this is a large hall space with a high thermal inertia, where temperature and humidity changes occur with a time interval of 2 - 3 hours. The installation of data loggers in the vicinity of machines or technology with the development of sensible heat can cause some distortion of measurement, slight temperature deviations of 0.5 to 1°C upward. On the basis of the data, it can be estimated that in large hall places where the effect of high thermal inertia can be achieved by adiabatic cooling, the required heat-technical parameters are met and the thermal load can be effectively eliminated.

Adiabatic cooling, however, can´t maintains the exact parameters of the indoor environment without external influences. Cooling power decreases significantly with rising external relative humidity. The open system only works with outdoor air (ODA) in summer operation. For outside air parameters e.g. (ODA 34 °C, 30 % RH), the adiabatic cooler delivers air in the air conditioned room with parameters (23.2 °C, 60 % RH). From a particular measurement it was found that the interior temperature by evaporating cooling installed in the industrial hall was able to drop by 16 °C.

Temperature monitoring of the working environment and functionality has been done by the thermal analysis of individual production lines in the industrial hall. Thermal analysis is used to determine the surface temperature emitted by the thermal radiation component. Thermal infrared radiation measurement is the basis for non-contact temperature measurement. Images show the infrared portion of the spectrum.

Temperature monitoring of the working environment and functionality has been done by the thermal analysis of individual production lines in the industrial hall. Thermal analysis is used to determine the surface temperature emitted by the thermal radiation component. Thermal infrared radiation measurement is the basis for non-contact temperature measurement. Images show the infrared portion of the spectrum.

In the figures shown, it is possible to see and compare that the temperature by adiabatic coolers installed in the industry hall can be reduced to the acceptable temperature in the workers' residence zone. The above findings and results can be stated that the adiabatic cooling is also suitable for industry halls with the intensity of radiation technology to 350 W / m^2.

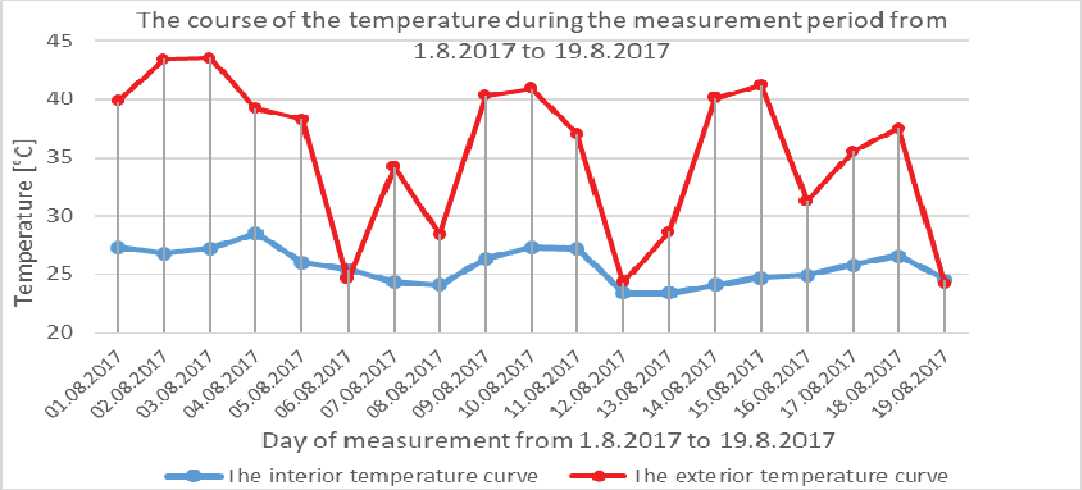

Fig.4 Monitoring chart of outdoor and indoor temperature in industry hall

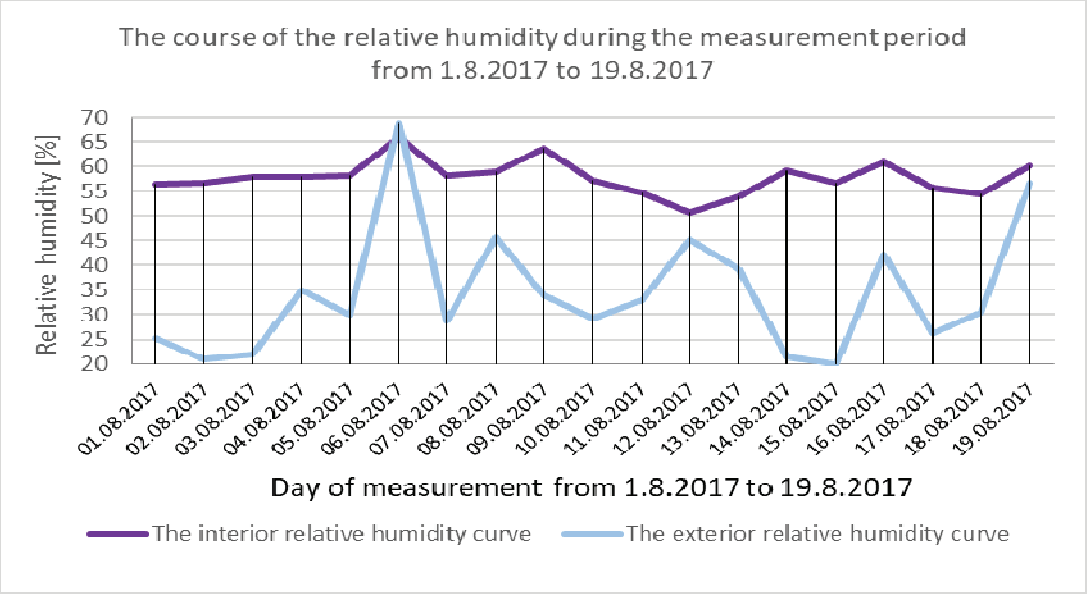

Fig.5. Monitoring chart of outdoor and indoor relative humidity in industry hall.

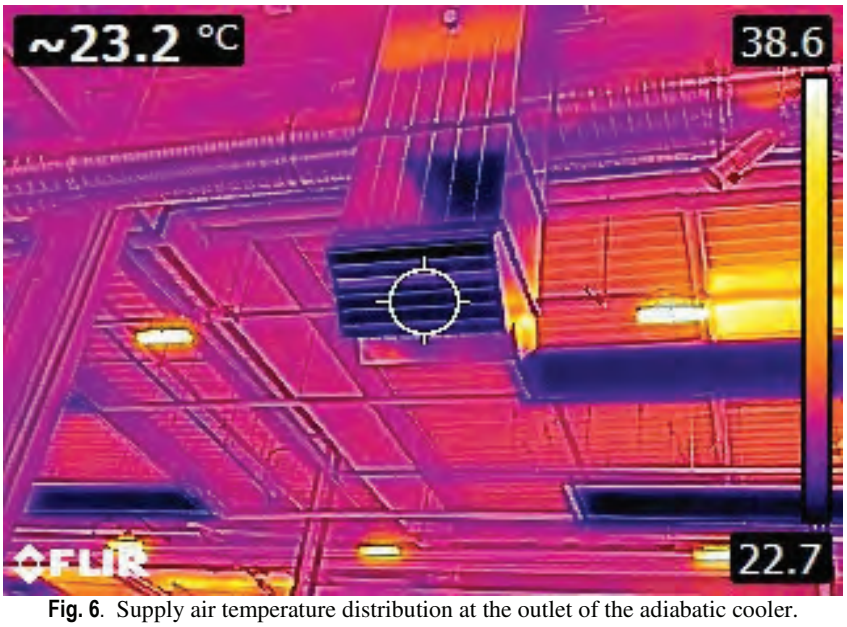

Fig. 6. Supply air temperature distribution at the outlet of the adiabatic cooler.

Fig. 7. Temperature distribution in the residential zone

4. Conclusions

This article presented a methodology and systematic study related to evaporative cooling systems applied to mild climate zone. The methods presented here are useful to evaluate the technical viability of evaporative cooling systems for human thermal comfort. It allows to the correct determination of where and how evaporative cooling systems can be efficiently used. Evaporative cooling systems, although not widely used in middle Europe, have a very large potential to produce thermal comfort and can be an alternative to the conventional systems in regions where the wet – bulb temperature is relatively low. Moreover, it may also be used with conventional systems where only the evaporative system can´t supply all of the needs for comfort. Some possible alternatives are the multistage systems and the adsorption pre-humidifying systems.

The most important data for an engineers or designers, however, when considering evaporative system applications, is updated climatic registers for the specific region in order to find out what can be done with regard to thermal comfort. The methods presented in this paper, although illustrated for evaporative cooling, may also use for other air conditioning systems.

Using water for evaporative as a mean of decreasing air temperature is considerably the most environmentally friendly and effective cooling system. Evaporative cooling differs from common air conditioning and refrigeration technologies in that it can provide effective cooling without the need for an external energy source. If the power consumption can reduce to a moderate level, then it will become serviceable in all sorts of requirements. Evaporative cooling is also important to the development of independent temperature and humidity control air conditioning systems.

Acknowledgment

This work was supported by the Ministry of Education, Science, Research and Sport of the Slovak Republic under VEGA Grant 1/0847/18

References

[1] Ferstl K., Vetranie a klimatizácia priestorov s vyššou produkciou vlhkosti (Ventilation and air conditioning in areas with higher humidity production), SSTP, Bratislava, 2001

[2] Ferstl K., Masaryk M., Prenos tepla (Heat transfer), STU, Bratislava, 2011, ISBN 978-80-227-3534-6

[3] Foster R. E. Dijskstra E. Evaporative air-conditioning fundamentals: Environmental and economic benefits worldwide. Refrigeration Science and Technology Proceedings. International Institute of Refrigeration, Danish Technological Institute, Danish Refrigeration Association, Aarhus, Denmark, pp. 101-110. 1996

[4] Watt J. R., 1963, "Evaporative air conditioning", The Industrial Press, New York., 1963

[5] Koçak S. S. Atmaca I. Doğan, A. The Online Journal of Science and Technology – July 2016, Volume6, Issue 3, pp. 36 – 39. www.tojsat.net

[6] Testo, http://www.testo.sk.

[7] Nyers J., Pek Z., 2014, Mathematical Model of Heat Pumps' Coaxial Evaporator with Distributed Parameters. Acta Polytechnica Hungarica, Vol.11, No.10, pp. 41-54.

[8] Nyers J. (2016), A new analytical method for defining the pump's power optimum of a water-to-water heat pump heating system using COP, Thermal Science, doi: https://doi.org/10.2298/TSCI161110324N.

[9] Kalmár T., Kalmár F. (2010), Comfort and energy analysis of heating up, International Review of Applied Sciences and Engineering, 1-2, 35-43.

[10] Kajtár L., Kassai ., Bánhidi L., Computerized simulation of the energy consumption of air handling units. 2011. Energy and Buildings, ISSN: 0378-7788, (45) pp. 54-59.

[11] Kajtár L., Kassai M., A new calculation method to analyse the energy consumption of air handling units. 4th International Symposium on Exploitation of Renewable Energy Sources: EXPRES 2012. Subotica, Serbia, pp. 10 ISBN:978-8685409-70-7

[12] Szabo J, Kajtar L, Expected thermal comfort in underground Spaces. EXPRES 2016, Subotica, Serbia. pp. 76-80. ISBN:978-86-919769-0-3

EXPRES 2018
ISBN: 978-86-919769-3-4

ECONOMIC ANALYZES AND ENERGETIC EFFICIENCY OF SMALL HYDRO-PLANT

D. GOLUBOVIC [a], *P. KOVAC* [b], *D. JESIC* [c], *B. SAVKOVIC* [b], *D. SARJANOVIC* [d]

[a] Faculty of Mechanical Engineering, University of East Sarajevo
71123 East Sarajevo, Vuka Karadžića 30, Bosnia and Hercegovina
E-mail: dusan.golubovic54@gmail.com
[b] Department for Production Engineering, Faculty of Technical Sciences, University of Novi Sad
21000 Novi Sad, Trg D Obradovica 6, Serbia
E-mail: pkovac@uns.ac.rs, savkovic@uns.ac.rs
[c] International Technology and Management Academy – MTMA,
Trg D.Obradovića 7, 21000 Novi Sad, Serbia
E-mail: dusanjesic@hotmail.com
[d] Sara-Mont. Doo,
11000 Belgrade, Milića Rakić 7, Serbia
E-mail: sarjanovicd@gmail.com

The paper describes the principles of work, types and characteristics of SHP, economic analyze as well as a proposal for improving their energy efficiency by changing the parameters of a small hydropower plant. For the subject of research in this work, SHP in the Republic of Srpska, power of 3 MW, was taken. It was built in 1950 and is constantly in operation. The subject of the research will be economic analyze the change in the technological parameters of SHPs and the construction of a new SHP using the same dam and pipeline. In the end, a comparison of old and new SHPPs will be carried out, and their advantages and disadvantages will be analyzed.

Keywords: *energy efficiency, economic analyze, small hydropower plant*

1. Introduction

The question of energy utilization is a very topical issue. The resources they use are not unproductive but are limited. Therefore mankind is increasingly turning towards renewable sources of energy. Hydro energy or water energy is the most important renewable energy source, and it is also the only one that is economically competitive with fossil fuels and nuclear energy. It has all the advantages of renewable energy, because it is unlimited, clean and cheap in the long run [1, 2].

In this paper, the working principles, types and characteristics of SHPP are described in detail and the proposal for improvement of energy efficiency by changing the parameters of a small hydropower plant [3–5].

For the subject of research in this work, SHPP in the Republic of Srpska, power of 3 MW was taken. It was built in 1950 and is constantly in operation. The subject of the research will be the change of technological data of SHPP and the construction of new SHPP using the same dam and pipeline.

The great advantage of small hydroelectric power plants is that the electricity production price is far below the production price of electricity generated by solar energy, wind energy and other renewable energy sources.

The production price of electricity in small hydropower plants is lower than the production price of conventional power plants, such as fossil fuel or gas fired power plants, nuclear power plants, and the like.

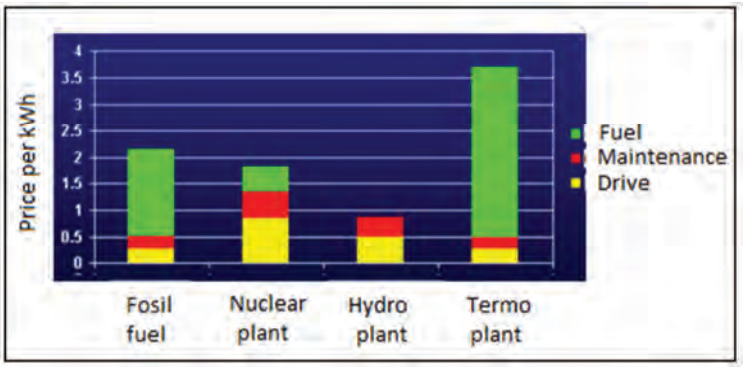

Fig. 1. Comparative overview of the cost of energy production in conventional power plants

2. Material and method

[1]

Taking into account the strength of the total number of awarded concessions: [6]

- 35 are small hydro power plants up to 1 MW
- 24 are power from 1 to 2 MW,
- 36 are power from 2 to 5 MW,
- 5 are power from 5 to 10 MW and
- 6 small hydropower plants with a power exceeding 10 MW.

Figure 2 shows the diagram with the granted concessions according to the power of a small hydropower plant.

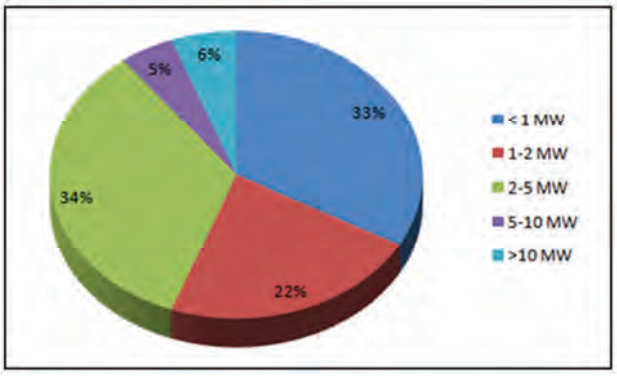

Fig. 2. Overview of the granted concessions by the power of a small hydroelectric power plant [6]

Most of these small hydropower plants are located in poorly populated mountainous areas and are of a derivative type. Although the Government of the Republic of Srpska has given a large number of concessions for the construction of small hydropower plants, so far only few small hydroelectric power plants have been realized, primarily because of:

- Relatively high costs per installed kW,
- Inadequate hydrological data and technical solutions,
- Lack of spatial planning documentation,
- Lack of adequate transmission network,
- Low electricity prices,
- Limited or insufficient participation in government funding,
- There are no domestic equipment manufacturers, most of the necessary equipment is imported (import equipment is about 20% more expensive),
- Complicated administrative procedures and the like.

In order to achieve the realization of these concessions, active participation of the state and Elektroprivreda Republike Srpske is necessary. Difficulties faced by investors can be solved if the following would be done:

- Timely and optimal development of the industry for the construction of equipment and materials for SHPPs that would influence the level of costs and time of construction,
- Development of new and more detailed hydrological and geological studies at the planned locations for SHPPs (municipal services could be done for their areas)
- Each kWh of energy produced should be taken over by the Electric Power Company of RS in the general energy network,
- The conditions for connection of SHPP to the general energy network to be simplified,
- Permits, consents and other awareness to the minimum,
- The planned small hydropower plants, wherever possible, will be multifunctional (water supply, irrigation systems, tourism, fishing, etc.)

3. Results and analysis

Fig. 3. SHPP Mesići dam [7]

Table 1. Basic technical and energy characteristics of SHPP Mesići-Nova [8]

Parameter	**Units**	**Size**
Mean annual intake of inflow	(m^3/s)	7,63
Eco-friendly flow	(m^3/s)	0,53
Upper water level of the plant	(mnm)	530,00
Bottom level of the of the plant	(mnm)	476,89
Instaliran protok:		
Aggregate 1	(m^3/s)	4,00
Aggregate 2	(m^3/s)	4,00
Aggregate 3	(m^3/s)	4,00
Plant	**(m^3/s)**	**12,00**
Number and type of aggregate		3,Francis
Gross plant drop	(m)	52.311
Losses fall for installed flow	(m)	4,85
Net plant drop	(m)	47,46
Installed flow:		
Aggregate 1	(kW)	1,633,33
Aggregate 2	(kW)	1,633,33
Aggregate 3	(kW)	1,633,33
Plant	**(kW)**	**4,900**
Possible plant production	**(kWh)**	**23.958.986**
Investment	**(KM)**	**8.990.000**

Table 2. Structure of total investments of SHPP Mesići-Nova

No	Item	Amount (KM)
I	Construction works	
A	Preparatory works	15,000
B	Main Construction works	
01.	Dam and entrance building - Machine plant	25.000
02.	Inlet tunnel	2.890.000
03.	Pressure pipeline	300.000
04.	Machine plant	300.000
Total main construction works:	3.515.000	
C	Unspecified works	105.000
Total construction works (A + B + C)	**3.635.000**	
II	Equipment	
01.	Electromechanical equipment	5.085.000
02.	Hydromechanical Equipment	90.000
Equipmenttotal:	**5.175.000**	
III	Founding investment	
01.	Design and design control	130.000
02.	Costs of the investor	50.000
Total Founding Investment:	180.000	
Total investments (I + II + III)	**8.990.000**	

Table 3. Calculation of fixed operating costs of HPP Mesići-Nova [9]

Item	Investment	Costs maintenance	Insurance costs	Other Costs	Total costs
Rate Total Costs		Rate Total Costs		Rate Total Costs	
(KM)	**(KM)**	**(KM)**	**(KM)**	**(KM)**	**(KM)**
Construction works	3.635.000	0,50% 18.175	0,10% 3.635	0.10% 3.635	25.445
EMO	5.085.000	1.30% 66.105	0,50% 25.425	0.10% 5.085	96.615
HMO	90.000	1.30% 1.170	0,50% 450	0.10% 90	1.710
Total	**8.810.000**	85.450	**29.510**	**8.810**	**123.770**

Figure 4 gives comparative graphical data of average production by months from 1950 to 2015 at SHPP Mesici and production at SHPP Mesići in 2016.

From the diagram in Figure 5 it can be seen that the production in 2016 of the Mesići-Nova SHPP is around 8000 kWh higher than the average annual production at SHPP Mesići.

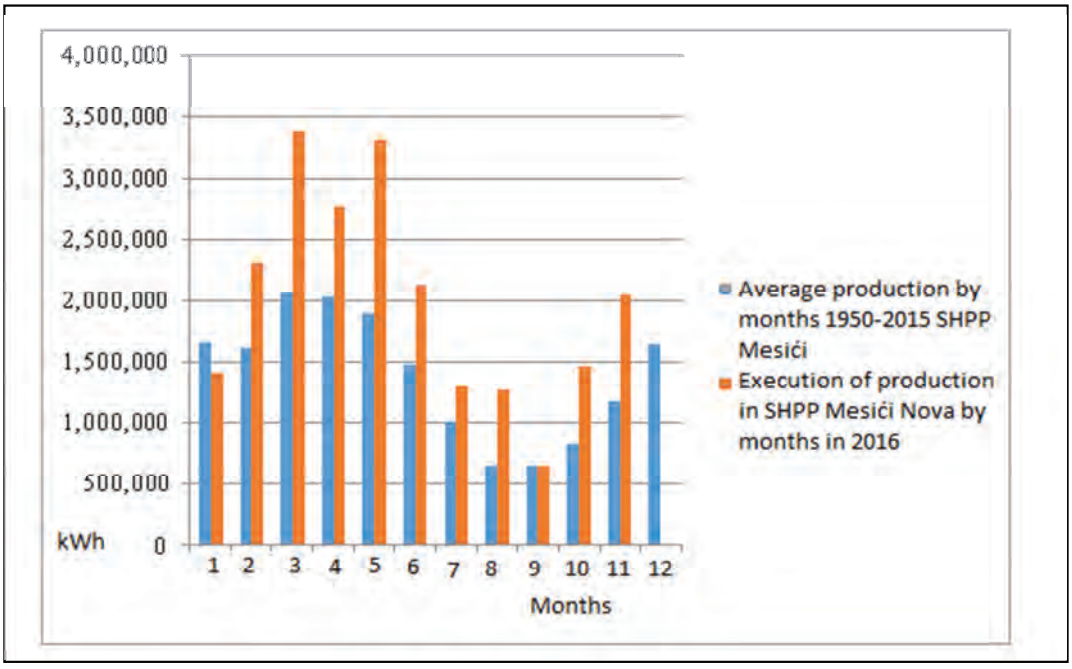

Fig. 4. Comparison of average production by months from 1950 to 2015 at SHPP Mesići and production at SHPP Mesići Nova in 2016, [9]

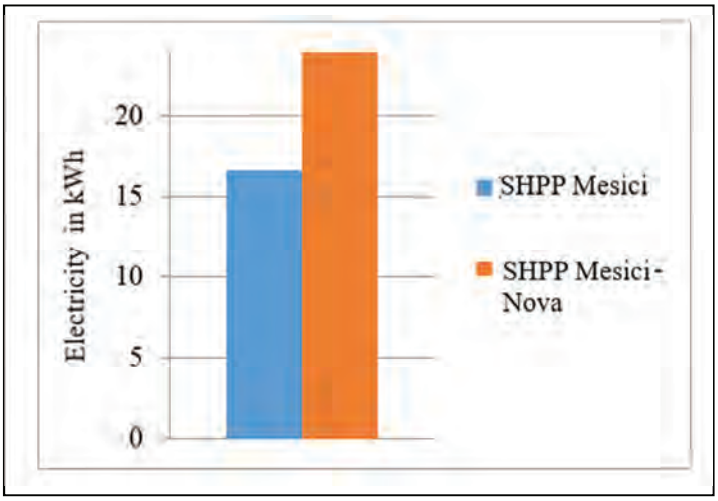

Fig. 5. Comparison of average annual production of electricity on SHPP Mesići and SHPP Mesići-Nova [9]

4. Conclusions

SHP equipment in BiH is mostly older, with lesser characteristics compared to new technical solutions. Also, the lifetime of the equipment in some SHPPs is nearing completion, so replacement or reconstruction is necessary. In these cases, the possibility of changing the technological parameters of SHPPs is often analyzed in order to revitalize and change the power of SHPP.

Changing technological data and technical characteristics of the equipment caused an increase in electricity production and improved energy efficiency.

This means that in our conditions it is possible to modernize the plant in accordance with the modern world plant. In this way, it will surely increase energy efficiency, total electricity production, process automation and reduce the harmful impact on the environment.

Comprehensive analysis brings new knowledge for use in similar plants. Based on the trend of growth in the use of renewable energy sources, a more intensive construction of SHPPs can be expected.

Acknowledgement

Results are part of bilateral project SRB-SK and project TR 35015.

References

[1] Labudović: Obnovljivi izvori energije, Energija vodenih tokova, Zagreb, 2002.
[2] Kovač P, Palkova Z.: Proizvodno mašinstvo i obnovljivi izvori energije
[3] Gojković,V.: Tehničko rješenje male hidroelektrane u Republici Srpskoj, Master rad, Mašinski fakultet Istočno Sarajevo, 2014.
[4] Djurić , B. Ilić, V. Male hidroelektrane, ETA Beograd, 2013.
[5] Milojević, A.: Male hidroelektrane, javno ili privatno dobro, 2007.
[6] Enkos: Studija mogućnosti ekonomkse opravdanosti hidroenergetskog potencijala korišćenja prelivnih voda HE Mesići, Sarajevo, 2010.
[7] Institut za građevinarstvo „IG“: HE „Mesići-Nova“, glavni projekat, oprema hidroelektrane, mašinska oprema, Trebinje, 2014.
[8] Enkos: Studija ekonomske opravdanosti izgradnje HE „Mesići Nova”,Sarajevo, 2014.
[9] Mješoviti Holding „ERS“ MP a.d. Trebinje, ZP „ELEKTRODISTRIBUCIJA“ a.d. Pale, HE Mesić.
[10] Nyers J., Pek Z., 2014, Mathematical Model of Heat Pumps' Coaxial Evaporator with Distributed Parameters. Acta Polytechnica Hungarica, Vol.11, No.10, pp. 41-54.
[11] Odry A., Kecskés I., Burku E., Odry, P., 2017, Protective Fuzzy Control of a Two-Wheeled Mobile Pendulum Robot: Design and Optimization, WSEAS transactions on systems and control 12:(#32) pp. 297-306.
[12] Nyers J.: "COP and Economic Analysis of the Heat Recovery from Waste Water using Heat Pumps".International J. Acta Polytechnica Hungarica Vol. 13, No. 5, 2016, pp. 135-154. DOI:10.12700/APH.13.5.2016.5.8.

EXPRES 2018
ISBN: 978-86-919769-3-4

COMPARISON OF A CONICAL AND A SPIRAL ABSORBER FOR A SOLAR DISH COLLECTOR

S. PAVLOVIC[a], E. BELLOS[b], V. STEFANOVIC[a], C. TZIVANIDIS[b]

[a]Faculty of Mechanical Engineering, Department of Energetics and Process technique, University in Niš, Nis, Serbia
[b]Thermal Department, School of Mechanical Engineering, National Technical University of Athens, Zografou, Heroon Polytechniou 9, 15780 Athens, Greece.
Corresponding author: Sasa R. Pavlovic (saledoca@gmail.com)

The objective of this paper is to compare two different absorbers for a solar dish collector. The conical and the spiral absorbers are compared thermally performing a computational fluid dynamics study with SolidWorks Flow Simulation. The existing installation has a spiral absorber cavity and the goal is to investigate if the use of another conical cavity would increase the system performance. The first step of this work is the validation of the developed methodology for the spiral absorber, using experimental results. The next step is the examination of the conical absorber with the simulation tool in order to determine its performance. The analysis is performed with water as working fluid for inlet temperatures up to 85°C. According to the final results, the conical absorber leads close to 7.5% higher thermal efficiency due to the increase in the optical performance. For inlet temperature of 50°C for instance, the thermal efficiency of the spiral absorber is 32.38% while it is 34.93% for the conical absorber. The enhancement in the exergy efficiency is higher and it is about 11%. These results clearly indicate that the conical design is beneficial compared to the existing spiral design.

Keywords: Conical absorber, Spiral absorber, Thermal analysis, Optical analysis, Solar Dish collector

1. Introduction

Solar energy utilization is vital for reducing the fossil fuel consumption and to face important environmental problems. Concentrating solar collectors are able to produce high amounts of thermal energy at various temperatures up to 500°C. The most usual concentrating technologies are parabolic trough collectors, linear Fresnel reflectors, solar towers and solar dishes. Among these concentrating technologies, solar dishes are a technology which evolves with high speed and a lot of research has been focused on it. The last years, a lot of research has been focused on the optimization of the solar dish receivers. Various shapes have been tested as cylindrical, conical, spherical, hemispherical and spiral have been examined as possible configurations of the solar dish absorbers. Loni et al. [1] examined a cylindrical cavity absorber and they optimize it by determining the optimum opening diameter. Moreover, Loni et al. [2] have examined a prismatic cavity receiver. Shuai et al. [3-4] compared cylindrical, dome, heteroconical, elliptical, conical and spherical absorbers. Finally, they found that the spherical receiver has the most uniform heat flux distribution. Daabo et al. [5-6] stated the conical absorber is a better design than the cylindrical and the spherical configurations.

The use of a spiral absorber has been investigated by Pavlovic et al. [7-10] experimentally and numerically. They examined this system optically, thermally and exergetically and they determine that the optimum operating conditions are for temperature levels close to 150°C. Moreover, they indicated that the present design presents low optical efficiency. The objective of the present work is to examine the conical absorber with the reflector of the previous studies [7-10] in order higher optical and thermal efficiency to be achieved. The conical design is a promising solution according to refs [5-6]. In the present study, a numerical analysis is performed with SolidWorks Flow Simulation for both spiral and conical design. The developed model is validated with experimental results for the spiral design. The final results can be used for evaluating the idea of using a conical design in the solar dish system of refs [7-10].

2. Material and methods

The physical model of the solar dish collector with spiral absorber is depicted in figure 1. Figure 2 shows the designed models with spiral and conical absorber in SolidWorks. For more information about the examined collector, refs [7-10] can be used.

Fig. 1. The Physical model of the solar collector with spiral absorber

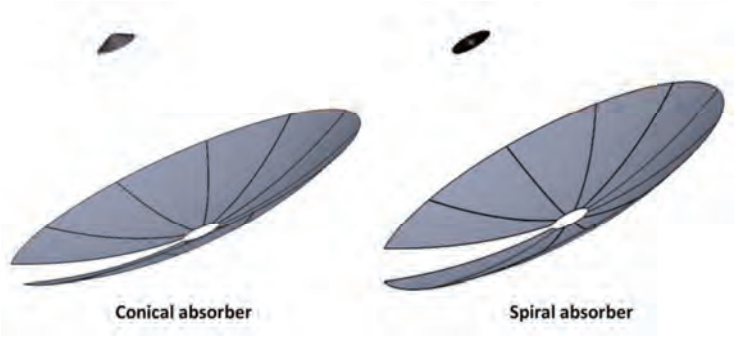

Fig. 2. The two examined solar dish collectors designed in SolidWorks

It is essential to state that the designed conical model has the same opening as the spiral coil (400 mm), while its height is about 25 mm. Below, some important mathematical equations about the examined system are given. The solar beam energy is calculated as the product of the dish aperture (A_a) and the solar beam radiation (G_b):

$$Q_s = A_a \cdot G_b, \quad (1)$$

The useful energy production (Q_u) is given as:

$$Q_u = m \cdot c_p \cdot \left(T_{out} - T_{in}\right), \quad (2)$$

The thermal efficiency of the collector (η_{th}) is calculated as:

$$\eta_{th} = \frac{Q_u}{Q_s}, \quad (3)$$

The useful exergy production is calculated as [7]:

$$E_u = Q_u - m \cdot c_p \cdot T_{am} \cdot \ln\left[\frac{T_{out}}{T_{in}}\right], \quad (4)$$

The exergy of the solar radiation is calculated by the Petela model, as below [7]:

$$E_s = Q_s \cdot \left[1 - \frac{4}{3} \cdot \left(\frac{T_{am}}{T_{sun}}\right) + \frac{1}{3} \cdot \left(\frac{T_{am}}{T_{sun}}\right)^4\right] \quad (5)$$

The sun temperature (T_{sun}) can be taken equal to 5770K. The exergy efficiency is calculated as:

$$\eta_{ex} = \frac{E_u}{E_s} \quad (6)$$

The mass flow rate (m), the specific heat capacity (c_p), the inlet temperature (T_{in}), the outlet temperature (T_{out}), the ambient temperature (T_{am}) are used in the previous calculations.

At the end of this subsection, it is important to state that the simulation at SolidWorks has been performed by developing a model in this program. The optical and the thermal analysis have been performed simultaneously with this tool. Moreover, the mesh has been created by this program. The proper boundary conditions, radiative surfaces and materials have been inserted in this model. More details about this methodology can be found in the Refs [9-14].

3. Results

The results of this work are summarized below. The first step is the validation of the developed model with spiral absorber using the experimental results which have been presented in Ref [7]. Table 1 proves that the mean deviation in the outlet temperature is 0.9% and it is 4.1% in the thermal efficiency. These small deviation values prove that the developed model in SolidWorks is accurate enough to be used.

Table 1. Validation results for the spiral absorber case

Measured parameters				Experimental		Spiral		Deviation	
Time	V	T_{in}	T_{out}	T_{out}	η_{th}	T_{out}	n_{th}	T_{out}	η_{th}
(hr)	(l/h)	(^oC)	(^oC)	(^oC)	-	(^oC)	-	-	-
10:15	194	33.22	830	44.87	0.3073	45.92	0.3350	2.34%	9.01%
10:30	194	34.63	840	47.53	0.3362	47.46	0.3344	0.15%	0.54%
10:45	195	35.13	845	47.72	0.3278	47.97	0.3343	0.52%	1.99%
11:00	198	36.00	848	48.98	0.3420	48.67	0.3338	0.63%	2.39%
11:15	197	36.51	850	49.54	0.3408	49.28	0.3340	0.52%	2.00%
11:30	201	36.85	849	49.56	0.3395	49.34	0.3336	0.44%	1.73%
11:45	201	37.79	858	50.03	0.3236	50.40	0.3334	0.74%	3.02%
12:00	194	38.61	862	51.21	0.3200	51.71	0.3327	0.98%	3.97%
12:15	190	39.24	865	52.49	0.3284	52.65	0.3324	0.30%	1.21%
12:30	195	39.80	869	52.51	0.3218	52.94	0.3327	0.82%	3.38%
12:45	190	40.06	871	53.47	0.3301	53.57	0.3326	0.19%	0.75%
13:00	194	40.88	873	53.37	0.3132	54.13	0.3323	1.42%	6.08%
13:15	194	41.31	876	54.34	0.3256	54.06	0.3321	0.48%	2.00%
13:30	194	41.78	865	55.02	0.3351	54.89	0.3318	0.24%	0.98%
13:45	194	41.78	857	54.87	0.3344	54.77	0.3318	0.18%	0.76%
14:00	194	42.05	859	55.18	0.3346	55.07	0.3318	0.20%	0.84%
14:15	194	42.37	855	55.91	0.3467	55.32	0.3316	1.06%	4.36%
14:30	194	43.61	845	56.11	0.3238	55.39	0.3051	1.28%	5.76%
14:45	197	44.43	846	56.52	0.3177	57.02	0.3308	0.88%	4.14%
15:00	197	44.77	839	55.66	0.2885	57.24	0.3304	2.84%	14.51%
15:15	194	45.71	830	56.46	0.2835	58.23	0.33018	3.13%	16.47%

In the following analysis, the collectors are examined only numerically. The solar beam irradiation is 850 W/m^2, the ambient temperature 27^oC and the inlet temperature is examined parametrically. Figure 3 gives the thermal efficiency for different flow rates and inlet temperature equal to 50^oC. This figure clearly indicates that the conical design leads to higher thermal efficiency. Moreover, the flow rate has a small impact on the results. The value of 200 l/h s selected as one reliable choice which leads to high values of the thermal; efficiency for both systems.

Figure 4 depicts the thermal efficiency curves of the collector. It is obvious that the thermal efficiency is about 7.5% higher with the conical absorber. This increase is explained by the optical enhancement with the new absorber. Below, the thermal efficiency equations for both collectors are given.

$$\eta_{th}[Conical] = 0.3603 - 0.4244 \cdot \frac{T_{in} - T_{am}}{G_b} \quad (7)$$

$$\eta_{th}[Spiral] = 0.3345 - 0.4272 \cdot \frac{T_{in} - T_{am}}{G_b} \quad (8)$$

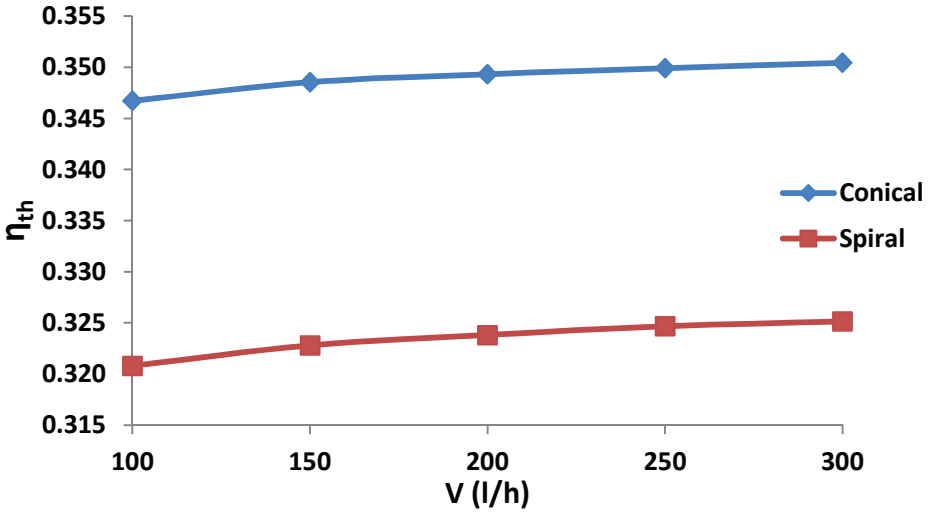

Fig. 3. The impact of the flow rate on the collector performance (spiral and conical cases) for inlet temperature equal to 50°C.

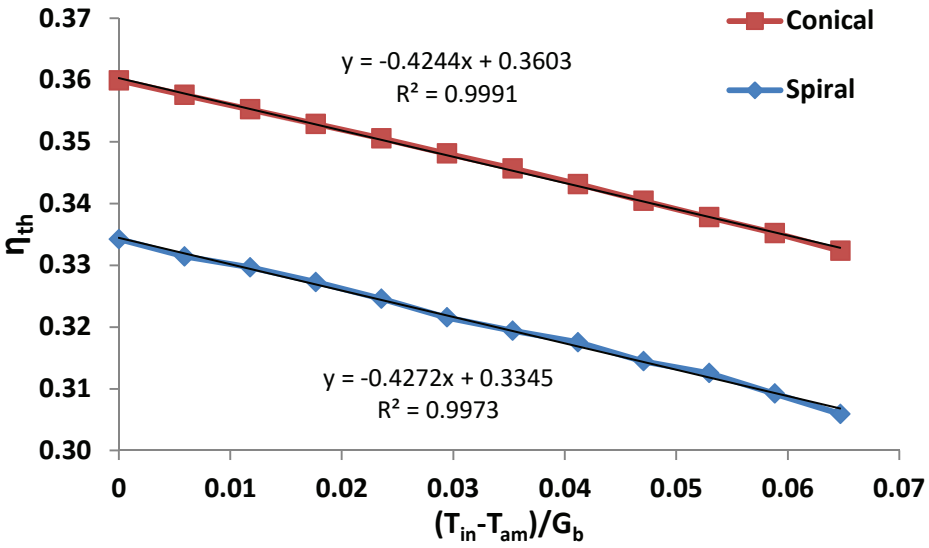

Fig. 4. Thermal efficiency curves for the tow examined cases

The exergy efficiency is enhanced with the conical absorber, according to figure 5. The mean exergy enhancement is about 11%, a high value which indicates again the conical design as the proper one. Figure 6 gives the absorber temperature for both cases when the inlet temperature is 30oC. It is obvious that the conical design is warner at the end, a result which is explained by the higher solar irradiation absorbance. This result shows that higher amounts of solar energy are cached at the end of the conical absorber.

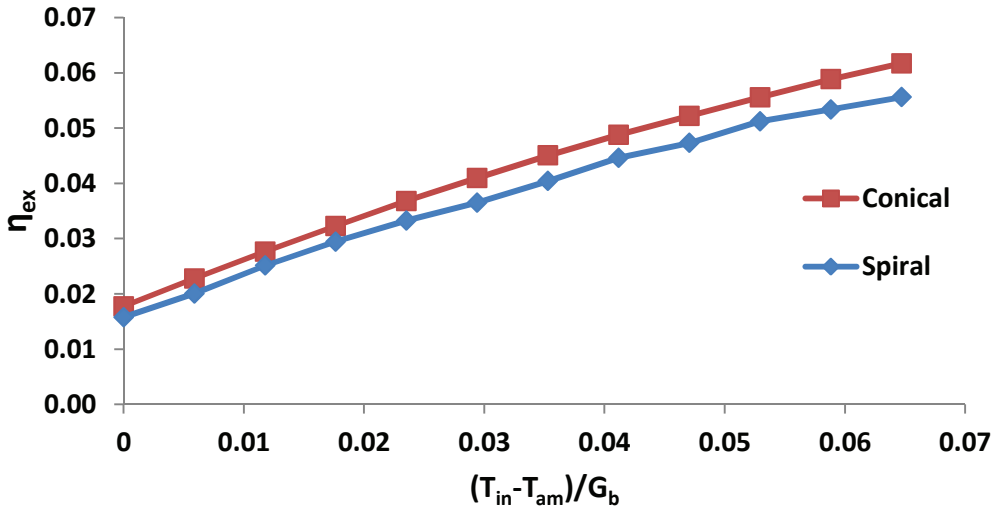

Fig. 5. Exergy efficiency curves for the tow examined cases

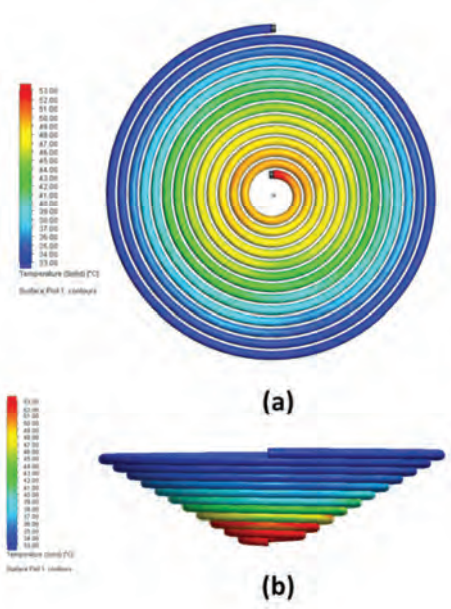

Fig. 6. Absorber temperature for inlet temperature equal to 30°C a) Spiral absorber b) Conical absorber

4. Conclusions

The objective of this work is to investigate the use of a conical absorber in a solar dish collector. The present design has a spiral absorber and this design has been examined experimentally and numerically under various conditions in refs [7-10]. The present comparison between the conical and the spiral absorber proved that the conical design leads to higher performance. More specifically, the conical design leads to 7.5% higher thermal efficiency and to 11% higher exergy efficiency. The main reason for these results is the increase in the optical efficiency of the conical configuration. In the future, the conical design can be examined experimentally in the present system, as well as more designs as cylindrical and spherical can be also tested.

References

[1] R. Loni, A.B. Kasaeian, E. Askari Asli-Ardeh, B. Ghobadian, Optimizing the efficiency of a solar receiver with tubular cylindrical cavity for a solar-powered organic Rankine cycle, Energy 2016;112:1259-1272

[2] R. Loni, A.B. Kasaeian, E. Askari Asli-Ardeh, B. Ghobadian, W.G. Le Roux, Performance study of a solar-assisted organic Rankine cycle using a dish-mounted rectangular-cavity tubular solar receiver, Applied Thermal Engineering 2016;108:1298-1309

[3] Y. Shuai, X.-L. Xia, H.-P. Tan, Radiation performance of dish solar concentrator/cavity receiver systems, Solar Energy 2008;82(1):13-21

[4] Y. Shuai, X. Xia, H. Tan, Numerical simulation and experiment research of radiation performance in a dish solar collector system, Front. Energy Power Eng. China 2010;4(4):488-495 (DOI 10.1007/s11708-010-0007-z)

[5] A.M. Daabo, S. Mahmoud, R.K. Al-Dadah, The effect of receiver geometry on the optical performance of a small-scale solar cavity receiver for parabolic dish applications, Energy 2016;114:513-525

[6] A.M. Daabo, S. Mahmoud, R.K. Al-Dadah, The optical efficiency of three different geometries of a small scale cavity receiver for concentrated solar applications, Applied Energy 2016;179:1081-1096

[7] S. Pavlovic, E. Bellos, W.G. Le Roux, V. Stefanovic, C. Tzivanidis, Experimental investigation and parametric analysis of a solar thermal dish collector with spiral absorber, Applied Thermal Engineering 2017;121:126-135

[8] S. Pavlovic, A.M. Daabo, E. Bellos, V. Stefanovic, S. Mahmoud, R.K. Al-Dadah, Experimental and numerical investigation on the optical and thermal performance of solar parabolic dish and corrugated spiral cavity receiver, Journal of Cleaner Production 2017;150:75-92

[9] S. Pavlovic, E. Bellos, R. Loni, Exergetic investigation of a solar dish collector with smooth and corrugated spiral absorber operating with various nanofluids, Journal of Cleaner Production, 2017, (https://doi.org/10.1016/j.jclepro.2017.11.004)

[10] S.R. Pavlović, E. Bellos, V.P. Stefanović, C. Tzivanidis, Z.M. Stamenković, Design, simulation and optimization of a solar dish collector spiral-coil thermal absorber, Thermal science 2016;20(4):1387-1397

[11] E. Bellos, C. Tzivanidis, D. Tsimpoukis, Multi-criteria evaluation of parabolic trough collector with internally finned absorbers, Applied Energy 2017;205:540-561

[12] E. Bellos, C. Tzivanidis, D. Tsimpoukis, Thermal enhancement of parabolic trough collector with internally finned absorbers, Solar Energy 2017;157C:514-531

[13] E. Bellos, D. Korres, C. Tzivanidis, K.A. Antonopoulos, Design, simulation and optimization of a compound parabolic collector, Sustainable Energy Technologies and Assessments 2016;16:53-63

[14] Nyers J., Kajtar L., Slavica T., Nyers, A. (2014) Investment-savings Method for Energy-economic Optimization of External Wall Thermal Insulation Thickness, Energy and Buildings, 86, 268-274.

EXPRES 2018
ISBN: 978-86-919769-3-4

ANNUAL ENERGY CONSUMPTION ANALYSIS INFLUENCED BY THE USER HABITS IN DIFFERENT CLIMATE ZONES IN TURKEY

[a]T. CSOKNYAI, [a]U. KINAY

[a]Budapest University of Technology and Economics,
The Department of Building Service and Process Engineering,
csoknyaitamas@gmail.com,
uygurkinay@gmail.com

This article aims to identify and gain an understanding of the effect of occupants' energy consumption behaviour. Design engineers calculate the building loads taking into account the requirements specified in the standards. The operating conditions of the same type of buildings in different climate regions can be different and it is influenced by other factors such as the users' habits. The comfort conditions maintained by the users is often different from what was considered during design phase. On one hand, the economic income level (energy poverty) is one driving factor to influence comfort conditions that they can afford and on the other hand, awareness of energy efficiency and climate change-aims can have a significant impact as well.

For the analysis of the effect of actual users' behaviour on annual heating and cooling energy consumption in kWh/m^{2}year, a typical detached house is modelled in different climatic regions. Scenarios created with different user habits are modelled in TRNSYS software.

Keywords: Energy simulation, User habits, TRNSYS, Single family house

1. Introduction

Buildings have the greatest potential for climate change mitigation. For this reason, the European Union is preparing the necessary actions and directives to improve energy efficiency in buildings. The largest energy saving potential is in existing buildings, but on long term new buildings built according to NZEB requirements integrating renewable energy sources will also take a role. The energy consumption is strongly influenced by occupant behaviour, which is a factor often underestimated.

Turkey has different climate zones and different user habits. Since 2000, legislations and standards are continuously improved for new buildings in Turkey following the improvements carried out in EU member states. First, revision of the Thermal Insulation Requirements for Buildings Standard (TS 825) was finalized in April 1998 and latest revisions on TS 825 were done in May-2008 issued by the Turkish Standards Institute. Under this standard the country is divided into four climatic zones on heating degree day's basis. The HDD and CDD values for different temperature is shown at table 1.

Table 1 Heating and cooling degree day for Ankara and Izmir[i]

	Heating degree days			Cooling degree days		
	14^{0}C	16^{0}C	18^{0}C	22^{0}C	24^{0}C	26^{0}C
Ankara	1773	2199	2677	109	37	8
Izmir	562	845	1188	559	319	147

The degree day regions (DDR) can be seen in Fig 1.

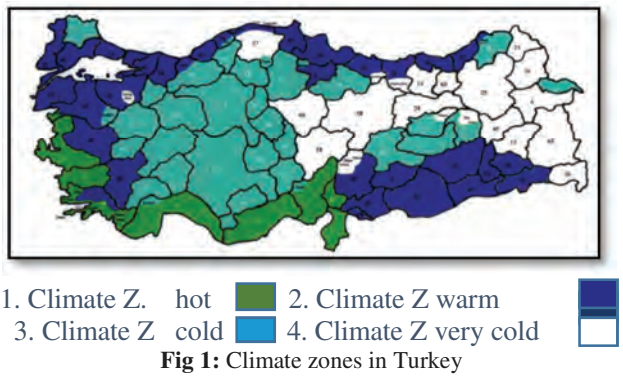

Fig 1: Climate zones in Turkey

In parallel to the introduction of the EPBD[ii] (2002 and 2010 recast) in European Union member states, the

Energy Efficiency Law[iii] has been put in force on 2 May 2007 in Turkey followed by the "Building Energy Performance Regulation" [iv](BEPY) on 5 December 2008 with related National Calculation Methodology[v] and tool (BEP-TR).

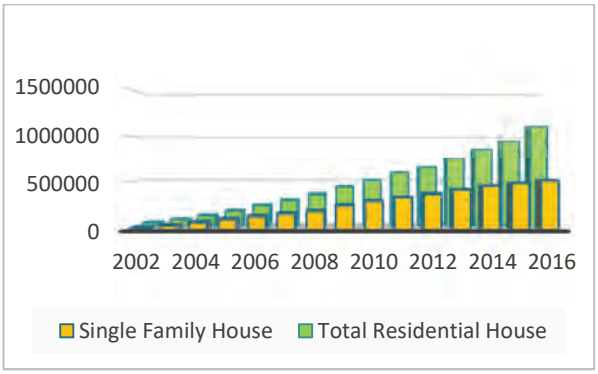

Fig. 2 Cumulative building usage permits

In existing buildings, the occupants according to both age group and employment situation have different heating and cooling needs. Partial and intermittent heating and cooling is rather general resulting in a big difference between design and real actual energy consumption. In order to model the consequences of such consumption habits, a reference single family house with individual heating and cooling system has been selected and analysed. The reference house was selected so that it should reflect the average properties of Turkish single-family houses: the average square meter area is calculated on the basis of building use permit data published by the Statistical Institute of Turkey[vi] during the period 2002-2016 and the outputs of Instrument of Pre-accession Assistance project (IPA).

The weighted average area is calculated as 160 m^2 using The Turkish Statistical Institute's (TUIK) data. The defined single-family reference house is a two-storey building with 160 m^2 floor area in two variations: with and without an unheated basement area. According to questionnaire results of the IPA project, majority of the family houses do not have a basement (out of 167 houses 112 does not have a basement). But it is considered important to have a variation of the family house with basement. Facade material is composed of brickwork and outer walls with thermal insulation except for climate zone 1. The building is equipped with double-glazed windows with plastic frame and sloped roof, except for climate zone 1, where single-glazed window and flat roof applications are wide-spread.[vii]

The current situation of building sector has also been reviewed taking year 2000 as a baseline. The reason for selecting this year is related to the facts that the Building Heat Insulation Regulation incorporating TS 825 standard became mandatory in June 2000.

2. Definition of the reference single family house and its simplified model

Two storey detached house, kitchen, living room, hall and toilet are on the first floor and two bedrooms and bathroom are on the second floor. The single-family house model total area is assumed to be 160 m^2 on the basis of TUIK[viii] and IPA Project output. The three-dimensional model is created with using Google Sketch up. The two-dimensional model building is also established through the TRN-Build software. In Trnsys predefined components can be used to simplify the modelling.

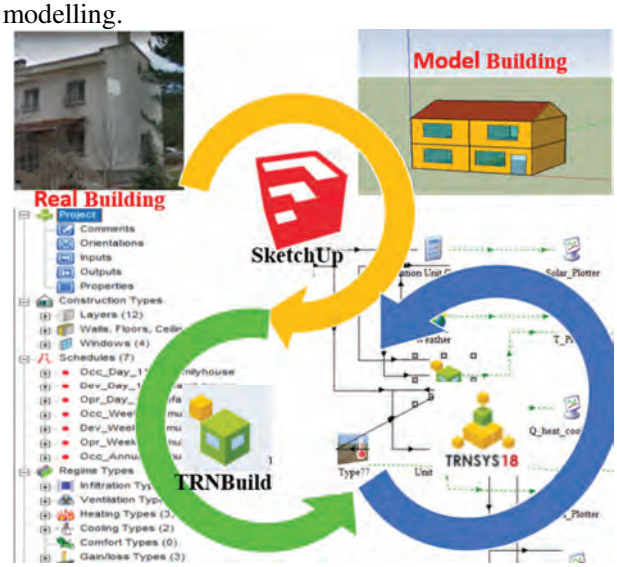

Fig. 3 Simulation steps

In our simulation component type 56 was used. Type 56 describes a building with multiple thermal zones, i.e. rooms. Each room has a homogenous room air temperature. Heat gains (loads) from solar direct and diffuse radiation is calculated for each room depending on window and heat transfer properties.[ix] The multizone single family house is divided into 4 zones and airnodes. (an airnode is an area of the building that can be characterized by a single air temperature.)

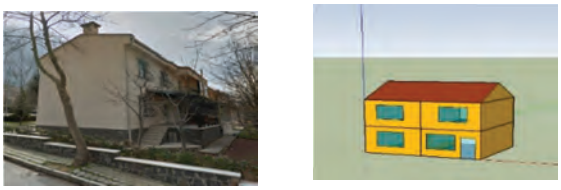

Fig. 4: Real house and Simulated model house

The model building zones are named Zone 1 Kitchen, Zone 2 living room, Zone 3 bedroom1, Zone 4 bedroom2. Every zone has same floor area which is 40 m^2 and window ratio which is 15% percent. Trnsys software zone can include more than one airnode depending on the structure of zone such as atrium.

3. Simulated model construction properties

The U-values of the simulated model are determined by recommended U-values at the TS 825 standard for the climate region. A data entry example is shown in figure 4. Building materials can be created with the materials of the TRNSYS Library; or on the other hand, the user can create his / her library by identifying his / her own materials. Note that the thermal conductivity of the materials must be entered in kJ / hmK, the thermal conductivity value is given in kW / mK on the tables.

Ankara is located in 3th climate zone and Izmir is located in first climate zone; the recommended U-values in the TS 825 standard are shown in the table below.

Table 4 Suggested U-values for climate zones

Cities	Climate Zone	U_{wall} W/m^2 K	U_{roof} W/m^2 K	U_{ground} W/m^2 K	$U_{win.}$ W/m^2 K
Izmir	1.	0,70	0,45	0,70	2,4
	2.	0,60	0,40	0,60	2,4
Ankara	3.	0,50	0,30	0,45	2,4
	4.	0,40	0,25	0,40	2,4

The building layers according to table 4 are defined in the software; U-values have been adapted by changing the insulation thickness for Izmir.

4. Weather data

The model building was simulated within a weather pattern dictated by TMY2. The location and weather data were imported from the Meteonorm database, Europe Region[x] separately identified in Meteonorm by "Switzerland"[xi], and the output format is TMY2. The location of building in Ankara; latitude 39,95^0 N, longitude 32,883^0 E altitude 902m, climatic zone 3, solar radiation data period 2004-2010. The location of building in Izmir, latitude 38,433^0 N longitude 27,167^0 E altitude 25m, climatic zone 1, using solar radiation data period: 2005-2013 (interpolating). The heating season is between September 15 and May 1 for both locations used in the calculation.

5. Schedules

Trnsys software allows to define time schedules which can be used for calculating internal gains from people, electrical devices and also manage mechanical systems.

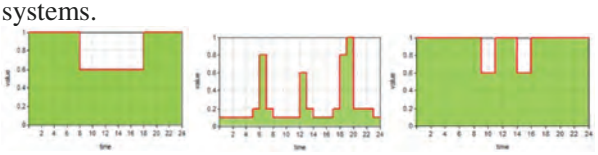

Fig.5 Occupancy Electric Operative daily schedule

Schedules were set to express typical Turkish residential habits. Daylight control was chosen and adjusted with illuminance set points, which is the set point 1 500 lux lighting is off and the set point 2 300 lux lighting is on. Weekly and annual schedules are defined with daily schedules given Fig.5 as an example. Occupancy schedule was used for calculating internal gains from people, device schedule was used for electrical devices gains and operative schedule was used for lightening gains. Weekends are defined as occupied and operated all day (Figure 6).

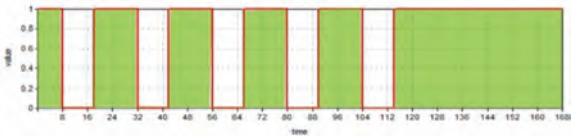

Fig.6 Weekly occupied schedule for scenario 3.

These daily and weekly charts are used for calculating internal gains and for partial heating and cooling scenarios. The heating season is restricted in accordance with the actual application. Some days in summer the need for heating occurs, but since the heating system is not working, only the heating season is considered (figure 7).

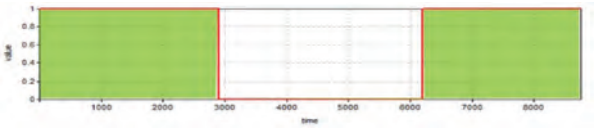

Fig.7 Heating season period.

6. Determination of heating and cooling loads

Simulations were conducted in order to determine the effect of various changes to the building operation on total annual energy consumption since the final objective is to simulate the occupant habits. For the heating and cooling season, the air change rate in the model was estimated 0.8 1/h according to TS 825 Thermal Insulation Requirements Standard[xii]. The annual heating and cooling demands were investigated by below scenarios;

Scenario 1: All zones were heated and cooled (design scenario) in this scenario the single house model fully heated and cooled. Heating set temperature is 24^{0}C and cooling set point 26^{0}C for all zones except

loft. Roof space which means between exterior roof and adjacent ceiling is accepted unconditioned area for all scenarios.

Scenario 2: **All zones were just heated (design scenario without cooling)** it was simulated only for heating loads. Without cooling load, the change in heating energy is observed.

Scenario 3: All zones were adjusted with the periodic heating and cooling time schedule (intermittent operation scenario). This scenario was aimed to explore occupant'sbehaviour. The people who live in single family house have full time employed and they operate the mechanical system at the setback point during unoccupied hours. Assuming occupants leave the home between 8:00 AM and 6:00 PM for a 9:00 to 5:00 work schedule, at occupied hours the system is operated at temperature 24 ° C for heating and 26 ° C for cooling. At unoccupied hours the heating setback point is 15 ° C and cooling is off.

Scenario 4: The first floor (kitchen and living room zones) was heated to comfort conditions and the second floor (bedroom1 and bedroom2 zones) was heated and cooled with the setback temperature. To save on energy consumption, partial heating and cooling scenario is applied whereby, kitchen and living room on the first floor is kept at 24 ° C and bedrooms on the upper floor are set at 15 ° C degrees for heating and at 26 ° C &28 ° C respectively for cooling

Scenario 5: The first floor (kitchen and living room zones) was heated to comfort conditions and the second floor (bedroom1 and bedroom2 zones) was unconditioned (real use scenario). This scenario aims at modelling the real case operation habits. The first-floor zones are kitchen and living room. The second-floor zones are bedroom1 and bedroom2. The user using first floor and the second floor is unconditioned during heating and cooling seasons.

7. Results and discussion

The building converted from the real building to the Trnsys model was simulated in accordance with the scenarios specified in the before section. Ankara is located in the 3rd climatic zone; Izmir is located in the 1st climatic region. Trnsys hourly simulation results using with the Meteonorm climate are below.

Fig. 8 Summary of Ankara

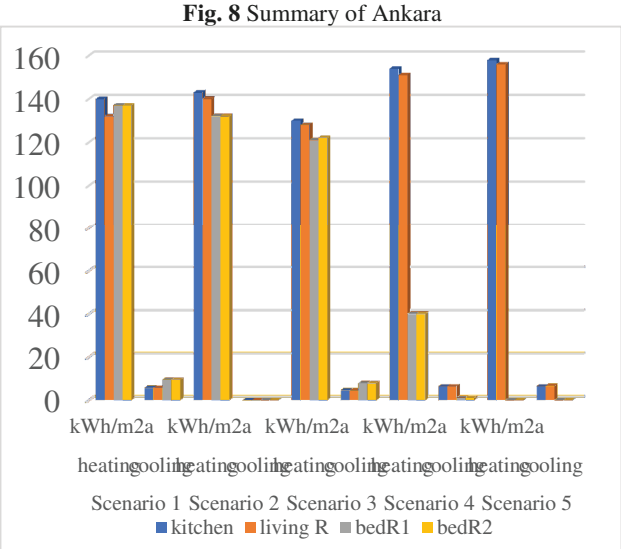

Because of Ankara's climate zone, heating load has a significant share in energy cost. From September to May there is a need for heating which amounts to 95% of the annual energy requirement used for heating. Energy saving potential has been explored in different scenarios. Mechanical systems are operated under comfort conditions when the house is occupied and are kept at setback temperature during unused times (scenario 3). When the mechanical systems are operated in this way, 10% savings is achieved according to the simulation results. Moreovere, 32% of savings are achieved when comfort conditions are provided on the first-floor zones and the second-floor zones are kept at the setback temperature (scenario 4). However, only two zones are heated and cooled in the first floor (scenario 5); savingrate is 44%.

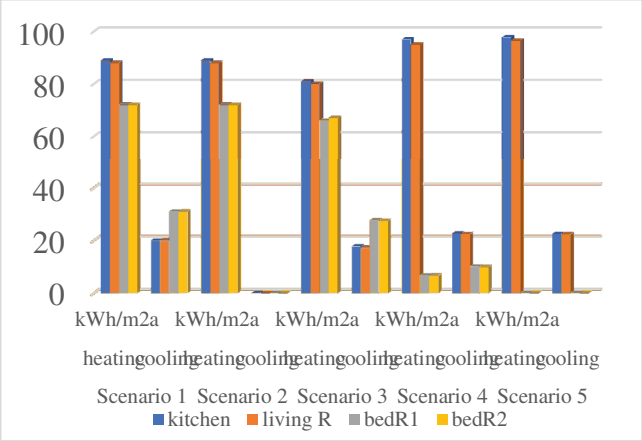

Fig. 9: Summary of the Izmir simulation results;

In Izmir besides the heating load, cooling load is also important to the energy consumption as understood from HDD and CDD values. Here 25% of annual energy consumption is used for cooling and 75% is used for heating energy. In simulations based on scenarios; 9% savings is experienced in case of intermittent operation (scenario 3). 36% savings is achieved if the mechanical systems were partially

operated (scenario 4). In the last scenario; when only the first floor was heated and cooled, the saving rate is 44% (scenario 5).

In the graph, the red zones show the need for heating load per m^2 during the heating period, the blue lines indicate the need for cooling load per m^2 in summer. The fluctuations in the graph consist of the variability of the energy consumed to keep the indoor temperature in balance with the changing outdoor temperature. As seen in the graphic, it is important for the Ankara climate region with the saving potential in the heating energy (figure 10).

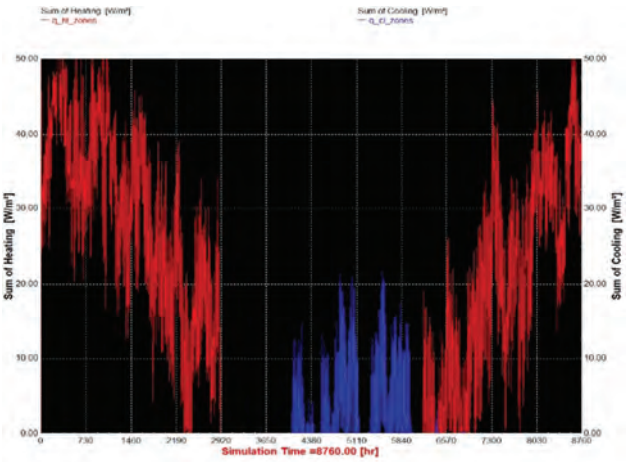

Fig.10 Simulation results for sum of zones in Ankara (scenario 1)

Figure 11 shows the need for heating and cooling of İzmir during summer and winter. It is important in the blue lines that show the cooling energy as well as the red lines showing the heating energy. It is necessary to take different actions according to the regions in national regulation.

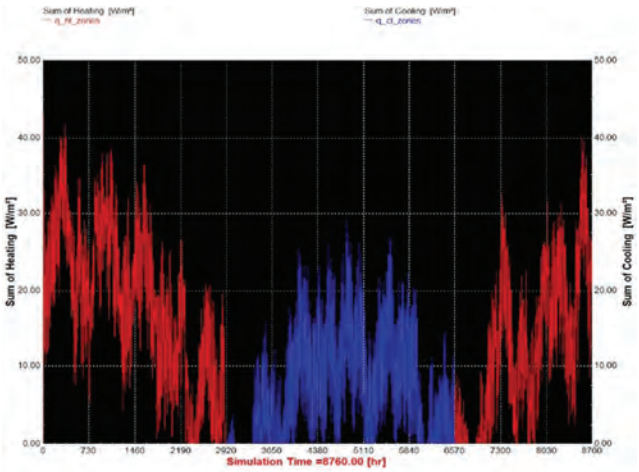

Fig.11 Simulation results for sum of zones in Izmir (scenario 1)

Figure 12 shows the zone temperatures simulated in scenario 4. The first floor shown with purple colour being conditioned and the second floor shown with green colour kept at setback temperature. As seen in the graphic, the upper floor is moving in the temperature range of 15-28 ^{0}C while the entrance floor is kept at 24-26 ^{0}C.

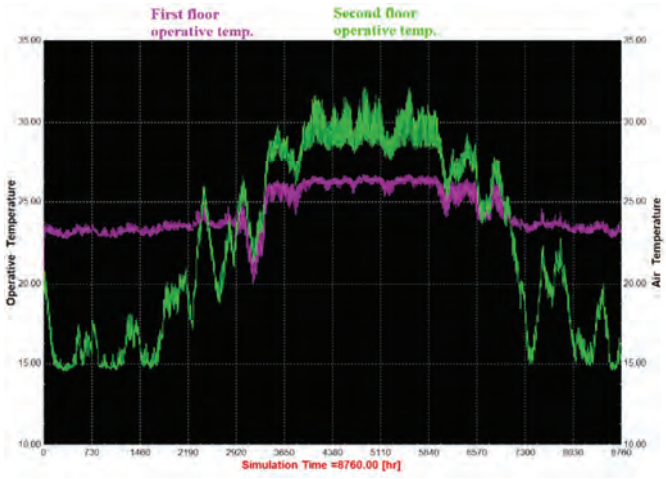

Fig.12 Simulation results for zone temperature in Izmir (scenario 4)

Figure 13 displays the yearly heating and cooling loads intermittent operation. The blue represents the cooling and the red represents the heating and black lines in between the two representing the condition of no heating or cooling.

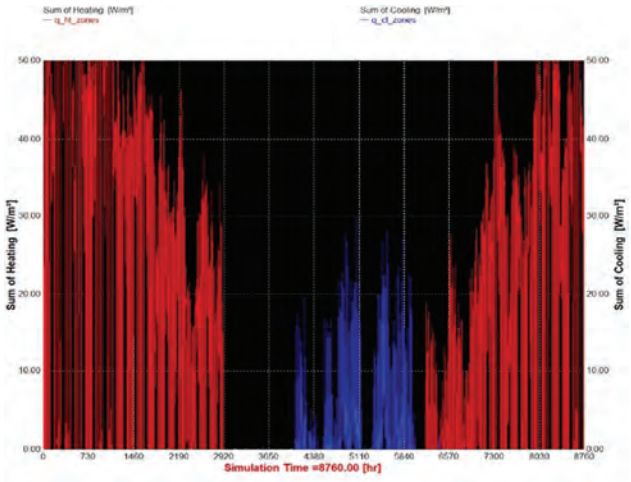

Fig.13 Simulation results for Ankara (scenario 3)

The same building components are modelled in the Bep-TR software with scenario 1 for Ankara and the results are close to the results of the TRNSYS software. There is a difference in the results because of the climate data and methodology used in the calculation. The certificate is compulsory to obtain for all new buildings; the time has been given for existing buildings. It is used to control the suitability of building projects to a minimum class “C”.

In figure 14-15 showed energy performance certificate which is output of Bep-TR software.

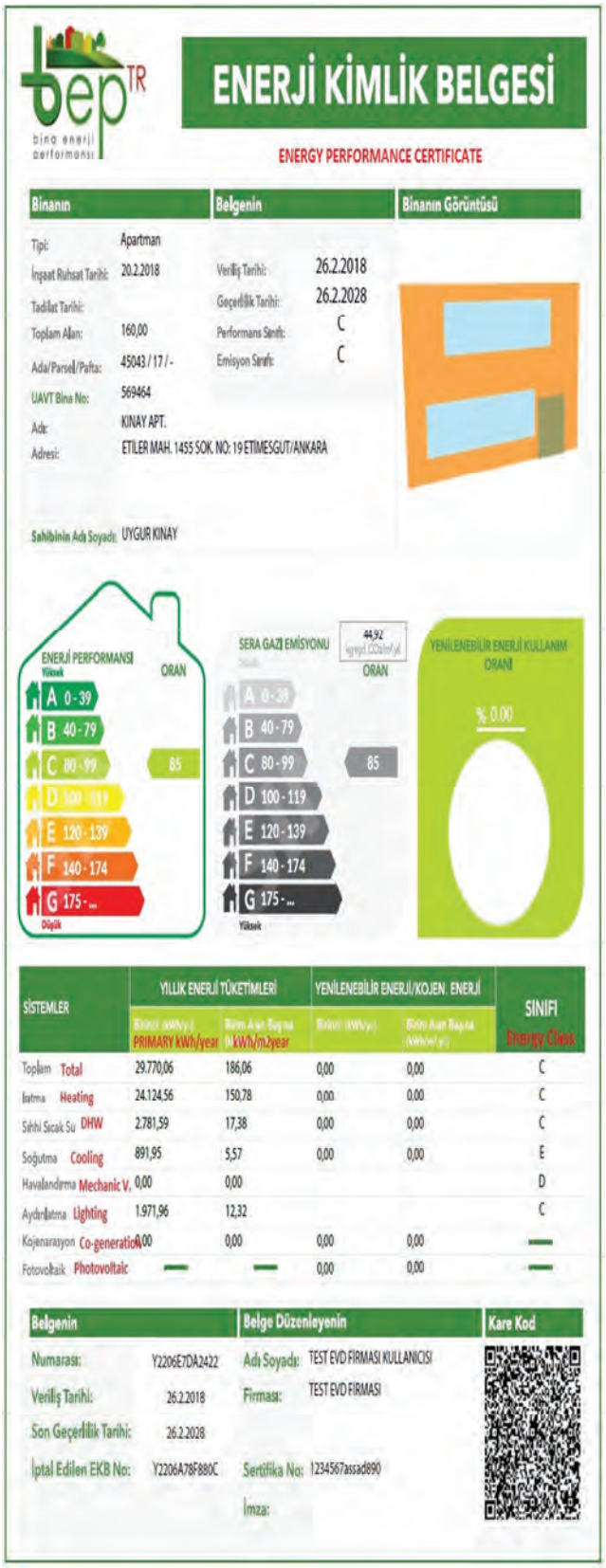

Fig.14 Bep-TR Certificate for Ankara (Building Energy Class)[xiii]

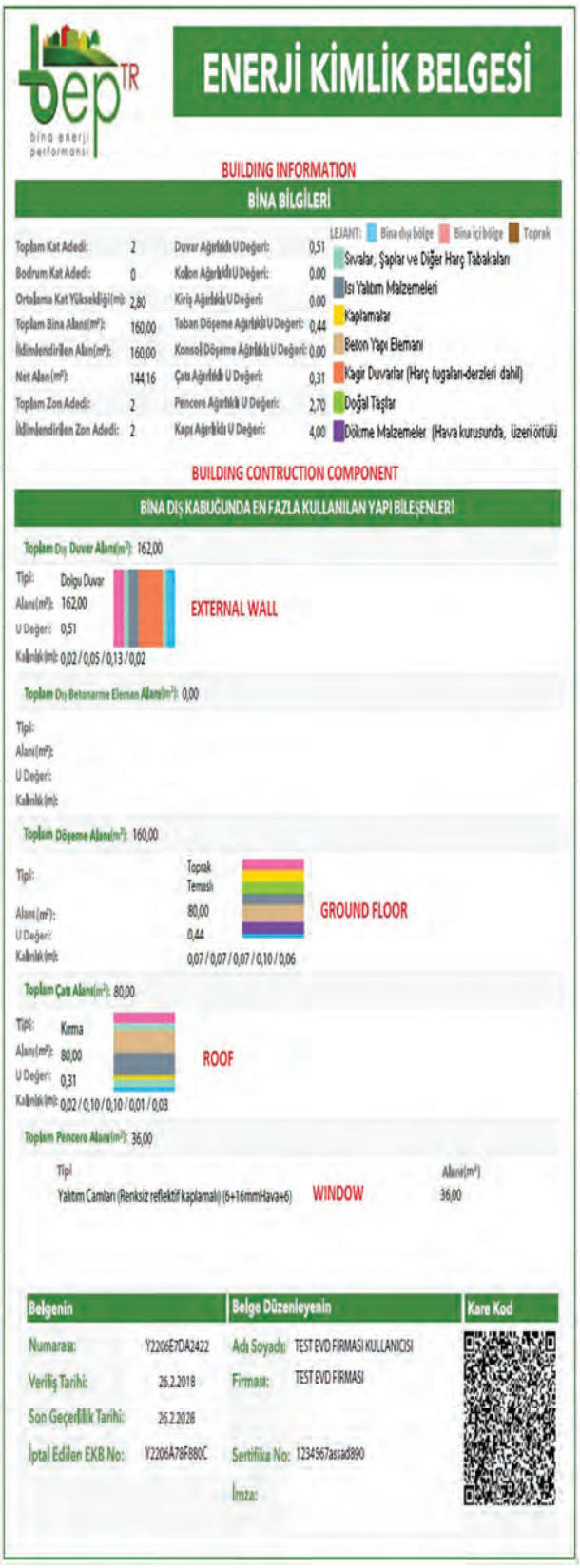

Fig. 15 Bep-TR Certificate (Building information)

8. Conclusion

The simulation showed that partial and intermittent heating and cooling makes a significant drop in the energy consumption compared to standard permanent use. This finding (which has been supported by numeric results) can explain the large gap between modelled and measured results in real situations. On the other hand the result can also be interpreted as a great potential for energy savings by taking the responsibility of important energy-consuming aspects out of the hands of occupants and put under the purview of a comfort controlling system.

It can also be concluded that model building input parameters are important to take realistic results.

One key simulation input is related to weather database; in order to simulate a real situation detailed and verified weather data are needed. The humidity level in Izmir is higher than Ankara and the sensible air temperature varies with the humidity.

Total energy consumption for the model house is 23152 kWh/year in Ankara and for heating 21920 kWh/year. And from the natural distribution company webpage[xiv], 1 TL/kWh = 0.0942485. Hence, annual heating costs can

be calculated for 2018 from the energy consumption and unit price. The calculated heating cost for the model house is 445 Euro per year (2065 TL/year). Scenario 5 showed that there it can be decreased by 194 Euro by partial and intermittent operation. For the scenario 3 which represents a full-time working people's house the saving potential is 40 Euro (Minimum wage for Turkey is 343 Euro in 2018[xv]). The model home is an average single-family house, but it is possible to make an assumption with lower income family house which is app. 75 m^2 [xvi].

The impact of different users' habits on the energy consumption of an average detached house also depends on the climate zone. Automation of mechanical systems with artificial neural networks can reduce the influence of user habits in order to achieve targeted energy efficiency of zero-energy buildings.

References

[i] http://eng.harran.edu.tr/~hbulut/ULIBTK07a.pdf

[ii] http://eur-lex.europa.eu/legal-content/EN/ALL/;ELX_SESSIONID=FZMjThLLzfxmmMCQGp2Y1s2d3TjwtD8QS3pqdkhXZbwqGwlgY9KN!2064651424?uri=CELEX:32010L0031

[iii] http://www.mevzuat.gov.tr/MevzuatMetin/1.5.5627.pdf

[iv] http://www.mevzuat.gov.tr/Metin.Aspx?MevzuatKod=7.5.13594&MevzuatIliski=0&sourceXmlSearch

[v] http://www.mevzuat.gov.tr/Metin.Aspx?MevzuatKod=9.5.24045&MevzuatIliski=0&sourceXmlSearch=Binalarda%20Enerji%20Performans%C4%B1

[vi] http://www.turkstat.gov.tr/PreTablo.do?alt_id=1055

[vii] Technical Assistance for Improving Energy Efficiency in Buildings Project Output (TR2011/0315.20-01/001)

[viii] https://biruni.tuik.gov.tr/yapiizin/giris.zul?dil=ing

[ix] Helena Persson, Bengt Perers , Bo Carlsson "Type12 and Type56: a load structure comparison in TRNSYS" World Renewable Energy Congress 2011-Sweden

[x] http://www.meteonorm.com/en/downloads/documents

[xi] TRNSYS18/Documentation/08-WeatherData.pdf

[xii] http://www1.mmo.org.tr/resimler/dosya_ekler/cf3e258fbdf3eb7_ek.pdf

[xiii] https://beptr.csb.gov.tr/bep-web/#/index/main

[xiv] https://online.baskentdogalgaz.com.tr/MusteriOnline/faces/genel/dogalgazsatisfiyatlari.jsf

[xv] https://www.csgb.gov.tr/home/Contents/Istatistikler/AsgariUcret

[xvi] https://www.toki.gov.tr/en/housing-programs.html

EXPRES 2018
ISBN: 978-86-919769-3-4

MEASURING AND MODELING THE MIXING POWER OF THE HULLED MILLET IN AN AGITATED DRUM DRYER

T. POÓS [a], *D. HORVÁTH*[b], *K. TAMÁS*[c]

Budapest University of Technology and Economics/ Department of Building Services and Process Engineering, Faculty of Mechanical Engineering, Budapest, Hungary
Budapest University of Technology and Economics/ Department of Building Services and Process Engineering, Faculty of Mechanical Engineering, Budapest, Hungary
Budapest University of Technology and Economics/ Department of Machine- and Product Design, Faculty of Mechanical Engineering, Budapest, Hungary
[a]poos@mail.bme.hu,
[b]daniel.horvath.nk@gmail.com,
[c]tamas.kornel@gt3.bme.hu

In the agricultural, food, chemical and pharmaceutical in-dustries, the mixing of granular materials often occurs. To select the mixing motors installed in the equipment, the speed of the mixer and the performance for the propulsion engine are required. The main purpose of this research was to create a discrete element simulation model capable of determining the mixing power consumption of an agitated drum dryer and to validate it with laboratory measurements.

Keywords: *agitated drum dryer, mixing, discrete element method.*

1. Introduction

In the agricultural, food, chemical and pharmaceutical industries the mixing and moving of granular materials are often encountered. The dynamics of mixing solid substances show different behaviors compared to fluid mixing, to describe these, the parameters of the mixed material and the geometric and operating parameters of the mixer (filling rate, rotational speed) are needed. There were several research to investigate this mixing process. Bridgwater, 2012 [1] collected the mixer geometries used to mix powders and granular materials and the phenomenas occuring during operations and the researches which describe them. As a result of which he found that studies of easily bulking materials without internal cohesion and hard-to-bulk materials with internal cohesion require further research. Kuo et al., 2003 [2] using Positron Emission Particle Tracking examination (PEPT), observed the behavior of a horizontal axis shovel mixer. During their measurements, the movement of the granules within the assembly was divided into three motion ranges. The active range of motion was considered around the blades. A further transient range has been defined, beyond which the inactive range is located away from the paddle, which is slowly moving away on the surface and at the bottom slowly approaching to the shovel. Their investigations were limited to partcile movements within the grain assembly, which served as a basis for analyses of later mixing quality studies. Gijón-Arreortúa & Tecante, 2015 [3] investigated the mixing of normal maize starch and icing sugar in a U-shaped horizontal axis mixer. While the former material mentioned above is insoluble in water, the latter mentioned is well soluble in the water, so that homogeneity can be well examined during mixing. The mixing power requirement and mixing time were observed at various filling rates and rotational speeds. A correlation was established with respect to the calculation of the mixing power consumption based on the physical properties and characteristic sizes of the granular materials and parameters of the mixer. It was found that the mixing power consumption is proportional to the increase in the rotational speed and filling rate. They illustrated the relationship between the effective cohesion number and the performance number, and based on the obtained curve, a correlation between the two numbers was made. Masiuk, 1987 [4] investigated the effect of the rotational speed, the filling rate and the moisture content of the mixed sand on the mixing power consumption of a double spiral band mixer. It has been found that the mixing power requirement increases linearly by increasing the mixing speed or the filling rate but decreases with increasing the moisture content. Many of the laboratory and plant tests and measurements carried out by the researchers have, in the majority of cases, produced appropriate results to determine mixing power requirements and the mixing properties of the materials. However, conducting these measurements is extremely

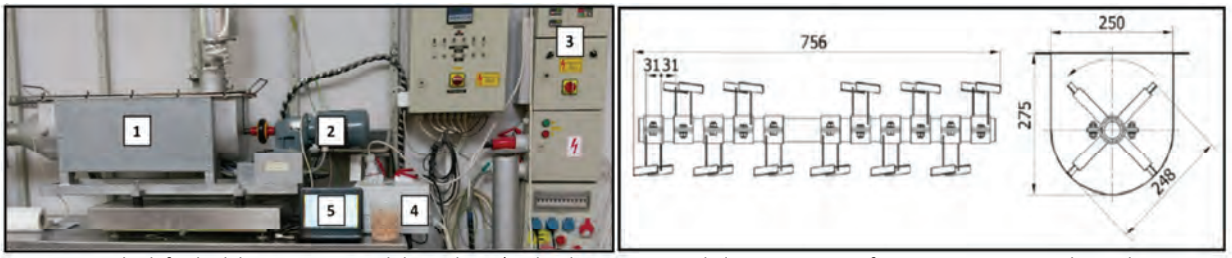

Figure 2. On the left, the laboratory agitated drum dryer (1. the drum , 2. geared electric motor, 3. frequency inverter, 4. three-phase power meter, 5. computer) and on the right side, the design of the drum and the mixer

time-consuming and only a few parameters have been observed. By Geng et al., 2009 [5] a 3D DEM model was created for simulating the operation of a horizontal axis rotary drum. In their simulations, the granules used in laboratory tests were modeled with good approximation. However, during their research, only frictional contact model was used. The effect of moisture content on cohesion in grain assembly have not been investigated.

The aim of this research is to create a simulation model of a horizontal axis drum dryer with mixing blades based on discrete element method (DEM), which is suitable for determining the mixing power requirements.

Figure 1. Hulled millet

2. Material and methods

For the measurements hulled millet was used, which material characteristic size have already been determined in previous studies [6]–[8]. Before starting the measure-ments, it is important to prepare the material. The materi-al assembly must be cleaned of dust, other contaminants and broken particles in order to obtain a precise charac-teristic size of the given material assembly.

a. Material

The hulled millet is a suitable agricultural material for the measurements, because it is small-scale (typically 1.7 ± 0.1 mm [8]), properly homogeneous, spherical, wettable and relatively cheap. In addition, the material itself is prone to arch building and has hydrophilic properties, so its moisture content greatly influences its material properties. Its real look is shown in Figure 1.

First, the granular material have been cleansed and provided the roughly same particle size with a wind-sorting device (which selects by gravity deposition speed). It is also important to determine the moisture content because it greatly influences the specific properties of the material. The exact moisture content on wet basis was determined by a drying chamber.

b. B. Laboratory equipment and measurement method

The measurements were performed in the agitated drum dryer which can be seen on the left side of Figure 2. The electric performance of the mixing motor was measured with a special three-phase power meter at 1 s sampling intervals and recorded on a computer. The mixing of the material is carried out by a bladed mixer driven by the geared electric motor in the drum. The motor is connected to the power transmitter via the frequency inverter, which records the actual performance, from which the idling performance must be deducted. In order to determine the idle performance, the idle measurement at each speed (0.48; 0.63; 0.79; 0.95; 1.11; 1.27; 1.43; 1.58 1 / s) was

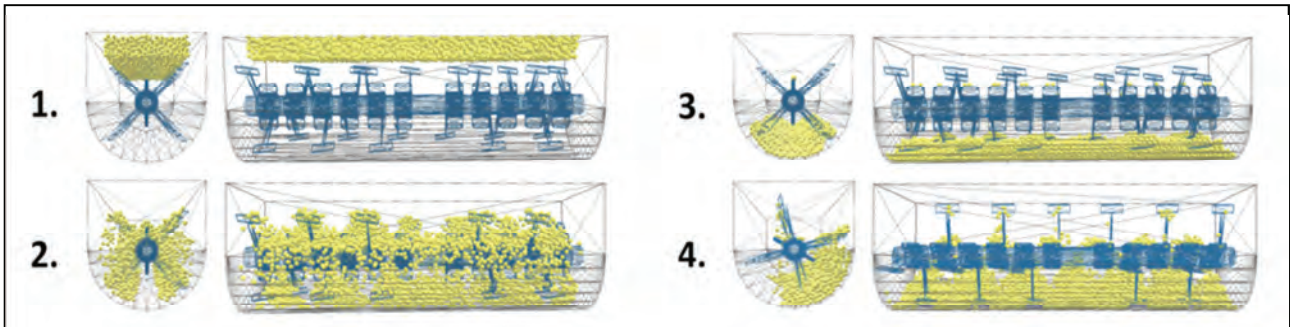

Figure 3. The discrete element model of the mixer (1. generating the particle assembly, 2. gravity deposition of the assembly, 3. activation of the cohesive contacts, 4. start of the mixing)

Table 2. The global default parameter settings of the DEM simulations

Filling factor [%]	Global numerical damping [1]	Number of the particles [1]	Proportionality factor of the critical time step [1]	Time step [s]
15	0	3713	0.7	$3.58 \cdot 10^{-5}$

performed. The data per minute for a given setting was averaged. The idle performance was deducted and we considered this the mixing power requirement for the given conditions. Knowing the mixing power consumption (P) and the rotational speed (n), the mixing torque required (M) can be calculated:

$$M = \frac{P}{2\pi n} \quad (1)$$

The batch operational agitated drum dryer dimensions and arrangement are shown on the right side of Figure 2. 765 mm long, 250 mm wide and 275 mm high U-section drum that is covered by a flat plate. There are 22 mixing blades on the same axis as the drum shaft, each of which is 20 mm high, 50 mm wide and their horizontal angle is 10°.

c. Discrete element method

In this research, the Yade open source discrete element software was used in which the modeling is done in Python [9]. Several types of so-called motors, such as particle contact models, were available to describe the rheological processes between the particles (eg. frictional, cohesive and capillary, etc.). In the model we used a frictional-cohesive (CohFrictMat) contact model [10] due to the nature of the task being investigated, which is suitable for simulating the cohesion of moisture in the granular material. The first stage of the simulation is to generate the particles with the filling rate (Figure 3/1.). Then the gravitaty deposition of the assembly starts (Figure 3/2.). It lasts until the magnitude of the unbalance force ratio drops below 0.001 (Figure 3/3.). During the next phase, cohesion relationships between the particles will be activated, which will be re-activated each time for every new particle contact. Finally, at a given rotational speed, the mixing starts (Fig. 3/4). The sampling of the torque applied to the axis was performed at every second for 30 seconds by the discrete element software.

The mixing power requirement (P) can be calculated based on the Equation (1) in terms of torque (M) and rotational speed (n). Table 1 summarizes the parameters of the equipment's material used in the simulations, which were taken from the material properties of the steel [11].

Table 1. The DEM parameters of the equipment's material [11]

Density [kg/m^3]	Elasticity modulus [GPa]	Poisson ratio [1]	Friction angle [°]
7750	200	0.3	40.1

The mixing's global default parameter settings for the discrete element simulations are summarized in *Table 2* The time step is divided by the proportional factor and it is equal to the critical time step [9] defined by Yade software.

3. Measurement and simulation results

The dimensions and setting parameters of the granules used during the simulation of the mixing process are summarized in Table 3, which was determined by static measurements and simulation calibrations in previous studies [6]–[8]. Because of the small size of millet grains, during the simulations, hundreds of thousands of particles would be needed, which the software could not handle. Thus the diameter of the particles was increased. The mixing and simulation results are shown in Figure 4. It can be stated that the simulation model of the mixer underestimated the results of the measurement. The mixing power consumption increased polynomially by increasing the rotational speed. The simulational curve showed similar characteristics to the result of the laboratory measurement.

Table 3. The parameters of the hulled millet used for the DEM simulations

Measured granule diameter [mm]	Measured moisture content (wet basis) [%]	Measured granule density [kg/m^3]	Chosen elasticity modulus [MPa]	Measured internal friction angle [°]	Calibrated strengths of the cohesion [kPa]	Calibrated dimensionless strengths of the cohesion [1]
10±1*	22.5	2092 [3]	20 [6]	40.3 [3]	61 [1]	0.05 [1]

*The real mean diameter of the hulled millet was 1.7 ± 0.1 mm [3].

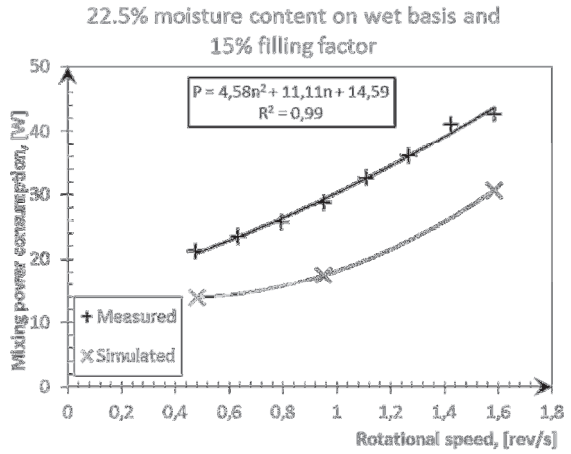

Figure 4. The measured and the simulated mixing power consumption in the case of hulled millet with a filling rate of 15% and 22.5% moisture content on wet basis depending on the rotational speed

Further calibration of the model is required, in which parameter sensitivity tests should be performed for the simulated material parameters chosen from the literature. It could be a solution to increase the elasticity modulus of the particles because it was taken from the literature [11] or slightly distorting the geometric shape of the particles, thus increasing their interdependence.

4. Conclusion

In this research, the mixing power requirement of a horizontal shaft agitated drum dryer was determined by mixing millet with a given moisture content. The mixing equipment and its operation were modelled with discrete element method, taking into account the operating parameters used during the measurement. Then simulation of the mixing was performed with material parameters determined by previous static measurements and simulational calibrations. Measured and simulated results were compared. The mixing power increased polynomially by increasing the rotational speed. The simulational curve showed similar characteristics to the result of the laboratory measurement. It has been found that the model underestimated the laboratory results. Therefore, additional calibrations are required in which parameter sensitivity tests are required to be performed on the simulational material parameters chosen from the literature.

Acknowledgment

Special thanks for “Richter Gedeon Talentum Foundation (H-1103 Budapest, Gyömrői str. 19-21, Hungary)” and by Hungarian Scientific Research Fund (NKFIH/PD-116326) for financial supporting this research. The publication of the work reported herein has been supported by ETDB at BME.

References

[1] J. Bridgwater, “Mixing of powders and granular materials by mechanical means—A per-spective,” Particuology, vol. 10, no. 4, pp. 397–427, 2012.

[2] H. P. Kuo, P. C. Knight, D. J. Parker, A. S. Bur-bidge, M. J. Adams, and J. P. K. Seville, “Non-equilibrium particle motion in the vicinity of a sin-gle blade,” Powder Technol., vol. 132, no. 1, pp. 1–9, May 2003.

[3] I. Gijón-Arreortúa and A. Tecante, “Mixing time and power consumption during blending of cohe-sive food powders with a horizontal helical double-ribbon impeller,” J. Food Eng., vol. 149, no. Sup-plement C, pp. 144–152, Mar. 2015.

[4] S. Masiuk, “Power consumption, mixing time and attrition action for solid mixing in a ribbon mixer,” Powder Technol., vol. 51, no. 3, pp. 217–229, 1987.

[5] F. Geng, Z. Yuan, Y. Yan, D. Luo, H. Wang, B. Li, and D. Xu, “Numerical simulation on mixing kinet-ics of slender particles in a rotary dryer,” Powder Technol., vol. 193, no. 1, pp. 50–58, Jul. 2009.

[6] T. Poós, D. Horváth, and K. Tamás, “Modeling the movement of the granular material in a static equipment with discrete element method,” present-ed at the International Scientific Conference on Advances in Mechanical Engineering (ISCAME 2017), Debrecen, Hungary, 2017.

[7] T. Poós, D. Horváth, and K. Tamás, “The compare of angles of repose with discrete element method and measurement,” in 8th International Scientific Conference, Trebinje, Bosnia-Herzegovina, 2017, pp. 65–70.

[8] D. Horváth, “Statikus berendezésekben mozgó szemcsés anyaghalmaz modellezése,” presented at the Tudományos Diákköri Konferencia, Budapesti Műszaki és Gazdaságtudományi Egyetem, 2017.

[9] V. Šmilauer, E. Catalano, B. Chareyre, S. Dorofeenko, J. Duriez, A. Gladky, J. Kozicki, C. Modenese, L. Scholtès, L. Sibille, J. Stránský, and K. Thoeni, “Dem formulation. In Yade Documen-tation 2nd ed.,” Yade Proj., p. 37, 2015.

[10] F. Bourrier, F. Kneib, B. Chareyre, and T. Fourcaud, “Discrete modeling of granular soils re-inforcement by plant roots,” Ecol. Eng., vol. 61, no. Part C, pp. 646–657, 2013.

[11] J. Horabik and M. Molenda, “Parameters and con-tact models for DEM simulations of agricultural granular materials: A review,” Biosyst. Eng., vol. 147, no. Supplement C, pp. 206–225, Jul. 2016.

EXPRES 2018
ISBN: 978-86-919769-3-4

OPERATIONAL DESIGN OF HEAT TREATMENT EQUIPMENT FOR AGRICULTURAL GRANULAR MATERIALS

T. POÓS [a], *T. KOVÁCS*[b]

Department of Building Services and Process Engineering,
Faculty of Mechanical Engineering
Budapest University of Technology and Economics,
H-1111 Budapest, Bertalan Lajos u. 4-6., Hungary
[a]poos@mail.bme.hu,
[b]tamassmth@gmail.com

A screw conveyor heat treatment machine was designed to treat agricultural granular materials. A thermodynamic model was created to describe heat transfer with continuous material flow. The cases of shell side steam heating, steam injection, shell side water cooling and cooling by air injection were examined. In the calculation algorithm based on the model, the parameters can be modified arbitrarily. During a series of laboratory measurements, the required material properties of ground corn cob were determined and used as input parameters for the calculations. The sensitivity of the model was tested by modifying a number of parameters, and observing their effect on the heat treatment conditions.

Keywords: *sterilizing, heat transfer, screw conveyor.*

1. Introduction

The quality of animal derived food products largely depends on the animals' living conditions and the nutrition they get. Different types of animal feed additives are widely available which can be used to increase productivity (e.g. milk yield) and ensure the health and well-being of animals. During our work, a heat treatment machine is operationally designed, which is part of the production line for animal feed. The machine operates continuously, first sterilizing then cooling the ground corn cob, and a fungi culture is also added for later fermentation. Several methods are found in the literature for the sterilization of agricultural granular materials, which can be divided into three groups: heat treatment (using hot air, saturated steam, or hot water with steam injection), radiation sterilization (using UV-, gamma-, and electron radiation sterilization) and sterilization with chemicals (e.g. ammonia, sodium-hypochlorite, ethanol vapor).

A number of methods based on radiation exist which may be viable for the sterilization of agricultural materials. Machines based on UV, cathode and gamma rays are mentioned below. In an experiment by Y. Hidaka and K. Kubota [1], wheat was sterilized by UV radiation to increase hold up and residence time. As the sterilization effect of radiation mostly occurs on the surface of the seeds, they had to be spread in a thin layer on a conveyor belt, and the long necessary treatment time is also a disadvantage of this method.

The sterilization of barley malt, which is commonly used in the alcohol industry, was examined using different technologies. Stratton and Coulter studied the sterilization of barley malt using cathode radiation [2], where they determined that the necessary amount of radiation is decreased when the material to be sterilized is heated, but the technology was not cost effective at the time the article was written. In another experiment [3], gamma radiation was used for the same purpose, and it was concluded that it is possible to choose a dose of radiation where an adequate amount of bacteria was destroyed, and the amount of extracted alcohol did not decrease, in other words the radiation did not deteriorate the quality of the ingredient. Similarly, to the cathode radiation method, the costs of this technology also proved to be high. In other processes, chemicals or other added agents are used in the sterilization of materials. One of these methods is sterilization using ethanol vapor [4], which was successfully applied for spices, treatment at 1,3 bar pressure and 100°C for 10 minutes resulted in a sterile product for smaller samples. It proved more effective than hot water treatment for larger sample sizes. The sterilization of maize using chemicals were also examined in different experiments, using e.g. ammonia [5] and sodium-hypochlorite [6]. Using these methods, sterile state was reached at a treatment duration of 5 hours. This process cannot be used for our product,

as it is intended for animal consumption.
During a fermentation process, the carbohydrate content of a material is transformed into usually an alcohol or acid, in the presence of microorganisms. In the case of Solid State Fermentation (SSF from now on), microorganisms are grown on the surface of a material, without the presence of unbound water. The process can be further categorized, whether the solid material takes part in the reaction as a growth media or stays inert and only provides a surface area for the process. Another type of technology used for fermentation is Submerged Fermentation (SmF from now on), where the transformation process takes part in a water solution. In industrial conditions, the application of SmF is less prone to problems [7], as homogenous operation parameters are easier to achieve, even at larger operation sizes. Conversely, there are operations which are only possible with the use of SSF, or the quality of the product is vastly improved compared to one produced by a SmF meth-od. [7] SSF technology is used in the production of enzymes, citric acid, koji, in ethanol fermentation and to improve the nutritional value of agricultural materials [8]. To ensure a successful fermentation process, a number of operational parameters have to be monitored and controlled, which are mostly influenced by the type of microorganism in the process. During the design of a machine the temperature tolerance and oxygen requirement (aerobe on anaerobe) of the microorganism have to be taken into account, in addition to its sensitivity to shearing forces and mixing. As some microorganisms might be sensitive to most parameters, it is not sufficient to upscale a well-functioning laboratory sized equipment to an industrial sized one, [7], as this can lead to an inhomogeneous distribution of the parameters, so the quality of the product will not be identical to the ones produced in smaller batches

2. Measurement of material properties

From the standpoint of equipment design, the precision of the calculations of our model can be increased by measuring the following material properties: specific heat, density, porosity, power requirement for mixing, and distribution of granule sizes. A part of these were measured at different material moisture contents (8%, 31%, 57%), which are the moisture content values at certain points in the manufacturing recipe. The exact moisture content values were determined using a drying chamber.

Figure 1: Measuring equipment: a) calorimeter, b) vibratory sieve shaker, and c) Hofsäss-type air pycnometer

The measurement of specific heat was done in a calorimeter using the mixing method. With taking the heat capacity of the calorimeter (Fig.1/a)) into account, the specific heat of the material is calculated using the following equation:

$$(c_v m_v + C)(T_v - T_k) = c_a m_a (T_k - T_a) \qquad (1.1)$$

where c is specific heat [J/kgK], m is mass [kg], C is the heat capacity of the calorimeter [J/K], T [°C] is temperature, the indices mark the following: v-water, a-material, k- common. The results are shown in Fig. 2.

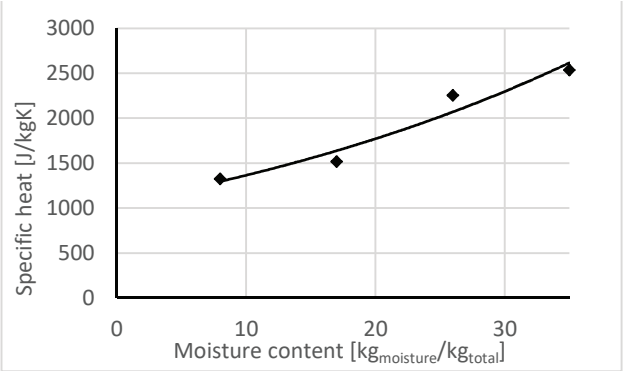

Figure 2. Specific heat of ground corn cob as a function of moisture content

The bulk density (ρ_h) of the material was determined using mass and volume measurements. Using an air pycnometer (Fig. 1./c)) the porosity (ε), the particle density (ρ) of the material were determined. The device is capable of measuring the pressure difference created during the compression between given volumes of the air inside the pycnometer, from which the volume of air trapped in the device can be calculated. After loading in the material and repeating the measurement, and taking the difference between the trapped volumes, the solid volume of the material can be calculated. From this, the

particle density and porosity of the material can be determined, the results for different moisture contents is shown in Table 1. The effects of volume increase due to the added moisture can be observed in these results.

Table 1. Results of porosity measurement for ground corn cob

	x_0=0,08 [kg_{mst}/kg_{tot}]	x_1=0,31 [kg_{mst}/kg_{tot}]	x_2=0,57 [kg_{mst}/kg_{tot}]
ρ [kg/m3]	2255	2072	2144
ρ_h [kg/m3]	520	316	467
ε [1]	0,759	0,846	0,774

The measurement of the distribution of granule sizes for x_0 moisture content was done using a vibratory sieve shaker (Fig.1/b)), the results are shown in Fig. 3.

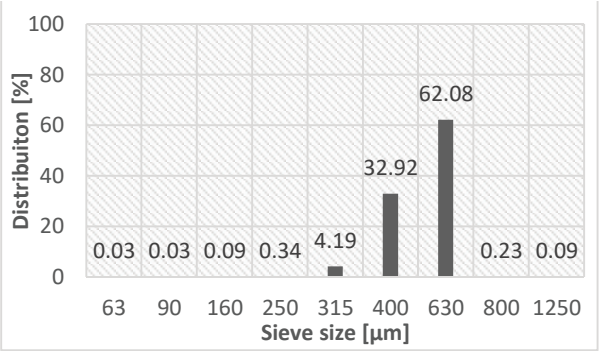

Figure 3. Granule size distribution of ground corn cob for x0 moisture content

3. Calculation model

a. Model of the heat treatment equipment

The planned machine is a multi-stage screw conveyor equipment with a vertical layout, shown in Fig.4. The following technological steps are performed in the machine:

1. Loading of ground corn cob and water;
2. Heating with steam injection and shell side steam heating;
3. Hold time for sterilization;
4. Shell side water cooling and air injection cooling;
5. Addition of microorganisms and removal of material for further fermentation

The heat treatment of the products is possible using shell side steam heating, and steam injection can be used to speed up the heating process. The subsequent cooling is done using shell side water cooling, and can be improved by air injection. The number of stages shown in Figure 4. are subject to change based on the operational parameters.

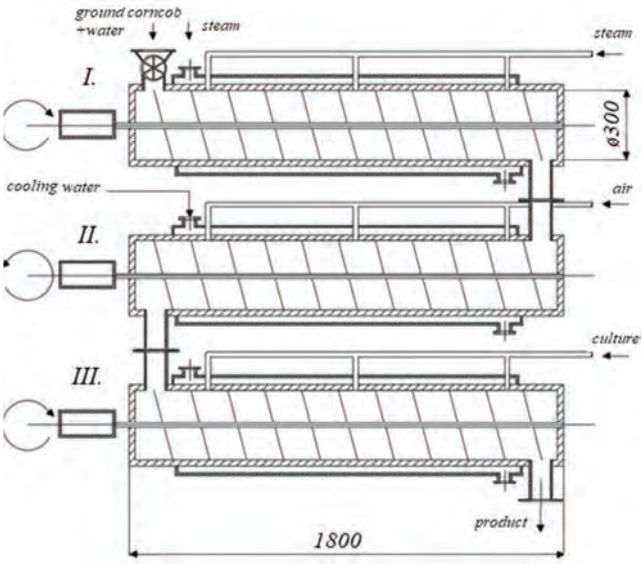

Figure 4. Model of the equipment with 3 stages: I. heating, II. cooling, and III. addition of microorganisms

In the model the following thermodynamic phenomena were taken into account:

- Heat transfer between the cooling water/ condensating steam in the shell side and outer surface of the screw housing, which were calculated using empirical formulas for the different cases.
- Thermal conduction in the wall of the screw housing, the heat conductivity of the wall was approximated using stainless steel
- Thermal conduction in the material layer formed on the inner wall

The main determining factor of the thickness of the forming material layer is the distance between the inner wall of the screw housing and the screw edges. Continous mixing takes place inside the cylinder, but the screw is not in direct contact with the wall, therefore a material layer forms in the gap between them. Beyond this layer mixing was considered intensive and all heat was transferred to the material. The width of this gap was changed between 1-20 mm for the purpose of this study. The thermal conductivity of the material was approximated based on literature [9].

b. Formulas

The formulas used to model the heat treatment process are shown below: shell side steam heating and water cooling, and steam and air injection. Furthermore, the parameters of the screw conveyor were also chosen to carry material according to the manufacturing recipe.

To determine the heat transfer area required for shell side steam heating, the condensation heat transfer coefficient has to be determined. Using the following equation, laminar film condensation can be described around a horizontal cylinder [10]. To calculate the condensation heat transfer coefficient, the apprent latent heat is needed:

$$r^* = r + 0{,}68 \cdot c_{p,foly} \cdot (T_s - T_w) \qquad (3.1.)$$

Utilizing this, the condensation heat transfer coefficient can be calulated:

$$\bar{\alpha}_{kond} = 0{,}729 \cdot \sqrt[4]{\frac{\lambda^3 \cdot \rho \cdot (\rho - \rho_g) \cdot g \cdot r^*}{\mu * (T_s - T_{w)} \cdot D}} \qquad (3.2.)$$

The effect of the steam injection –because injection happens inside the cylinder, where mixing is intensive – was considered without heat loss. It was assumed that the inejcted steam transfers its full latent heat to the material.

Heat transfer coefficient for shell side water cooling was determined using the following empirical formula, valid for forced convection in a tube [10]. The material properties of the cooling water were taken on T specific temperature, where the T_w wall temperature is taken as the average of the water (T_∞) and the material inside.

$$Nu = \sqrt[3]{3{,}66^3 + 1{,}61^3 \cdot Re \cdot Pr \cdot \frac{D}{L}} \cdot \phi_{T1} \qquad (3.3.)$$

where Φ_{T1} is a temperature correction factor for liquids.

$$\phi_{T1} = (Pr/Pr_w)^{0{,}14} \qquad (3.4.)$$

While calculating the effect of air injection, the following equations were used [10] :

$$Nu = \frac{0{,}037 \cdot Re^{0{,}8} Pr}{1 + 2{,}443(Pr^{\frac{2}{3}} - 1)/Re^{0{,}1}} \cdot \phi_{T2} \qquad (3.5.)$$

where Φ_{T2} is the temperature correction factor for gases.

$$\phi_{T2} = (T_\infty/T_w)^{0{,}12} \qquad (3.6.)$$

This assumed the least effective case, considering the flow as a forced flow over a plane.

The screw conveyor dimensions and parameters were determined using the following equations [11]: Volume transported by the screw:

$$\dot{V} = 3600 \cdot A \cdot v \cdot \rho_h \cdot \xi \qquad (3.7.)$$

Transportation speed of the material:

$$v = \frac{s \cdot n}{60} \qquad (3.8.)$$

where s [m] is screw pitch, n is rotational speed [1/min].

The maximum rotational speed:

$$n_{max} = \frac{K}{\sqrt{D}} \qquad (3.9.)$$

where K=60 because the material is not abrasive, and ξ filling factor was considered to be 0,2 based on the reccomendations of [11]. The screw must carry the amount of material in the production recipe while maintaining a minimal rotational speed to increase time spent in one stage during heat treatment. Volume increase caused by added moisture was not taken into consideration, but the model can be expanded by measuring it.

4. Results

The parameters of the calculation model were set in the following way: according to the recipe, 100 kg/h ground cob and 100 kg/h water were added in the equipment, during steam injection 2 bara steam was used, the condensed steam results in an added 30 kg/h of water. In the last stage, the mass flow of the broth containing culture was 225 kg/h. The starting temperature of the ground corn cob, the water, and the air was 20 °C, during heating the material reached 90°C, then cooled to 50°C before adding culture. During cooling the mass flow of the cooling water was 330 kg/h, the flow of air was 6,35 m^3/h (pipes used for steam and water injection have a diameter of 15 mm, and there were 10 pcs every stage). The lenght of a stage was 1,8 m, the inner diameter of the screw conveyor was 300 mm, the case wall was 5 mm wide stainless steel, the rotational speed was 30 [1/min]. Fig. 5 shows that the determining factor of thermal conduction was the material layer that formed on the inside wall of the cylinder.. Therefore, the distance between the edge of the screw and the inner wall of the cylinder is an important factor to take into consideration during construction desgin. It can also be observed that the addition of air injection cooling only reduced the number of required stages in a few cases, mainly at larger layer thickness. The necessity of steam injection is shown, as with its addition the number of required heating stages could be significally reduced.

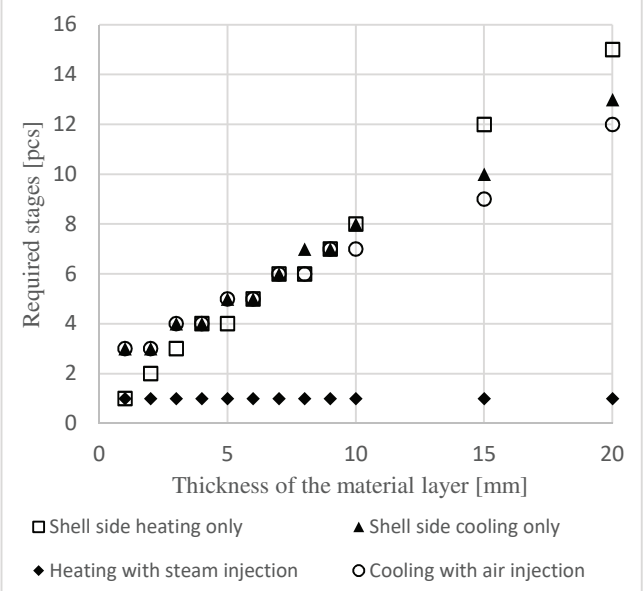

Figure 5. Number of required heating and cooling stages as a function of material layer thickness at inner wall

If the sterlization of material is goal in the device, more stages are required to have sufficient hold time. As only heat loss has to be counteracted in these stages, the heating capability of the equipment is considered sufficent. With the corresponding of the thermal destruction of microorganisms, we can determine a required temperature-time pair. Time spent on one stage is determined by the rotational speed of the screw conveyor. The correlation between the number of

required stages for holding and the rotational speed can be approximated linearly with good accuracy.

5. Conclusion

During this study, a model was created to describe the heat transfer properties of heating, cooling, and the addition of culture for continuous mass transport. Heat transport was described for shell side heating, steam injection, shell side water cooling and cooling by air injection. The parameters of the screw conveyor were chosen to transport the required amount of material. In the program based on the model, the parameters of the technology can be modified arbitrarily. The sensitivity of the model was tested, and parameters defining the size of the equipment were shown. Areas for further improvement of the model include: more accurate description of heat transfer for steam and air injection, determination of maximum cooling air velocity without carrying away the material, undertaking more measurements for specific heat to improve the accuracy of results, measuring the volume increase caused by added moisture and taking it into account when sizing the screw conveyor. For further construction design, the angle of repose also has to be determined for different moisture contents, as the flow of material between stages has to be ensured.

Acknowledgment

Special thanks to Dr. Mária Örvös for her help in this work. Special thanks to “Richter Gedeon Talentum Foundation (H-1103 Budapest, Gyömrői str. 19-21, Hungary)” and to Hungarian Scientific Research Fund (NKFIH/PD-116326) for financially supporting this research.

References

[1] Y. Hidaka és K. Kubota, „Study on the sterilization of grain surface using UV radiation: Development and evaluation of UV irradiation equipment”, *Jpn. Agric. Res. Q.*, köt. 40, o. 157–161, ápr. 2006.

[2] J. R. Stratton, C. J. Coulter, W. H. Day, és C. S. Boruff, „Malt Sterilization, Cathode Radiation as a Means of Sterilizing Distiller’s Barley Malt”, *J. Agric. Food Chem. - J AGR FOOD CHEM*, köt. 4, márc. 1956.

[3] L. L. Kempe, J. T. Graikoski, J. R. Stratton, és W. H. Day, „Malt Pasteurization, Sterilization of Barley Malt with Gamma Radiation”, *J. Agric. Food Chem. - J AGR FOOD CHEM*, köt. 12, 1964.

[4] „Ethanol vapor sterilization of natural spices and other foods”.

[5] M. Broda és G. Włodzimierz, „Ammonia disinfection of corn grains intended for ethanol fermentation”, *Acta Sci. Pol. Technol. Aliment.*, köt. 8, okt. 2009.

[6] R. E. Girton, „STERILIZATION OF CORN GRAINS WITH SODIUM HYPOCHLORITE”, *Plant Physiol.*, köt. 11, sz. 3, o. 635–639, júl. 1936.

[7] D. A. Mitchell, N. Krieger, és M. Berovic, *Solid-State Fermentation Bioreactors: Fundamentals of Design and Operation*. Springer Science & Business Media, 2006.

[8] A. Pandey, C. R. Soccol, és D. Mitchell, „New developments in solid state fermentation: I-bioprocesses and products”, *Process Biochem.*, köt. 35, sz. 10, o. 1153–1169, júl. 2000.

[9] M. Jiřičková, Z. Pavlik, és R. Černý, „Thermal properties of biological agricultural materials”, *Proc. Thermophys. 2006*, 2006.

[10] Dr. Bihari Péter, Both Soma, Dobai Attila, és Györke Gábor, „Segédlet a Hőtan tárgycsoport tárgyaihoz, Első kiadás”. 2014.

[11] Greschik Gyula, *Anyagmozgató gépek*. Budapest: Tankönyvkiadó vállalat, 1987.

EXPRES 2018
ISBN: 978-86-919769-3-4

REVIEW OF EVAPORATION RATE AT NATURAL CONVECTION

T. POÓS[a], *E. VARJU*[b]

Department of Building Services and Process Engineering,
Faculty of Mechanical Engineering
Budapest University of Technology and Economics,
H-1111 Budapest, Bertalan Lajos u. 4-6., Hungary
[a]E-mail: poos@mail.bme.hu
[b]E-mail: varjuevelin@mail.bme.hu

The aim of the simultaneous heat and mass transfer research is to analyze evaporation intensity induced by heat convection. Phenomena of simultaneous heat and mass transfer can be observed in the case of evaporation from open water tanks as well as during the evaporation of surface moisture when drying materials. Relationships for determining the evaporation rate at natural convection were collected within this work. New measuring apparatus has been installed and equations for determination of evaporation rate were validated. Most of the correlations showed high deviation, although Box, Bower and Saylor equations are recommended for calculation of evaporation rate at such measuring conditions.

Keywords: *evaporation rate, dimensionless numbers, simultaneous heat and mass transfer,*

1. Introduction

There are numerous processes in the industry, the household and the environment where heat and mass transfer occurs on the water-air contact surface, resulting water vapor diffusion from the saturated water surface to the unsaturated air, this is called evaporation. Study of evaporation processes has come into view at up-to-date building cooling services and examination of water loss of heated reservoirs. Evaporation of water has to be taken into account regarding water reservoirs, lakes, internal and external pools, sewage treatment, drying, irrigation, and spent fuel pools of nuclear power plants, where it is necessary to determine water loss to resupply water and to specify the amount of toxic material in the air.

During the evaporation process, a very thin layer of air above the water surface is saturated with water vapor due to molecular diffusion. If there is no air movement, further evaporation proceeds entirely by molecular diffusion to the air bulk, this phenomenon is called natural convection. However, if there is air movement, the saturated air layer is carried away by the air-stream, delivering relatively dry air to its place, therefore the evaporation proceeds rapidly. This phenomenon is called forced convection. In this work the evaporation rate at natural convection is investigated, when the air in contact with water surface gets saturated with water vapor, so the lighter, saturated air flows upwards, while the heavier, drier air moves downwards, thus making the evaporation process more intensive. Natural convection is generally assumed in indoor swimming pools and reservoirs, and nuclear power plant spent fuel pools, where the assumed air velocity is lower than 0.15 m/s [1]. Whereas forced convection occurs at outdoor swimming pools and reservoirs, where the air velocity exceeds this velocity limit.

2. Correlations for natural convection

According to certain sources, Dalton was the first in 1802 to discuss the issue and to describe the problem of evaporation by empirical hydrodynamic approximation, and taking his work as a basis several researchers dealt with the phenomenon of liquid evaporation in the last centuries. Correlations to best describe the phenomenon were identified by regression analysis based on measurements. For natural convection, a part of the experiments [2]–[10] was carried out in a laboratory under controlled and adjusted conditions, while the other part [11] was in indoor swimming pools, where the setting of the environmental and liquid properties was less controlled, these values had a higher deviation. The equations for evaporation rate from these studies are valid in different ranges of interpretation (different gas and liquid temperature, surface area) and under certain

conditions (natural or forced convection), which reduces their usefulness.

In equations [1]–[3], [5], [8], [11] the determination of the evaporation rate are created based on the gas velocity (v_G [m/s]) and the water vapor partial pressure difference in the gas ($p_{v,G}$ [Pa]) and the liquid surface ($p_{v,f,sat}$ [Pa]) temperature:

$$N = (a + bv_G)\left(p_{v,f,sat} - p_{V,G}\right)^n \quad (1)$$

where *a, b* and *n* are constants.

There are equations [6], [9] that use the analogy between Sherwood (Sh), Rayleigh (Ra_M) and Schmidt (Sc) numbers to describe the phenomenon:

$$Sh = a \cdot {Ra_M}^b \cdot Sc^c \quad (2)$$

Table 1 shows at natural convection the correlations of evaporation rate of the researchers described above. In addition to the equations, their interpretations of the liquid and gas temperatures, the relative humidity of air, evaporating surface area are also listed if these appeared in the publication.

3. Measuring Method

An experimental apparatus was built and measurements were conducted to validate the equations mentioned above, for the case of natural convection. The apparatus is shown in Figure 1.

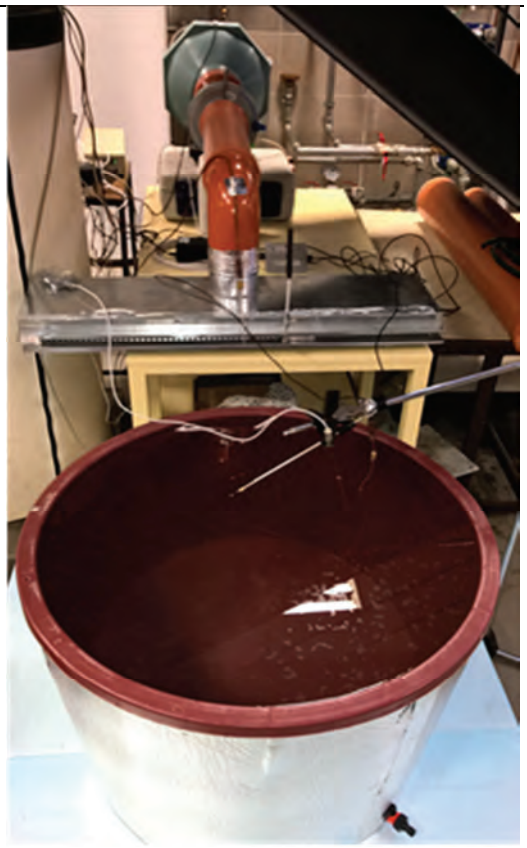

Fig. 1. The measuring apparatus

Table 1. Correlations for evaporation rate at natural convection

Ref.	Correlation*	T_L [°C]	T_G [°C]	φ [1]	A [m^2]
[2]/a	$N = 2.161 \cdot 10^{-8}(p_{v,f,sat} - p_{V,G})$	N.G.	14÷16	0.7	0.00475
[2]/b	$N = 10^{-10}\left(139.031 + 2.117\left(1.8T_f + 32\right)\right)\left(p_{v,f,sat} - p_{V,G}\right)$	21÷88	11	0.86	0.01
[3]	$N = (0.08893 + 0.07835v_G)\frac{p_{v,f,sat} - p_{V,G}}{r_w}$	N.G.	N.G.	N.G.	N.G.
[4]/a	$N = -2.032 \cdot 10^{-6} + 0.0055(c_f - c_G)$	17÷34	21.5	0.5÷0.54	0.073
[4]/b	$N = 1.5875 \cdot 10^{-3}(c_f - c_G)$**	17÷34	21.5	0.5÷0.54	0.073
[5]	$N = 2.627 \cdot 10^{-9}\left(p_{v,f,sat} - p_{V,G}\right)^{1.3}$	25÷95	N.G.	N.G.	N.G.
[11]	$N = -1.64 \cdot 10^{-5} + 2.19 \cdot 10^{-8}(p_{v,f,sat} - p_{v,G})$	24.3÷30.1	24.3÷34.6	0.4÷0.68	62.2
[6]	$Sh = 0.45 \cdot {Ra_M}^{0.25}$	N.G.	N.G.	N.G.	N.G.
[7]	$N = 0.00972(c_f - c_G)^{1.237}$	25÷50	20	0.5÷0.7	1.13
[8]	$N = (0.0038 + 0.1356v_G)$ $\left(p_{v,f,sat} - p_{v,G}\right)^{\left(-1.255v_G^3 + 2.182v_G^2 - 1.362v_G + 1.377\right)}$	26÷32	45	N.G.	1.5
[9]	$Sh = 0.230 \cdot Ra_M^{0.321} \cdot Sc^{1/3}$	43	24	0.52	0.0231 ÷0.371
[10]/a	$N = 0.00972\rho_f(\rho_G - \rho_f)^{1/3}(Y_f - Y_G)$**	7÷94	6÷35	0.28÷0.98	0.073÷425
[10]/b	$N = 0.011\rho_f(\rho_G - \rho_f)^{1/3}(Y_f - Y_G)$**	7÷94	6÷35	0.28÷0.98	0.073÷425
[1]	$N = 1.39 \cdot 10^{-8}(p_{v,f,sat} - p_{v,G})$	7÷94	6÷35	0.28÷0.98	0.073÷425

*The notations used in the table: r_w heat of vaporization [J/kg], c_f and c_G vapor concentration of the air on the water surface and in the air bulk [kg/m^3], ρ_f and ρ_G air density on the water surface and in the air bulk [kg/m^3], Y_f specific humidity of air on the water surface [kg of moisture/kg of air], N.G. not given.

Before starting the measurement, a tank with 230 l volume, 0.89 m diameter, and 20 mm thick aluminium coating polifoam insulation was fully filled with water and left overnight so that the temperatures would be equalized. The evaporation rate was deduced by weight measurement, the weight of the evaporated water vapoured was determined using a scale under the tank with 0.1 kg precision (Δm [kg]). The following data was collected during the evaporation process: the bulk water temperature (T_L [°C]) and the temperature of the ambient air (T_G [°C]), using T-type thermocouples, the liquid surface temperature (T_f [°C] with an AMiR 7842 infrared thermometer the air velocity using an Almemo hot-wire anemometer and air humidity (Y_G [kg/kg], φ [%]) using an Almemo FHAD 36 Rx type humidity meter. The data from the instruments was registered by a uniquely developed software with 10 minute sample rate. The changes of the ambient air properties during the multiple days of the measurement was disregarded. The resulting average values from the experiments are shown in Table 2.

Table 2. Measurement result for natural convection

T_L	16	°C
T_f	15,5	°C
T_G	21,8	°C
Y_G	0,0048	kg/kg
φ	30,3	%
v_G	0,11	m/s
Δm	3,5	kg
Δt	264920	s
N	0,0765	kg/m^{2}h

The evaporation rate was calculated using the following formula, as it was deduced by weight measurement:

$$N = -\frac{dm}{A \cdot dt}. \tag{3}$$

4. Results

Using these measurement results, the equations shown in Table 1. were tested for the same conditions. As all these formulas have different ranges of interpretation, not all of them fit the conditions of our experiment, these were marked with **. For equations where the rate of evaporation is given, were calculated using the measurement results. In other cases, where the Sh-Ra_M-Sc equation is given, the evaporation rate was calculated using the following formula:

$$N = \sigma(Y_f - Y_G) = k\rho_G(Y_f - Y_G) = \\ = \frac{D_{wG}}{L} \mathrm{Ra_M}^{\mathrm{b}} \mathrm{Sc}^{\mathrm{c}} \rho_G(Y_f - Y_G), \tag{4}$$

where σ is the evaporation factor [kg/m^{2}s], k is the mass transfer factor [m/s], D_{wG} is the diffusion factor [m/s], L is the characteristic length [m]. Percentage deviaton (δ [%]) was also calculated for the measured and calculated evaporation rates for comparison purposes:

$$\delta = \frac{N_{calculated} - N_{measured}}{N_{measured}} \cdot 100\%. \tag{5}$$

In Figure 2. these can be seen for all equations, where the numbers on the horizontal axis show the reference numbers of publications which are the sources of the equations. The red columns show equations with ranges of interpretation outside our measurement. Equations [10]/a and [10]/b are not shown because in they are valid only for positive air density differences, which is not the case in our measurement.

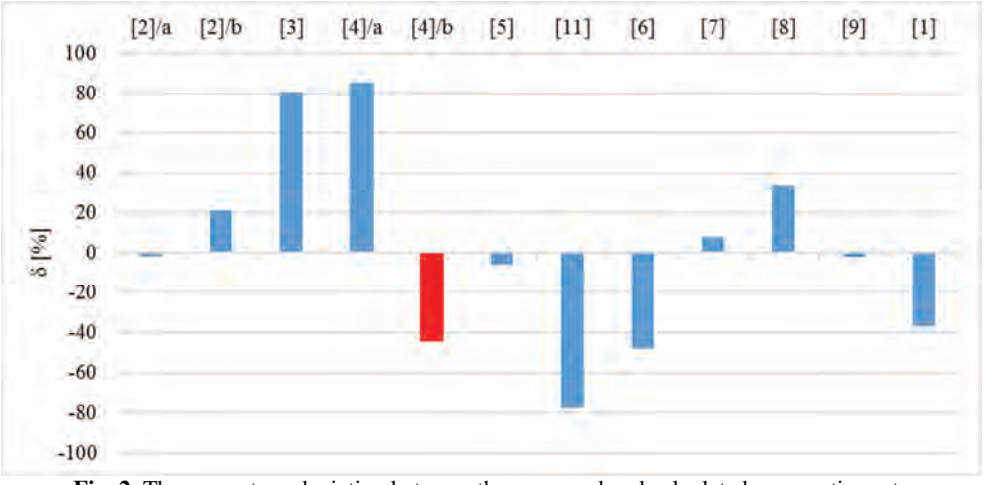

Fig. 2. The percentage deviation between the measured and calculated evaporation rate

The equations of Carrier [3], and Sharpley and Boelter [4]/a have shown the greatest positive deviation from our measurement results. This confirmed that according to literature, Carrier's equation usually overestimates the rate of evaporation. Sharpley and Boelter had similar temperature conditions to our measurement, still the differences in results are significant. On the other hand, the equation of Biasin and Krumme [11] have shown the same deviation as the ones mentioned before, only in a negative direction, underestimating the rate of evaporation. The cause of this difference may be that in their case, the temperature of the liquid and air was similar, therefore the driving force induced by temperature difference was smaller than the driving force induced by density difference, unlike our case.

The equations of Rao and Radhakrishnan [6] and Shah [1] show lesser deviation from the measurement result, the former is close to 50%, the latter is 40%. The evaporation rate was also underestimated, despite that all parameters were in their range of interpretation, they could not produce correct results. Similar or lesser differences was given by the equations of Box [2]/b and Moghiman és Jodat [8], but both of them resulted in a larger rate of evaporation than the measured. In the case of the equation of Moghiman és Jodat [8] is viable for higher temperature ranges, thus not providing appropriate results for the rate of evaporation.

The equations of Leven [5] and Tang et al. [7] resulted in minor, ±10% deviation in results, positive for the former two, and negative for the latter two. In the two equations, the partial vapor pressure difference (or concentration difference) is not a linear dependent factor, but a certain exponent is needed to describe the evaporation rate. Moghiman and Jodat thought that the current formulas in literature are so different because the assumption of linear dependence is false. The closest results were given by the equations of Box [2]/a and Bower and Saylor [9], where the deviation was smaller than ±3%. Bower and Saylor used Sherwood-, Rayleigh-, and Schmidt-numbers to describe the rate of evaporation, which may be most general way to describe this process.

5. Conclusion

During our research in simultaneous heat and mass transfer the intensity of evaporation by heat transfer was studied for natural convection. Literature proposing a way to determine the rate of evaporation for natural convection was collected. The validity of the equations is given by the temperature and humidity of air, temperature of the liquid, and the shape and size of the evaporation surface. Taking all these into account limits the general application of these formulas. During our research, these formulas were validated by measurements in a laboratory. As a result of this validation, the equations of Bower and Saylor, and Box proved to be the most precise (±3% deviation) and two equations (Leven, Tang et al.) showed ±10% deviation to our measurement results.

Acknowledgements

This paper was supported by Gedeon Richter's Talentum Foundation (H-1103 Budapest, Gyömrői str. 19-21, Hungary), and by Hungarian Scientific Research Found (NKFIH-PD-116326). Special thanks for Róbert Goda for her helps in this work.

References

[1] M. M. Shah, "Improved method for calculating evaporation from indoor water pools," *Energy Build.*, vol. 49, no. Supplement C, pp. 306–309, Jun. 2012.
[2] T. Box, "A practical treatise on heat, as applied to the useful arts : for the use of engineers, architects, etc. /," 1876. .
[3] W. H. Carrier, "The temperature of evaporation," *ASHVE Trans.*, vol. 24, pp. 25–50, 1918.
[4] B. F. Sharpley and L. M. K. Boelter, "Evaporation of Water into Quiet Air From A One-Foot Diameter Surface," *Ind. Eng. Chem.*, vol. 30, no. 10, pp. 1125–1131, Oct. 1938.
[5] K. Leven, "Beitrag zur Frage der wasserverdunstung," *Warme Kaltetechnik*, vol. 44, no. 11, p. 161–67., 1942.
[6] V. K. Rao and P. P. Radhakrishnan, "Evaporation of water from pools," *J. Indian Inst. Sci.*, vol. 59, no. 3, p. 106, 1976.
[7] T. D. Tang, M. T. Pauken, S. M. Jeter, and S. I. Abdel-Khalik, "On the Use of Monolayers to Reduce Evaporation From Stationary Water Pools," *J. Heat Transf.*, vol. 115, no. 1, pp. 209–214, 1993.
[8] M. Moghiman and A. Jodat, "Effect of air velocity on water evaporation rate in indoor swimming pools," *Iran. J. Mech. Eng.*, vol. 8, no. 1, pp. 19–30, 2007.
[9] S. M. Bower and J. R. Saylor, "A study of the Sherwood–Rayleigh relation for water undergoing natural convection-driven evaporation," *Int. J. Heat Mass Transf.*, vol. 52, no. 13, pp. 3055–3063, Jun. 2009.
[10] M. M. Shah, "Analytical Formulas for Calculating Water Evaporation from Pools," *ASHRAE Trans.*, vol. 114, no. 2, pp. 610–618, 2008.
[11] K. Biasin and W. Krumme, "Die wasserverdunstung in einem innenschwimmbad," *Electrowärme Int.*, vol. 32, no. A3, pp. A115–A129, 1974.

EXPRES 2018
ISBN: 978-86-919769-3-4

TESTING OF A VIBRATION FLUIDIZED BED DRYER DESIGN

T. POÓS [a], *V. SZABÓ*[b]

Budapest University of Technology and Economics/ Department of Building Services and Process Engineering, Faculty of Mechanical Engineering, Budapest, Hungary
[a]poos@mail.bme.hu,
[b]szabo.viktor@mail.bme.hu,

Vibrating fluid-bed dryer is widely used for drying granular material in chemical, agricultural, and pharmaceutical industries. The equipment contains a horizontal positioned perforated support plate with a metal grid. The dried material located on the grid forms into fluidized state in the effect of the drying gas, which flows through the grid and from the vibration of the plate. The grid's sealing damaged immediately after the first run. The purpose of our work is to make a proposal based on experiments to avoid this problem in the future. The experimental results are presented in this study.

Keywords: *vibrating fluid-bed dryer, perforated plate, metal grid, pressure drop*

1. Introduction

Vibration fluidized technology is widely used in chemical, food and pharmaceutical industries. During the operation the fluidized state is generated by vibration of the grid under the material to be dried and by the flow of air through it. The advantage of this operation is that it provides better heat and mass transfer between the drying gas and the material than the other drying processes, and the temperature and moisture content of the drying particles are homogeneous within the equipment due to the intense mixing of particles [1]. The technology can be advantageously applied to granules having a particle size distribution in a wide range, low strength, sticky or damp texture [2]. Any shape of the particles can be dried in the device as vibration can prevent the formation of air-generated ducts in the material layer. For the movement of the material, the vibration of the support plate has a greater effect than the flowrate of drying gas. For this reason, varying the flowrate of the drying gas has less effect on the system. Using the vibration is more advantageous to the movement than the airflow [3]. In the literature several authors deal with the mathematical modeling of the technology [4], [5], however, the description of the function of the support plate and the grid is incomplete.

2. Methods

The aim of our work is to determine the pressure drop of the support plate and the grid in a vibration fluidized bed dryer and to compare the pressure drop some variations of support plates. For this examination, a pilot plant fluidized bed dryer was used, in this case not for drying, but for flow test. Fig. 1 shows a photo of the fluidized-bed dryer equipment.

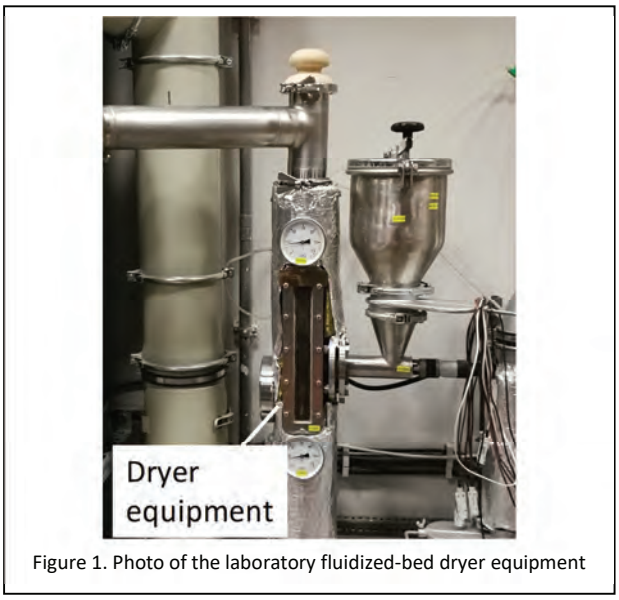

Figure 1. Photo of the laboratory fluidized-bed dryer equipment

During our experiments, three types of support plates and one type of grid were investigated. The plates are provided with perforations with different diameters and allocations. The smallest perforation size marked with number 1, the middle with number 2, and the largest one with number 3. Fig. 2 shows the photo of the plates.

Figure 2. Photo of the tested grids

The function of the support plate is to provide suitable strength support for the grid placed on it. In addition, it also has an airflow distributor function. Thus, the size of the perforation is determined by the strength and pressure drop considerations. While the flow is better, the higher the relative openness of the plate, but the strength at the same conditions also decreases its carrying capacity. The function of the grid is that the material to be dried should not fall off, so that the maximum hole size is determined by the smallest characteristic particle size.

Due to the flexibility of the grid, it could not be placed in the dryer itself because the edge was bent. A small weight ring from a thin ring was made, and placed it on the grid, keeping the shape of the grid. The flow resistance of this ring is negligible during the evaluations, because it was below the measuring accuracy of the instrument and was placed on each of them due to the nature of the comparative experiments. The position of the grid and the ring is shown in Fig. 3.

Figure 3. Position of the grid with the ring

The case, when the material was placed on the grid was also investigated. The tested material was chichory pulp coated feed as animal nutrition. So much material was placed on the grid so that the material height is approximately the same as the height used in the operating vibration fluidized bed dryer, approximately 30 mm. A picture taken during the experiments from the assembly is shown in Fig. 4.

Figure 4. The material in the dryer, below is the plate No. 2 and the grid

The exactly type of the grid is unknown, however, the diameter of the perforation was counted. It had fairly dense perforation with value of 82 mesh. A picture from the single grid is shown in Fig. 5.

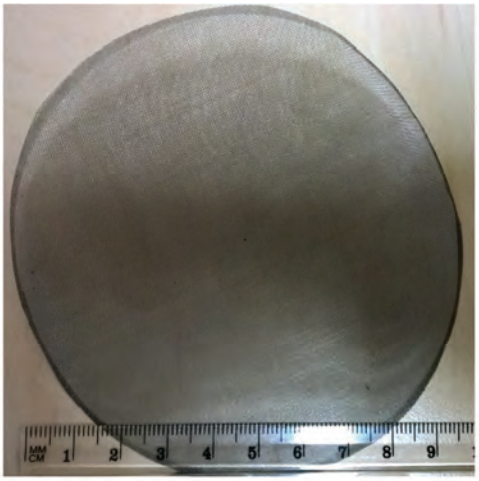

Figure 5. Photo of the grid

3. Results

The relative openness values were also verified by 3D modeling. The 3D models of the plates were prepared (Fig. 6.), and with the help of the software, the values of the size of perforated surfaces were measured then compared to the full disk surface. During the calculation and the experiments, the relative openness and pressure drop of the support plate and grid were determined.

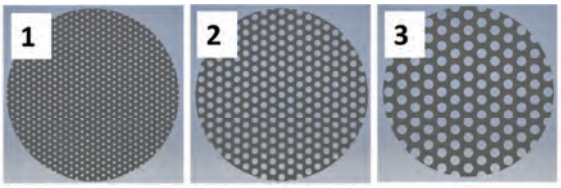

Figure 6. The model of the support plates

The relative openness of the plates were calculated from the ratio of the open surface (A_{open}) and the total surface (A_{total}) area:

$$A_{rel} = \frac{A_{open}}{A_{total}}. \quad (1)$$

Depending on whether the perforated plate has round holes in square, diagonal or regular triangles, the relative openness can be calculated in different ways (Fig. 7.).

Figure 7. Possibilities to allocate the holes on the plate. From left to right: square, diagonal, regular triangle layout [6]

The relative openness in the case of square layout:

$$A_{rel}^{square} = \frac{0.7853D^2}{C_1C_2}. \quad (2)$$

The relative openness in the case of diagonal layout:

$$A_{rel}^{diagonal} = \frac{1.5705D^2}{C_1C_2}. \quad (3)$$

The relative openness in the case of regular triangle layout:

$$A_{rel}^{3angle} = \frac{0.9067D^2}{C_1C_2}. \quad (4)$$

From the examined plates, there are regular triangle layouts in the holes. Thus, Eq. (4) was used for the calculations. The relative openness for each of the three support plates were calculated and summarized in Table 1. The table contains the geometric data of the support plates, the last but one column contains the values of relative openness with modeling, the last column contains of the relative openness values by the calculation. It can be observed, that both modeling and calculation are nearly the same values, so Eq. (4) can be used in a good approximation to calculate relative openness.

Table 1. The relative openness of the examined plates

Plate without perforation (mm2)	Real surface from model (mm2)	Rel. openness from model (%)	Rel. openness calculated (%)
7854.0	5663.6	27.9	28.0
	4690.5	40.3	40.3
	4631.7	41.0	40.3

Table 2 summarizes the pressure drop of the examined support plates and the grid.

Table 2. Pressure drop of the examined plates and grids

ID	Air velocity [m/s]	Temperature [°C]	Pressure drop [Pa]
Plate no. 1. + grid	4.61	31.6	44
Plate no. 2. + grid	4.66	30.0	24
Plate no. 3. + grid	4.60	26.3	28

In the function of the relative openness, the k-factor for perforated plates can be calculated [6]:

$$k = \begin{bmatrix} 0{,}707\left(1 - A_{rel}^{3angle}\right)^{0,5} \\ +1 - A_{rel}^{3angle} \end{bmatrix}^2 \frac{1}{A_{rel}^{3angle^2}}, \quad (5)$$

from where the pressure drop can be calculated:

$$\Delta p = k\left(\frac{\rho v^2}{2}\right). \quad (6)$$

The calculation were performed at an air velocity of 5 m/s and a gas temperature of 30 °C. At this air velocity, the pressure drop is significant due to the square exponent. When using a smaller value, the difference between the pressure drops was not significant. The results are summarized in Table 3.

Table 3. Relative openness and pressure drop at various type of support plates

No.	Rel. openness (calc) [1]	k-factor [1]	Δp [Pa]
1	0.280	22.25	314
2	0.403	8.05	114
3	0.403	8.05	114

In the case of examination of the grid was different from the support plates. The k-factor can be calculated with the following expression [6]:

$$k = 1{,}3\left(1 - A_{rel}^{grid}\right) + \left(\frac{1}{A_0^{grid}} - 1\right)^2. \quad (7)$$

The calculations were repeated with air velocity of 5 m/s and temperature of 30 °C. The results are shown in Table 4.

Table 4. Relative openness and pressure drop of the grid

Rel. openness (calc) [1]	k-factor [1]	Δp [Pa]	Δp [Pa/plate]
0.46	2.08	29	0.23

In the case when the material was placed on the grid, the velocity of air had to be reduced to the fluidization

region, otherwise the airflow would have transported the material from the drying chamber. Thus, the data provided in this way can not be directly compared to the previously presented. To compare the experiments, the pressure drop of the support plate and the grid was measured at the same reduced air velocity, then the material was placed on it under the same settings. The results are shown in Table 5.

Table 5. Pressure drop of the examined support plates and grid with and without material

ID	Air velocity [m/s]	Temperature [°C]	Pressure drop [Pa]
Plate no. 2. + grid	1.3	29.9	4
Plate no. 2. + grid + 3 cm height material	1.21	29.9	7

Using the calculation method, the effect of air velocity on the pressure drop of the support plate number 2 is illustrated in Fig. 8. The diagram shows the square effect of the velocity on the pressure drop.

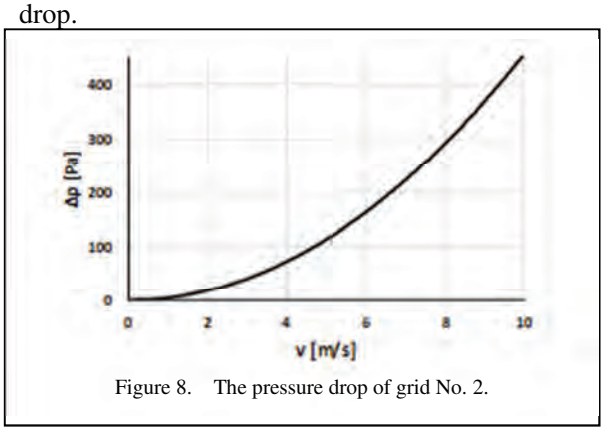

Figure 8. The pressure drop of grid No. 2.

4. Conclusion

The purpose of our work is to examine the pressure drop of the support plate and the grid in a fluidized bed dryer. The reason for this investigation was the damage of the grid and the detachment of the fastening screws in a vibration fluidized bed dryer. The cause of the problem was found in the high resistance of the grid, so we carried out experiments and calculations for the pressure drop of the system. First the perforation of the plates, their so-called relative openness were determined. Using laboratory experiments and calculations the pressure drop of each plate types were determined. According to our experiments, the plate number 2 is suggested of the three plates.

5. Acknowledgement

Special thanks for “Richter Gedeon Talentum Foundation (H-1103 Budapest, Gyömrői str. 19-21, Hungary)” for financial supporting this research and by Hungarian Scientific Research Found (OTKA-116326).

References

[1] M. Izadifar, D. Mowla, Simulation of a cross-flow continuous fluidized bed dryer for paddy rice, *Journal of Food Engineering* 58 (2003), 325–329.

[2] A. Picado, J. Martínez, Mathematical Modeling of a Continuous Vibrating Fluidized Bed Dryer for Grain, *Drying Technology* 30 (2012), 1469–1481.

[3] L. Xiang, W. Shuyan, L. Huilin, L. Goudong, C. Juhui, L. Yikun, Numerical simulation of particle motion in vibrated fluidized beds, *Powder Technology* 197, (2010), 25–35.

[4] N. Bizmark, N. Mostoufi, R. Sotudeh-Gharebagh, H. Ehsani, Sequential modeling of fluidized bed paddy dryer, *Journal Food Engineering* 101, (2010), 303–308.

[5] S. Soponronnarit, S. Wetchacama, S. Trutassanawin, W. Jariyatontivait, Design, testing, and optimization of vibro-fluidized bed paddy dryer, *Drying Technology* 19, (2001), 1891–1908.

[6] ‘Calculating Pressure Drop Across Sharp-Edged Perforated Plates’. [Online]. Available: http://www.aft.com/support/product-tips/entry/2017/06/14/calculating-the-pressure-drop-across-sharp-edged-perforated-plates. [Accessed: 05-Oct-2017].

ISBN: 978-86-919769-3-4

HEAT PUMPS THERMAL USE OF UNDERGROUND AND ABANDONED MINES ENERGY STORAGE FOR LARGE-SCALE RES UTILIZATION

MARIJA S.TODOROVIĆ

ME, FASHRAE, FREHVA, FWAAS, AESS,
Guest Prof. School of Energy and Environment,
Southeast University Nanjing, China,
CEO vea-invi.ltd, Belgrade, Serbia
E-mail: vea@eunet.rs

As fossil energy resources are closer to their exhaustion, global warming is in raise, and more catastrophic weather extremes are occurring worldwide, there are more and more warnings that the risks to the Earth humanity survival are also in growth. Using renewable thermal energy from environment (air-aerothermal, wate r-hydrothermal and underground thermal) HPs (heat pumps) increase energy and exergy efficiency and contribute to the reduction of final and primary energy demand, and reduction of CO_2 and other GHG emissions, particularly HPs use of underground is enabling high efficiencies to be reached at an annual bases because of its small temperature variations. Directive on the promotion of the use of energy from renewable sources (2009/28/EC RES Directive, § 2) heat pumps, recognizes heat pumps as clean renewable energy sources (RES) technology. Availability of most types of RES is interruptible and of variable intensity and therefore energy storage (ES) is important for the large-scale utilization of RES, and large-scale storage systems require large storage volumes. Worldwide, many abandoned mines (of coal or minerals) offer large storage volumes almost ready-made to be used directly for energy storage. This paper presents methodology and results of few feasibility studies on the underground water, ground, and energy piles used as heat sink/heat source for heat pump operation, as well as R&D and design methods using BPS for integrated building HVAC/energy supply systems optimization

, including BMS/smart control of heat pump use in energy, Abandoned mines, ed refurbishment of social multi-apartment housing and comprehensive refurbishment of old traditional village house.

Keywords: *Renewable energy sources, Energy storage, BPS, BMS/smart control, Smart grid, Abandoned mines*

1. Introduction

Ground source and ground water heat pumps have widespread use in Europe pioneered by Switzerland and Sweden and in North America (/2/-/4/, /10/-/13/) and are in very intensive implementation growth today worldwide. The reason is the fact that with current state of the art, the heat pumps represent much more efficient technology concerning to primary energy requirements compared to electrically or oil-heated boiler and to gas condensing boilers. Additional advantage is that instead of burning fossil fuel at the building site, through the use of electrical heat pumps the pollutant emissions (if the power plant is on fossil fuel) do not occur in situ but in power stations equipped with costly exhaust gas cleaning plant. Thus, an important reduction of emissions is obtained in densely populated urban commercial or residential areas. In addition Heat pumps transform renewable energy from air, ground and water to useful heat. They also can utilize waste energy from industrial processes and exhaust air from households.

As it is well known Heat Pump (HP further in this text) system consists of a heat source, the heat pump unit and a distribution system to heat/cool the building. Heat transfer fluid transports the heat from a low-energy source to a higher energy sink, but the direction of this cycle can be switched the same machine can be used for heating and cooling. Underground can be utilized as a heat source, a heat sink and a thermal energy reservoir, especially suitable for storing large quantities of heat or cold over longer periods of time. It is highly suitable for many applications in the low-temperature range, due to the large volumes available and its nearly uniform temperature. Apart from heating, such systems can also be used for space cooling. However, there is growing number of installations implementing direct cooling from the underground during the summer without application of a HP. Ioan Sarbu and Calin Sebarchievici provided in their paper /3/ detailed literature review of the fundamental technical, thermodynamic and engineering knowledge relevant for the GSHP's components and systems, and their recent advances.

Directive on the promotion of the use of energy from renewable sources (2009/28/EC RES Directive, § 2 /1/) HP is currently in revision stage (Jaap Hogeling's expectation is that its text related to HP's will be more clear explained by the 2009/28/EC Recital 31 as follows: HP's enabling the use of aero-thermal, geothermal or hydrothermal heat at a useful temperature level need electricity or other auxiliary energy to function. The energy used to drive heat pumps should therefore be deducted from the total usable heat. Only heat pumps with an output that significantly exceeds the primary energy needed to drive it should be taken into account. Which means that only the part after the deduction of the primary energy used by the HP (including the auxiliary) will be

considered as renewable useful heat. Concerning the development of specific guidelines for planning, design and construction of systems for thermal use of underground, as well as production of relevant systems components (e.g. heat pumps, pipes, thermal insulation materials etc.), German Association of Engineers (VDI) (/5/-/8/), and American Society for Heating, Refrigerating and Air-conditioning Engineers (ASHRAE) /9/ did provide the international community with appropriate engineering knowledge base, which has been transferred/used in this study as the most reliable source of technical information. Beside the extensive engineering experience in all relevant phases: planning, design, construction, operation and maintenance, the field of underground thermal utilization and related technologies are still in intensive development and R&D aimed to further technical advance in efficiencies and cost-effectiveness, particularly in design methods, suitable materials selection and correct execution of drilling, installation and integration of plants into systems, of plants for thermal use of the underground. When implemented corresponding series of standards and guidelines (EC, VDI and ASHRAE) economically and technically satisfactory plants can be guaranteed, which operate without disruption and without causing negative effects on the environment, even for long-term operation. In this paper reviewed projects has been implemented relevant design methodology optimization presented in four parts of guidelines series VDI 4640: Fundamentals, approvals, environmental aspects; Ground source heat pump systems; Underground thermal energy storage and forth - Direct uses. M. Reuss, E. Konstantinidou are authors of fine review of the first 10 years of implementation of the VDI 4640 – German guidelines for ground coupled heat pumps, UTES and direct thermal use of the underground /10/.

2. Systems characteristics and performance

Building site relevant data. In terms of energy efficiency, the building block has to be constructed in accordance with the relevant standards applicable to the building type and optimised with the reference to the energy efficiency. Although, there are different national, international as well standards of certain countries groups as EU, if our goal is realy sustainability, and it is to be, then ZFEB[1] should be the adopted optimization criteria what means that all kinds of energy loads are to be minimized. Hence, in accordance with such goals designers should explore solutions and take adequate decisions concerning the envelope wall the transfer coefficients and lighting quality levels necessary for certain human activities. Practices of energy efficiency maximization approach are to be applied. Combination of quasi-stationary calculations and dynamic sumulations of cooling and heating loads are performed concerning the virtual level architectural details and the feasibility character of the study. However, building/HVAC and energy supply systems much more accurate analysis, and final design/optimization via dynamic integrated building/HVAC and other technical systems performance simulations and energy efficiency optimization are to be implemented in the future project development focusing at: sustainable energy management, cost effectiveness, performance and reliability of the final selection of materials and technologies implementation. Later in this paper, reviewed case studies will demonstrate that such targets can be realized.

Systems Characteristics /6/. On the VDI 4640 the thermal use of the underground, up to approximately 400 meters depth is technically feasible and relevant technical guidelines are presented for the following applications:

Ground source heat pump systems - Part 2 /6/:

- Heat pump systems for heating,
- Heat pump systems for heating and cooling (in cooling operation, the cooling can be achieved via the heat pump and/or directly from the underground by circumventing the heat pump).
- Refrigeration machines for cooling.

Ground heat exchangers or the groundwater directly are used as heat transfer media, and ground heat collectors, borehole heat exchangers and other special ground heat exchanger models are in use as ground heat exchangers.

- Groundwater can stem from aquifers via wells, and from pits or from tunnel drainage.

Underground thermal energy storage - Part 3 /7/:

- Storage systems for heating (solar energy, waste heat, environmental heat are all used as heat sources).
- Storage systems for cooling (cold source: environmental cold)
- Storage systems for heating and cooling (in connection with heat pumps and without heat pumps, using environmental cold/heat

Ground heat exchangers or direct use of the ground-water as a heat transfer fluid (aquifer storage) are used.

Direct uses - Part 4 /8/:

A heat pump or a refrigeration unit are note used here: Cooling using groundwater; Heating using groundwater; and Air heating / cooling in the underground

Underground thermal regime. The temperature of the earth surface is on average at around 11 - 13 °C throughout the world. It is determined by an equilibrium between the radiating solar energy, thermal radiation into space, geothermal heat flow, and variants/interferences of these factors. Due to the, relatively very small heat flows from the interior of the earth natural state is disturbed by heat withdrawal or heat injection, the thermal deficit or thermal surplus must be rebalanced by heat transfer. In the case of ground source heat pumps, it is desirable that the underground has a high heat capacity and intensity of heat conduction as then the required heat reaches the wells or the ground heat exchangers particularly easily, or can be taken away from there in the underground. However, In the case of thermal energy storage, higher heat transfer capacity brings higher heat/cold losses. Heat transfer of underground by conduction, at steady state described by the thermal conductivity λ (in W/(m · K), and by the thermal diffusivity a (m^2/s), is to be determined taking in

[1] ZFEB – Zero Fossil Energy Building

account the hydraulic conductivity of the rocks in the underground (permeability in m/s) and the convective heat transport, as well as specific heat capacity ($\rho \cdot c$) to determine the storage of thermal energy (in kJ/ ($m^3 \cdot$ K)). In addition rock proportion and the liquid proportion must be taken into account as well as the fact that thermal conductivity of certain rocks can have different values in different directions.

The hydraulic conductivity depends on whether the underground is built up of unconsolidated or consolidated rock. There is difference between pore and fracture permeability. Guideline values for the permeability of unconsolidated rock are given in Table 2. in Annex. Consolidated rocks display greater variation in water permeability, due to the very irregular distribution of the fractures. This heterogeneity is particularly marked in consolidated rocks; therefore they should only be used for thermal purposes following a thorough investigation.

The contribution of geothermal heat flow in the overall thermal balance of the underground varies greatly with depth. In the case of plant close to the surface up to the neutral zone at a depth of approx. 10 to 20 m, the energy used to equalize the thermal deficit or surplus consists almost exclusively of solar radiation and percolating water, so that the influence of the geothermal heat flow can be ignored. Only at depths between 20 to 100 m a contribution of geothermal heat flow can be observed. Plants at greater depths (from approx. 100 m) are then primarily influenced by the geothermal heat flow.

System design approach. According to VDI 4640, design approach of plants for underground thermal use, two cases must be differentiated: short-term influence (operation of the plant with maximum output), and long-term influence (long-term operation of the plant with medium output). In both cases, the temperatures prescribed by the plant (e.g. minimum evaporation temperature of a HP) and the temperature limits determined by the underground must be observed. It is important that a clear differentiation is made between the heating and cooling requirements of a building or process and the heat extracted or added to the underground.

In the case of ground source HP's with ground heat collectors, an under-dimensioning of the collectors can lead to locally limited effects on the vegetation (extension of the cold period). In general, under-dimensioning results in lower heat source temperatures and thus a smaller annual performance factor. In extreme cases, heat source temperatures at the lower deployment limit for the heat pumps can occur. For ground source HP's with borehole heat exchangers, under-dimensioning during full load operation can have the consequence of very low heat source temperatures in the short term too, up to the lower deployment limits of the heat pumps. In addition, under-dimensioning can lead to falling heat source temperatures from heating period to heating period in the long term, if inadequate regeneration is provided.

3. GWHP assisted refurbishment of old village house to approach NZFE status

M.S. Todorovic and M.Cokic presented results of R&D on refurbishment design and technologies related particularly to old traditional village houses providing their residents with: improved thermally indoor environment IEQ (Indoor Environment Quality) by air-conditioning; sanitary water and electricity supply; and an access to the ICT networks /19/. Their research encompasses total BPS (Building Performance Simulation) and energy efficiency optimization of the reconstructed building for local typical meteorological year obtaining its zero fossil energy and healthy IEQ status.

The case study house was constructed of wooden skeleton and cob–a mixture of mud, straw, wood chips and sand (see Fig.1). Determined was strategy, reconstruction means, appropriate RES (Renewable Energy Sources) technologies and whole integrated sustainable building design to turn the building status to the contemporary living conditions, and environmentally conscious status preserving local architecture, construction traditions and culture. Analyzed is existing house renovated with the reference to its initial state, and compared with several scenarios of RES integrated refurbished house models using Bentley AECOsim Energy Simulator (see AECOsim Building Designer house model on Fig.1) integrated with the EnergyPlus. It has been shown, that enough minimized energy loads, can be satisfied exclusively by RES (PV powered Ground Water HP and biomass), and in addition based on RES use can be produced surplus electricity and sent to the grid. Heating and cooling loads are minimized, HVAC and all other technical systems energy efficiency is optimized, photovoltaic panels are used for the electrical energy supply for Air-Conditioning (in heating regimes extremes assisted by biomass), lighting, electronics, appliances and sanitary water heating. Further R&D needs: house structure/HVAC/RES integrated reconstruction technologies.

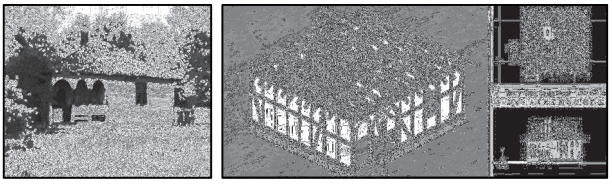

Fig. 1. AECOsim Building Designer house model with displayed roof and envelope structure (right)

Building's Energy Refurbishment Models. Energy analysis includes demands of five models. Model (MO1) is a house in its present state, while the other models have insulation layers added to improve the thermal properties of the building. In /1/ (Tables 1, 2) are given data on the house structural elements and data on the heat transmission coefficient values for current building and models of a the defined levels of energy refurbishment.

In addition to air-conditioning household total energy demand calculations include electricity use for interior lighting, home appliances, and sanitary water heating. Therefore, the additional use of electricity for domestic hot water, as well as the additional washing machine energy use was calculated for models MO2 - MO5. Fig. 2 displays the specific heat losses and gains and Fig. 3. shows heating and cooling loads in conditioned ground floor.

Interior lighting, home appliances and hot water supply (HWS) energy loads are shown in Table 3. The energy demands are calculated according to daily household needs, occupation and illumination.

Table 1. House elements - layers structure and thickness

Construction layers thickness d [m]					
(ins. to outside)	M O1	MO2-MO5	(above to below)	M O1	MO2-MO5
Ground floor			Ceiling/Internal floor		
Timber flooring	–	0.02	Timber board	–	0.03
Concrete screed	–	0.05	Mineral wool	–	Table 3
Vapor barrier	–	0.00017	Timber board	0.03	0.03
Mineral wool	–	Table 3.	Roof		
Bituminous waterproofing	–	0.003	Clay tile - Red/Brown	0.01	0.01
Clay, dry	50	*	Waterproofing	–	0.00038
Wall			Mineral wool	–	Table 3
Plaster	0.01	0.02	Glass wool	–	Table 3
Cob [9]/Wooden beams	0.15	0.15	Vapor barrier	–	0.00017
EPS	–	Table 3.	Gypsum board	–	0.0125
Plaster	0.01	0.02	Gypsum board	–	0.0125 (MO5)

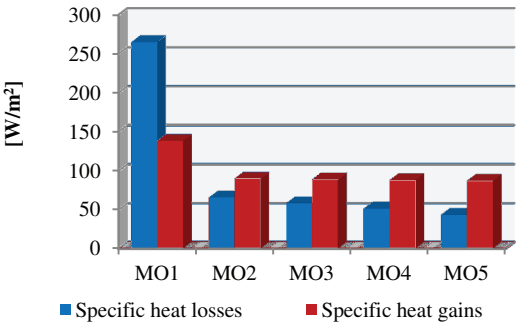

Fig. 2 Specific heat losses and gains

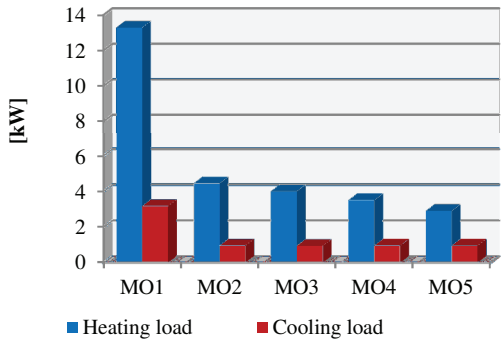

Fig. 3 Heating and cooling loads

With RES Energy Mix to NZFE house. Fig. 4. displays the annual solar radiation profile for the city of Ćuprija that was used for the calculation of solar PV equipment, and Fig. 5. displays groundwater temperature oscillation profile on the groundwater measuring station located about 1 km from Ribare village. For air-conditioning (AC), particularly summer cooling regime is foreseen by the PV electricity powered ground water heat pump (GWHP) REHAU AQUA type 7.

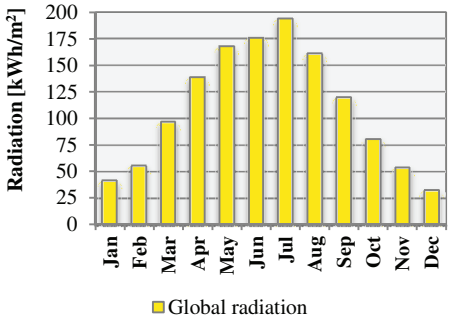

Fig. 4. Annual solar radiation profile, Ćuprija

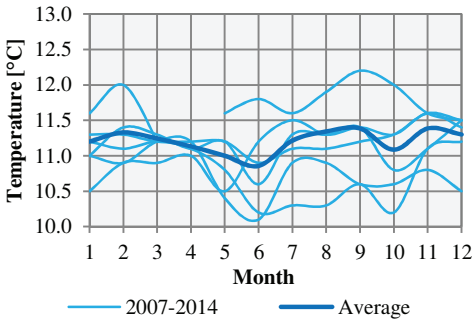

Fig. 5 Groundwater temperature profile, Ribare

Table 2. Heat transmission coefficient values

U values	MO1	MO2	MO3	MO4	MO5
Constr. element	U [W/m²K]				
Ground floor	1.162	0.374	0.294	0.196	0.098
Wall - Ground floor	1.920	0.378	0.285	0.192	0.097
Ceiling/Internal floor	2.187	0.367	0.309		
Wall - Attic	0.855	0.300	0.239	0.169	0.090
Roof	4.995	0.387	0.298	0.185	0.099
Door	5.333	1.333			
Window	5.801	1.039			

Table 3. Design Loads values

Design Loads [W]					
Process	MO1	MO2	MO3	MO4	MO5
Heating	13284	4460	4024	3522	2921
Cooling	3184	969	962	970	971
El. Appliances	360	463			
Lighting	320				
HWS	0	1500			

It has a vertical open circuit system that uses groundwater from production well as the heat sink (its working fluid to reject condensation heat to it). After realizing cooling process ground water returns to the injection well. In addition to powering the selected heat pump PV electricity is foreseen to supply all other electrical loads water heating (HWS), lighting, electronics and appliances. Determined area of PV panels sized to satisfy total electrical energy needs (AC, lighting, electronics and appliances are given in Table 4.).

Data given in the column PVmin correspond to sized PV area aimed to satisfy electricity needs when the largest PV produced power is (August), and PV max data relate to PV area sized to satisfy el. loads when PV produced power is smallest (December). It is to be drawn attention to the colored values light blue (PV power less than needed) and house is to use electricity from the grid, and light rose colored data (house integrated PV will produce more than needed and the refurbished house will send electricity to the grid). With more detailed analysis has been shown that

the PVmin sized PV resulted in so called net Zero fossil fueled house, and that PVmax is clearly Energy Plus house – producing more electrical energy and sending it to the grid than its electrical energy demand is.

The results of the analysis are imposing some additional questions that should provide the basis for further research. This raises the question of justification of the building renovation, which should be considered through the analysis of the current state of the building and its residual life, the total cost of rehabilitation and refurbishment, as well as the overall impact of the process on the environment through CO_2 emission. In Table 5 are presented preliminary calculated quantities: total investment costs (construction materials, components and works; all technical systems components and installations including biomass utilization unit and PV power plant); total energy saving values; and investment simple payback periods.

In terms of the preservation of traditional architecture and environmental sustainability, it is necessary to consider the construction method of new houses and renovation of existing ones, by use of the material with similar composition and properties, and that is accessible on-site or near the settlement. Primarily, this is the reference to the walls, made from earth material.

Table 4. Electricity demands and PV electricity production

MO2-MO5 – Total electricity demand and PV electricity production [kWh]					
Month	Demands	PVmin		PVmax	
		[kWh]	[%]	[kWh]	[%]
Jan	219.60	107	48.7	284	129.3
Feb	195.91	146	74.5	391	199.6
Mar	214.35	247	115.2	659	307.4
Apr	204.22	256	125.4	683	334.4
May	216.34	306	141.4	815	376.7
Jun	226.07	309	136.7	824	364.5
Jul	243.87	330	135.3	879	360.4
Aug	245.95	314	127.7	838	340.7
Sep	211.94	250	118.0	665	313.8
Oct	214.19	211	98.5	563	262.9
Nov	211.52	134	63.4	357	168.8
Dec	221.11	86	38.9	229	103.6
Total	2625.06	2696.00		7187.00	
PV panels power production					
Number of modules		9		24	
Installed PV power [kW]		2.25		6.00	
Total panels area [m^2]		13.14		35.04	

Table 5. Investment costs, annual energy costs, annual energy saving values and simple payback period

Model	Total investment costs [€]	Annual energy costs [€/year]	Annual energy costs savings [€/year]	Simple payback period [year]
MO1	0	1061	0	0
MO2	10408	142	920	11.31
MO3	10892	123	939	11.60
MO4	11735	104	957	12.26
MO5	14183	84	977	14.51

The above mentioned procedures are entailing the necessity of further governmental endorsed planning and realization of much broader "at large" implementation of similar projects to be reached transitions to the use of fully "green" energy sources, as well as its consequences on a households and its surroundings in a long term, particularly taking in account the highest impact on CO_2 emission reduction of MO5 model.

4. PV&GWHP integrated refurbishment of social housing

This case study addresses large large scale residential/municipal deep energy refurbishment (integrated with renewable energy soources (RES) of construction and HVAC system engineering of residential muiltiaparment social houseing /17/.

Numerous residential, social housing buildings erected in 1950s to 1980s, during the period of intensive construction in Belgrade, became dilapidated with visibly damaged façades, moisture penetration into the walls, inadequate indoor air temperature with too high air infiltration, of extremely high District Heating Systems (DHS's) energy consumption and increasing electricity use by split air-conditioning units (installed in approx. 80-90% of apartments) leading to the alarming summer peaking loads in the electricity distribution grid.

Architectural revitalization, through the application of energy efficiency improvement measures is to increase building's energy efficiency to the level which will ensure cost effective integration of renewable energy sources (RES) – integrated energy refurbishment. For "Case building" (Fig.6.) in New Belgrade (useful area 13000 m^2) a couple of scenarios/models of the retrofitted building (different levels of thermal insulation, reduction of window area and replacement of windows with new windows of a few different U-values and ratios between visible light transmittance and solar heat gain coefficients) have been defined and computer models were created. BPS (building Performance Simulations) were performed for the Typical Meteorological Year of Belgrade, for the construction models: MO1 model of the building current conditions according to the design of 1969; MO0 model of the building as it is today; MO2 - MO5 are the models of the building with improved energy efficiency construction; M – model in accordance with the DHS energy consumption monitoring data provided by the Belgrade DHS district heating system plant (measured at the DHS substation's heat exchanger).

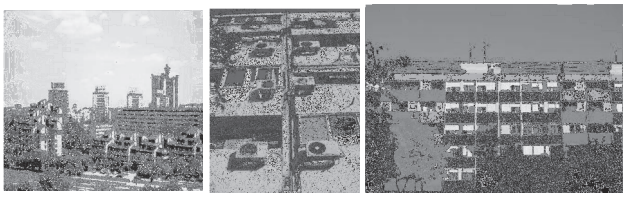

Fig. 6. Deep Refurbished building" with the BIPV

The results presented on Figure 7. (left) show that with the reference to the basic model MO0 specific heating losses are reduced ~4 times (from MO0 to MO5), and specific heat gains are reduced more than 4 times. Hence, installed heating power of the DHS heat exchanger in DHS substation in buildings after refurbishment is to be 4 times smaller, and similar order of magnitude will be reduction of necessary

installed power of air-conditioning split units. Diagram on the Figure 7. (right) shows that the annual energy demand for heating is reduced also by 4 times. There is fine similarity of the results of monitored (DHS heat exchanger) and energy use determined by the dynamic simulations (MO0).

By the preformed BPS predicted refurbishment results are excellent approval that approach to refurbishment can successfully lead to the effective integration of solar energy or other RES utilization. Namely, not only reduced loads by the refurbished envelope's thermal features, but the fact that building's envelope construction attacked by the moisture penetration needs intervention reconstruction to the ventilated façade offer challenge to perform "Synergetic refurbishment approach" increasing energy efficiency and integrated solar energy utilization. Concerning the construction works and existing building structure statics, low weight photovoltaic (PV) cells and PV system's simplicity would make it the most appropriate of the solar technologies candidate to be integrated in renewed façade. As the most cost-effective variant of interventions for architectural and energy reconstruction of the analyzed "case building" has been selected complete construction of a new residential floor (as financial potential source of funding by selling new-built apartments), ending with the green roof.

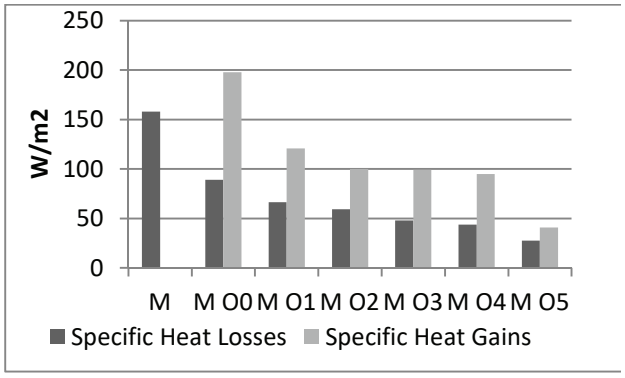

Fig. 7. Specific heating and cooling loads

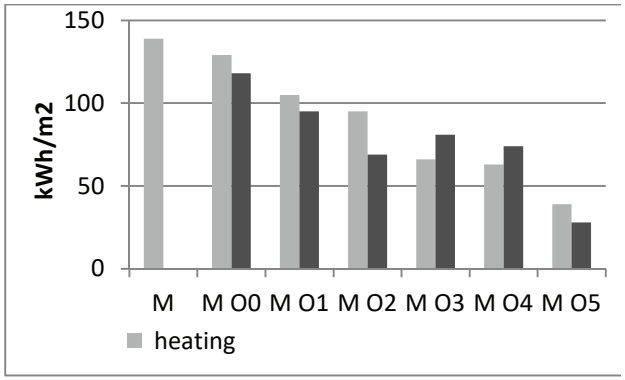

Fig. 8. Specific annual heating and cooling energy demand

The main relevant characteristics of selected PV modules type BP SX 3195 are: Maximal power 195W; Voltage on P_{max} 24,4V; Current at P_{max} 7,96A; Short-circuit current 8,6A; Open-circuit current 30,7V; and Area is 1,41 m^2. For the Belgrade Typical Meteorological Year, implementing BPS have been determined incident solar global radiation and potentially produced electricity by the BIPV – integrated PV in the building's facade (Fig. 6). For the total installed area on the west oriented facade of 1310 square meters total installed PV power potential for selected PV cells/panels is 179,7 kW. One third of that power would be enough to power all existing AC split units in the same building.

Thus, obtained result is more than significant justification to proceed with development of this project and other similar holistic approaches to the "Cost Effective Solar Integrated Refurbishment of Residential Buildings" and to accomplish fully integrated residential/municipal energy refurbishment, encompassing engineering solutions as follows:

- The facade's synergetic reconstruction to the highly thermally insulated PV integrated "ventilated – façade" did result in significant reduction of heating and cooling loads in building ~ 4 times with the reference to the existing; replacement of heat exchanger (4 times lower capacity and of higher energy efficiency at the current technology level) in building's substation of DHS).
- Thus liberated 75 – 80% of the existing installed DH capacity could be directed to other users - new built space in the same "Case building" or other new buildings spaces within the Belgrade municipal DHS.
- As New Belgrade has been built on "ground-water" existing air-source/sink split units are to be replaced by the ground-water heat pump (HP), resulting in reduction of necessary electrical power – order of the COP ratio change related to the source/sink (air/ground-water) temperature difference. Also, ground water PV powered HP can be used energy efficiently for heating in certain periods of year, what will further contribute to the DHS demand reduction and in the same time further increase of the renewable energy balance.
- As in the design conditions, one third of the potentially integrated PV panels would be enough to power all existing AC split units in the same building, there are prospects when there is surplus of produced electricity by the integrated PV for the HP operation with the reference to the HP demand, to use PV electricity for lighting, and appliances, etc. or even send it to the electrical grid, further increasing the renewable energy balance and cost-effectiveness of selling PV power at the very attractive Feed-in Tariff prices.

New vision on the prospective development of this project came up with the reference to the recently published in CIBSE Journal Tim Dwyer's CPD[2] article "Employing Distributed Mini Heat Pumps With A Shared Ground Loop In Social Housing" /20/ which presented how the use of mini heat pumps by apartments in social housing schemes that share a common ground loop (see Fig. 8) can be an effective way of reducing carbon output and cutting energy costs. A generic 16-floor, 95-apartment southern England lightweight concrete tower block that was originally completed in the mid 1960s, with an average apartment size of 50m^2, is used as an example. Cited CPD design proposes the application of distributed mini heat pumps that share a common

[2] CPD – Continuing Professional Development

ground loop as a means of reducing operational carbon impact – and cost – as part of the holistic improvement of this vital housing stock.

In any refurbishment project, the essential is first stage – following appropriate surveys and life-cycle cost benefit analysis. Building physics is to ensure heating and cooling loads to be minimized. The same way considering the cold weather building's performance, it is crucially important to ensure that the building alterations minimize the potential for overheating /19/. An example of a wall-hung 3kW mini heat pump driven by an almost-silent rotary vane (rolling piston, fixed vane) compressor is shown on Figure 3 (see boxout).

The evaporator of this vapour compression machine draws heat from the ground via the circulation of 'brine' through a ground loop and an internal building riser loop. The circulating working fluid used in the closed-loop ground heat exchanger is usually water with antifreeze (commonly ethylene glycol and propylene glycol) added to provide protection from freezing, plus inhibitors to prevent corrosion and bacterial growth. This offers freeze protection down to at least -15°C. /19/.

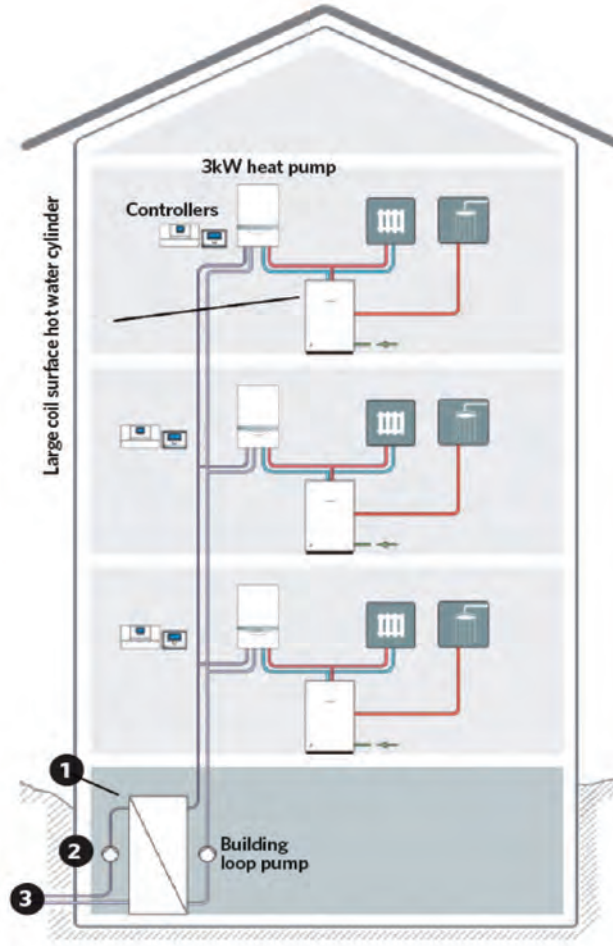

Fig. 8. Scheme of Distributed mini heat pumps with a shared ground loop: 1-Plate heat exchanger, 2-Ground loop pump, 3-To and from ground loop

At the building site, the ground temperature seasonally fluctuates to depths of about 15m where the temperature is approximately equal to the mean annual air temperature (8-11°C in the UK). Below this, the ground temperature increases at, on average, 2.6°C per 100m, Generally, mean temperatures at 100m depth in the UK vary between about 7°C and 15°C. Hence, in winter, the underground temperatures are higher than the air temperature, and in summer are lower than the air temperature. For the careful site assessment is required to determine an appropriate ground loop design and, particularly where bore holes are to be considered, the consultancy of geologists is needed.

A high-efficiency, low-pressure drop plate heat exchanger is required between the ground array and the internal building riser loop, to provide a hydraulic break. The internal riser must be sized to support all heat pumps running at the same time, taking in account that the heat pumps may have specific pressure limitations that influence the riser design.

Circulation pumps will be required for the ground array as well as for the internal riser, and both these will need to be sized for full flow requirements – careful system design is important to ensure effective hydronic operation. Since the circulating fluid is likely to be below the dew-point temperature of the surrounding air in the riser, proper insulation and vapour barriers are essential /19/.

The load anaysis confirmed that each flat could potentially be serviced by its own 3kW wall-hung R410a heat pump and DHW tank. The low-grade heat from a ground-sourced building loop is sufficient to deliver flow water temperatures of up to 60°C by the heat pump with the coefficient of performance (COP) of approximately 2.5 and is then used to heat the apartment through oversized radiators and to produce DHW.

The ground array has been sized to deliver brine to the heat pumps at a temperature of between 0°C and 8°C. 15450[4] indicates that a borehole in dry sediment can provide 20W per metre, and that 'normal' underground and water-saturated sediment can provide 50W per metre.) Considering the required heating temperature and predicted range of borehole extraction temperatures, the seasonal heating COP (SCOP) of the 3kW heat pump is 3.7, while the heating annual electrical requirement is 1,922kWh. For providing DHW at an satisfactory temperature, the average COP was estimated as 2.8 and so the annual electrical energy requirement is 818kWh.

5. Energy pile system performance

There are many encouraging results of energy piles systems design, construction and implementation worldwide (/21/-/23/-/24/). One of those is the Dock Midfield is the new terminal E of the Zürich airport. As the upper ground layer is too soft to support the loads of the building, 440 foundation piles have been built. More than 300 piles have been converted into energy piles in order to contribute to the heating and cooling of the building /11/.

Measurements of the energy pile system begun in October 2004 for a 2 years period. The results of the first year are presented. The measured system heat balance, and in particular the annual heating and cooling demands are close to the design values. Furthermore the thermal performances of the system are very good. It confirms the necessity and the suitability of a detailed and careful design process for this type of system. The design procedure has been based on detailed studies, involving response test analysis, thermal dynamic simulations of the building and the energy pile system.

The pile heat balance indicates that 39% of the annual extracted energy is injected by geo-cooling. This ratio is compatible and conform to the system design predictions. An improving potential lies in the cooling distribution. It could increase the global annual system efficiency from 4.9 to 5.4.

6. Energy storage in abandoned mines

Mining-energy-industrial system in Kosovo Basin (/26/, /27/) can serve as one case example of large lignite basin's most important aspects of the structural changes caused by the mining exploitation: consumption of large areas of land, degradation of eco-systems; people migration and changes in the pattern of settlements/villages; potential high level of environment pollution (air, water, land and living species) from the industrial complex (/25/-/28/). Development of the Mining-energy-industrial system in Kosovo basin have accelerated the socio-economic transformations (urbanisation, de-agrarisation) and caused the changes in the location and functions of town centers. Finally, the surface mining exploitation and the building and functioning of thermal energy and other systems for coal processing represent a major structural change which requires unique and specific approaches to planning in large lignite basins.

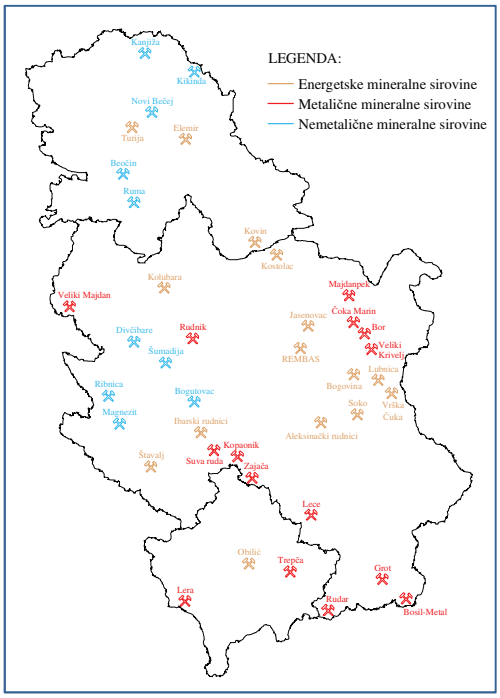

Fig.9. Energy, non- and metallic mineral mines in Serbia

Sustainable mining and consistent implementation of the mine closure planning approach require a developed mutual partnership of mining companies, spatial planners, investors, institutions and local communities to identify creative, profitable, environmentally-sound and socially-responsible management and reuse of mine lands /25/.

Transnational and cross-border cooperation between countries in the Danube River Basin is extremely important /25/, bearing in mind the transnational risks of large mining environmental hotspots in both countries which need ecological rehabilitation (accident of the cyanide spill into the river Tisa from the gold mines in northern Romania in 2000) left behind long-term consequences for the ecosystems in Romania, Hungary and Serbia /26/.

On Fig.9. is given map of Serbia with legend of main mines for energy, metallic and non-metallic mineral resources (Prof. Dr. S.Vujić, Mines Institute Belgrade). Abandoned mines (where mining activities occurred, but acceptable mine closure/reclamation did not take place or was incomplete) contribute to the legacy of environmental degradation left by historic mining which occurred before mine closure regulations were founded. In Canada regulators have initiated various programs to assess and remediate the abandoned mines within their jurisdictions.

7. Conclusions

Trying to find a way to make a turn from the current one-way irreversibility to sustainability, in addition to the uninterrupted R&D aimed to advance RES (Renewable Energy Sources) technologies it is necessary to find innovative ways of universal schemes, quantities, indicators and criteria relevant for the sustainable Earth resources utilization, environment protection and/or already damaged environment recovery) to reach humanity's resilience and sustainability. Availability of most types of RES is interruptible and of variable intensity. Therefore, energy storage is important for the large-scale utilization of RES, and large-scale storage systems require large storage volumes. Worldwide, many abandoned mines (of coal or minerals) offer large storage volumes almost ready-made to be used directly for energy storage, and thus, old cole mines could become even part of green future.

References

[1] Directive 2009/28/Ec Res Directive, § 2, Definition Of Heat Pumps And Their Use Of Renewable Energy Sources, Alex Vanden Borre, EU Policy, REHVA Journal, pp. 38-39, August 2011,

[2] Ground-Source Heat Pump Systems The European Experience, Ladislaus Rybach and Burkhard Sanner, CHC Bulletin, pp. 16-26, March 2000.

[3] General Review Of Ground-Source Heat Pump Systems For Heating And Cooling Of Buildings, Ioan Sarbu, Calin Sebarchievici, Energy and Buildings, Volume 70, February 2014, Pages 441-454

[4] Heat Pumps: A Gem In Energy Efficiency And Renewable Energy Use, www.ehpa.org/uploads/media/EHPA_heat_pumps_triple_dividend.pdf.

[5] Vdi-Richtlinien, Thermische Nutzung Des Untergrunds, Blatt 1 - Grundlagen, Genehmigungen, Umweltaspekt, ICS 27.010, 27.080, 27.200, June 2010.

[6] Vdi-Richtlinien, Thermische Nutzung Des Untergrunds, Blatt 2 - Erdgekoppelte Wärmepumpenanlagen, ICS 27.080, September 2001.

[7] Vdi-Richtlinien, Thermische Nutzung Des Untergrunds, Blatt 3 - Unterirdische Thermische Energiespeicher, ICS 27.080, Juni 2001.

[8] Vdi-Richtlinien, Thermische Nutzung Des Untergrunds, Blatt 4 - Direkte Nutzungen, ICS 27.080, September 2004.

[9] Methods Of Testing For Rating Of Multipurpose Heat Pumps For Residential Space Conditioning And Water Heating, Ansi/Ashrae Standard 206-2013, ISSN 1041-2336.

[10] 10 Years Vdi 4640 – German Guidelines For Ground Coupled Heat Pumps, Utes And Direct Thermal Use Of The Underground, M. Reuss, E. Konstantinidou, https://intraweb.stockton.edu/eyos/energy_studies/content/docs/FINAL_PAPERS/5A-3.pdf.

[11] Measured Thermal Performance Of The Dock Miffield Energy Pile System At Zuerich Airport, Daniel Pahud, Markus Hubbuch, 14th Schweizerische Status-Seminar "Energie und Umweltforschung in Bauwesen, 7.8. September 2006 ETH.

[12] History Of Heat Pumps Swiss Contributions And International Milestones, M. Zogg, 9th International IEA Heat Pump Conference, pp. 1-17, 2008.

[13] Ground Source Heat Pumps – History, Development, Current Status, And Future Prospects, Burkhard Sanner, 12th IEA Heat Pump Conference 2017 Proceedings, K.2.9.1,

[14] Case Study Of A Btes And Energy Piles Application For A Belgian Hospital, J. Desmedt, H. Hoes, http://citeseerx.ist.psu.edu/viewdoc/download?doi=10.1.1.507.2234&rep=rep1&type=pdf

[15] IEA HPP ANNEX 42: HEAT PUMPS IN SMART GRIDS Task 1 (i): Market Overview United Kingdom, Delta Energy & Environment, 2014.

[16] THE UNDERGROUND WATER, GROUND, AND ENERGY PILES USED AS HEAT SINK/HEAT SOURCE FOR HEAT PUMP OPERATION FOR HARBOUR CITY BRATISLAVA, Feasibility Study VEA-INVI for BDSP, Belgrade, 2008.

[17] Large Scale Residential/Municipal Res Integrated Refurbishment Construction And Hvac Systems Engineering R&D Needs, ASHRAE, Todorovic S. Marija, Transactions, Volume 118, Part 1, 2012.

[18] Energy And Exergy Analysis Of A Ground Water Heat Pump System, Lei Fei, Hu Pingfang, Physics Procedia, Volume 24, Part A, pp. 169 - 175, 2012

[19] Deep Energy Refurbishment Of An Old Traditional Village House To Approach Zero Fossil Energy And Healthy Ieq Status, Miloš Čokić#1, Marija S. Todorović#2, CLIMA 2016 Conference, Aalborg, May 2016.

[20] Employing Distributed Mini Heat Pumps With A Shared Ground Loop In Social Housing, Tim Dwyer, CIBSE Journal, pp. 42-45, 2017.

[21] Ground Source Heat Pumps–History, Development, Current Status, And Future Prospects, Burkhard Sanner, 12th IEA Heat Pump Conference, pp.1-14, 2017.

[22] T. Amis, F. Loveridge, Energy Piles And Other Thermal Foundations For Gshp – Developments in UK practive and research, REHVA Journal, pp. 32-35, January, 2014.

[23] H. Yousefi, M. Hamlehdar, S. Tabasi, Y. Noorollahi, Economic And Thermodynamic Evaluations Of Using Geothermal Heat Pumps In Different Climate Zone (Case Study: Iran), Proceedings, 42nd Workshop on Geothermal Reservoir Engineering Stanford University, Stanford, California, February, 2017

[24] Nyers J., 2016, COP and Economic Analysis of the Heat Recovery from Waste Water using Heat Pumps, International J. Acta Polytechnica Hungarica Vol. 13, No. 5, pp. 135-154.

[25] Florea Gabrian C., Turdean N., Closing The Mines In Romania - A New Challenge, *www.infomine.com/library/publications/docs/Florea.pdf*

[26] Sustainable Land Management In Mining Areas In Serbia And Romania**,** Vesna Popović, Jelena Živanović Miljković, Jonel Subic, Andrei Jean-Vasile, Nedelcu Adrian and Eugen Nicolăescu, *Sustainability 7*, 11857-11877; doi:10.3390/su70911857, 2015

[27] Recultivation And Sustainable Development Of Coal Mining In Kolubara BASIN, Ivica Ristović, Milan Stojaković And Milivoj Vulić, http://www.doiserbia.nb.rs/img/doi/0354-9836/2010%20OnLine-First/0354-98361000002R.pdf **9**

[28] WebGIS Cadastre Of Abandoned Mines In Autonomous Province Of Vojvodina, Ranka Stanković, Nikola Vulović, Nikola Lilić, Ivan Obradović, Radule Tošović, Milica Pešić-Georgiadis, *Mining And Environmental Protection*, 2015

EXPRES 2018
ISBN: 978-86-919769-3-4

DYNAMIC MODELING OF µCHP IN MATLAB-SIMULINK AND CAPABILITY FOR SMART GRID

M. KARACSI[a], *P. KÁDÁR* [b]

Department of Power Systems, Faculty of Electrical Engineering, Óbuda University
H-1034 Budapest, Bécsi út 94., Hungary
[a]E-mail: karacsi.mark@kvk.uni-obuda.hu
[b]E-mail: kadar.peter@kvk.uni-obuda.hu

Nowadays micro-CHP (Combined Heat and Power) devices are getting more popular. These devices are sold without communication interface yet, so they are not able to be part of a smart grid. If we could manage to fit this systems to the "Smart philosophy" we will have a serious advantage in power network balance keeping. This advantage can lead us to be able to handle the stochastics power production of renewables. In this paper we investigate the possibility to create a dynamic MATLAB-SIMULINK model of a µCHP device. If we can build a proper model of a µCHP device, we will be able to investigate further effects of µCHP devices to the electrical network and we will be able to test the ability of the µCHP for smart grid and urban energy production. This model will help also for the system operators to handle better the power systems, keep the quality of the electricity and increase the system stability and redundancy.

Keywords: *microCHP, MATLAB, SIMULINK, Smart Grid, Micro Grid, urban energy production*

1. Introduction

From 2010 step by step the energy production is getting decentralized. These fact is not only appearing because of the popularity small sized solar panels and wind turbines, but the old transmission lines have reached their capacity and the expansion cost of them is horrible. If we are not investing in the transmission lines extension, the only way to provide enough energy for our growing energy consumption is to build small sized local power generators. The µCHP devices are one of the solutions what we can choose.

µCHP systems are typically household scale power plants which are providing firstly heat and secondary electric power. The key of the machine success is the advanced efficiency. The advantage of the machine is not mainly coming from it parts, it comes from its place. In case regular (separated) heat (or gas) and electricity connection, we pay a lot of system usage fee. [1] These fees are covering not just the initial and maintenance cost of those huge infrastructures, but also includes all the energy losses which are hppening from the production till the consumption (in Hungary the system usage fee for electricity is ~50% of the total bill). If we are using a µCHP device, (depending on the fuel type), our total losses are significantly decreases. The µCHP systems heat efficiency are similar with the modern gas boilers, but next to the produced heat, the µCHP can provide us some mechanical energy as well. This mechanical energy can be used for ventilation, air condition, or (like in our case) electricity production.

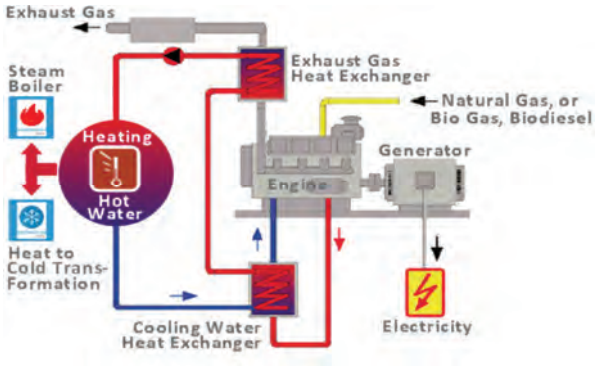

Fig. 1. Structure of a µCHP device [2]

In this case (compare to the regular heating system) the produced electricity is a clean profit for us. And this count not just the price of electron, but the price of system usage fee as well. This advantage is what can make a µCHP device to good environmental friendly investment. Next to the regular engined devices (LPG, natural gas, diesel, petrol) there are lot of R&D projects about Stirling engined and "green" fuel-cell powered µCHPs as well. [2] The traditional method of energy storage (in household scale) is still the batteries. This solution is still expensive, the cells lifetime is short and the LCA of these cells show us even more environmental problems. In case of series production of fuel-cell µCHP devices, there is a possibility to produce our hydrogen from renewable energy sources, and after store the H2 we can produce our heat and electricity whenever we want. But this solution needs some H2 producing development as well…

2. Modelling in MATLAB

Since we have only one test system at Óbuda University, the possibility to make different measurements on the system is limited. [3] The easiest way to cross this boarder is to build a dynamic µCHP model in MATLAB. At the beginning we were unsure that the software can handle this kind of models, but we had many previous measurements to test the software in case of success. This was also a useful method to validate our dynamic model what we make in MATLAB.

The first step was to create a board model. The development method was to build a simple model and make it more and more complex till we reach a realistic model, which can be used for tests. The first generation of the model includes just the asynchronous motor with network connection. In other hand our test system at Óbuda University is unique, because we use asynchronous machine for power production instead the regular synchronous generator.

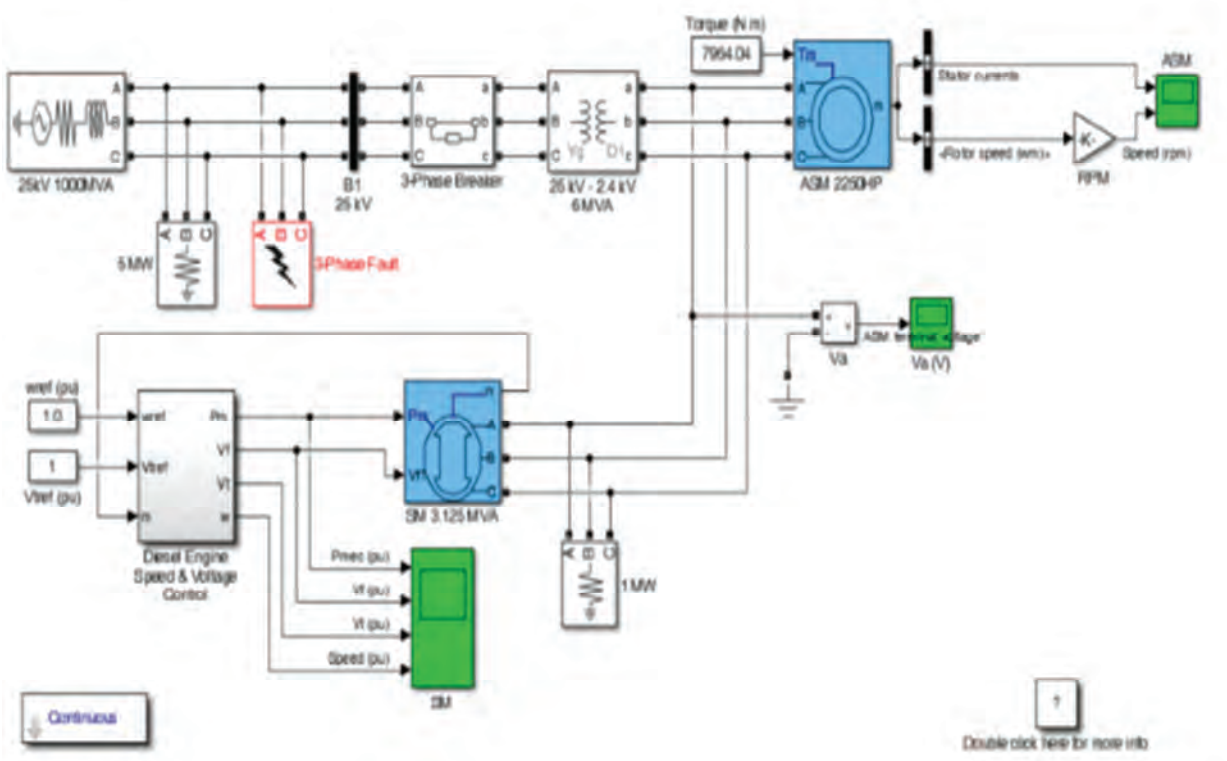

Fig. 2. First generation of µCHP model

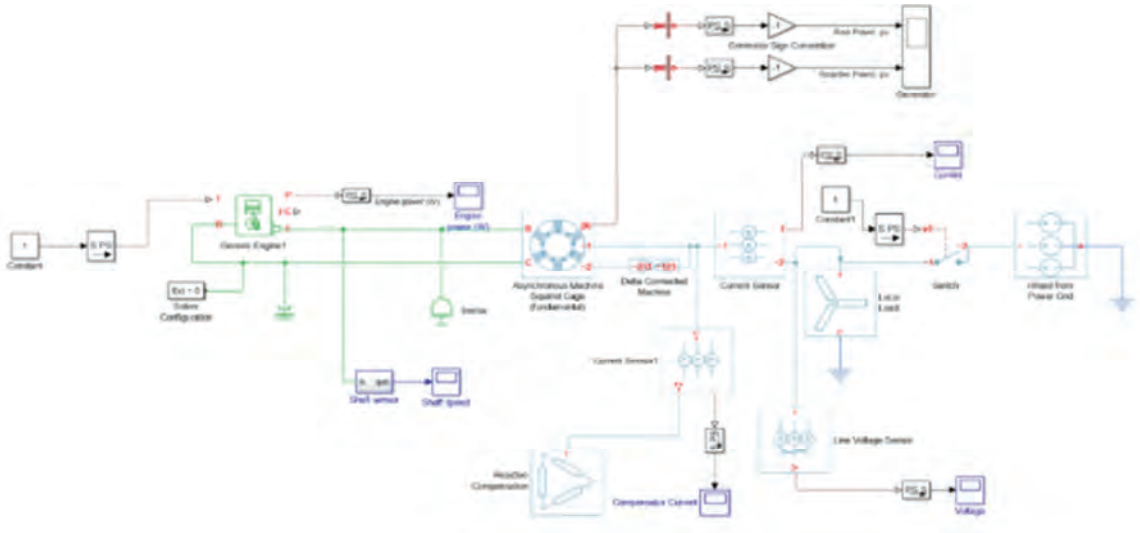

1. Figure Fifth generation of µCHP model

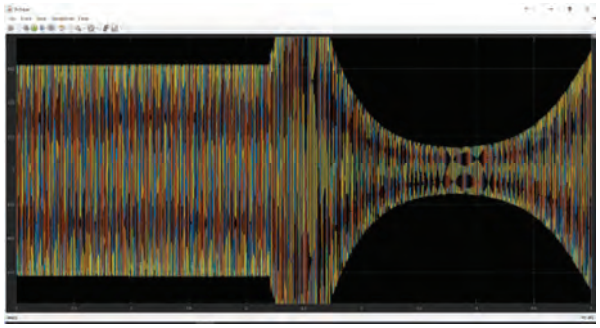

Fig. 4. Control crosscheck in case of network loss

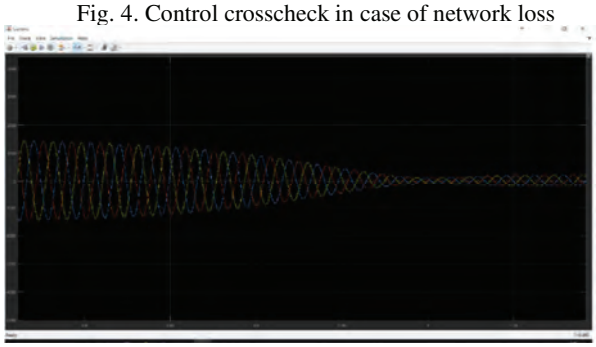

Fig. 5. Reactive power compensator check

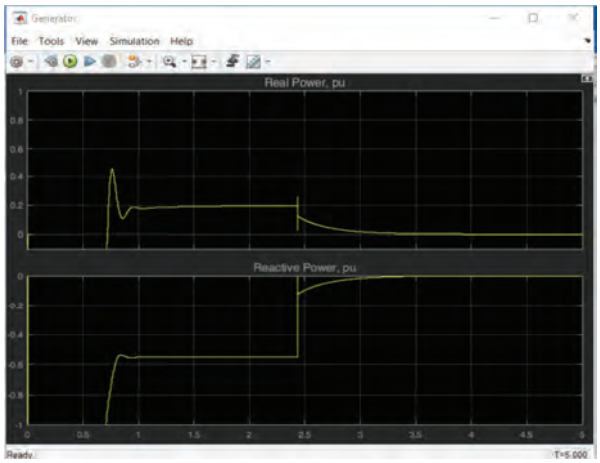

Fig. 6. Active and reactive power flow

In the second-generation model was the Otto engine integration with various measurements. This was a big step for us, because with the Otto engine we had to make many connections between different layers (power and mechanical), but finally we succeed. The third generation includes separate, variable loads, and more measurements. The fourth generation includes the switchable network connection, so from now on we could make separate island mode operation also. In this stage we realized, that the software works perfect. As we measured at the real system before, the dynamic model electromagnetic field was collapsing also whiteout reactive power compensation as well. So, in the fifth generation we built the compensation in the model also.

After every generation of the model, we had to make the validation progress. All the test results were surprisingly similar to the real-life measurements, so the validation of the dynamic µCHP model succeeded.

In the future we planning to make many different and more advanced test in MATLAB of µCHP systems such as µCHP massive spread effects to the power network, or integration of µCHP to Smart Grids. These tests will help us to define the number and sizes of µCHP systems to be part of the power network balancing in the system operator.

3. Fit to smart grid

"Smart grid" is a concept with many elements where monitoring and control of each element in the chain of generation, transmission, distribution and end-use allow our electricity delivery and use more efficient. [4] The active elements of the Smart Grid make able the network for self-healing and in case of power fail can crate and run stable standalone islands. For this concept can contribute to a smart µCHP device.

In a perfect Smart Grid, a µCHP device would have various measurements and connected interfaces to the system operator, which allows the system operator to use all µCHP device as a fully adjustable power plant within seconds.

Unfortunately, the Hungarian smart metering system is not so developed, and we cannot speak about smart grids as well. But we have two systems since decades, which are acting like a “semi smart” system. Both system has the same aim, but the communication line is different. The tone frequency ripple control system (the data goes thru the power lines) and the long wave ripple control system (you have one long wave radio tower, and you can cover 250km radius area). The only problem with this system, that the communication is only one way.

This system is called active DSM (Demand Site Management). Lot of household customer has a separate electricity meter and a relay box next to the “normal” one. Their network connection is the same, just has a separate subnetwork whit a complete different electricity meter. The tariff of this second electricity meter is lower (with 20-30%) than the regular energy price. They get this discount, because the allow the utility to switch this separate subnetwork on or off by the relay box (in case of need and next to the scheduled program). Mainly the users connect to this subnetwork massive energy consumer devices such as electrical water heater or heat storage stoves, which are not so sensitive for sudden power cut, or switching on. Because of the heat storage capacity of

these devices they even don't need to be turned on 7/24. The rules of switching by the law are the following:

- After switching on minimum one hour working
- Within 24 hours there must be a two-hour long period
- Within 24 hours must be eight hours of working time

Obviously in case of emergency, the utility can switch whenever wants. If we use this existing technology, to integrate µCHP devices, we will be able to give a start signal for them, to help us to create not just a DSM system, but an active power production system as well.
The µCHP devices mean new alternative for the distributed generation. These are fit to the small household generation and to the household measure emergency power source or also to larger microgrids.
In the figure 7 we provide a future map of the cooperation of the distributed power and heat generation devices in frame of a microgrid.
The only solution for extended microgrid is to have a distributed intelligent load, storage, generators and a central control facility that: [5]

- schedules the heat and power generation
- the load (DSM)
- cares for the reactive power and voltage regulation
- controls the island/net mode

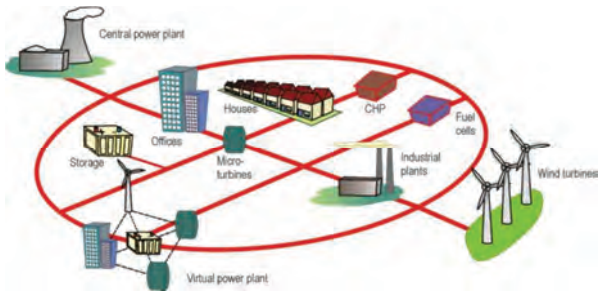

Fig. 7. Smart Grid with µCHP [4]

By our calculation we can built up a working Smart Grid with the existing ripple control technology and the µCHP systems.

Another problem when we are talking about distributed power generation, that the urban areas doesn't has any space. Because of the sizes, the noises and the exhaust gases the µCHP can be a good solution for urban areas as well. The cities where are common the natural gas network lines, and most of the household use natural gas to provide the heat and hot water need is a perfect place for µCHP systems. Since we know that µCHPs are mainly made to cover heat need and the ROI gets shorter as the running hours per year is growing, one household in not big enough for a complete µCHP. That's why you must install it for a bigger institute, office or industrial zone, or should connect more households to one µCHP. In this case we are maximizing annual occupancy.

Having a concrete example for office/schools opening hours category, applying the parameters of average consumptions of gas for electricity generation with 150 MWh/a, for heating we need 900 MWh/a, and assuming a government support like for this project in Germany. The results show that you will have the ROI for this investment in five years as the figure shows below. [7]

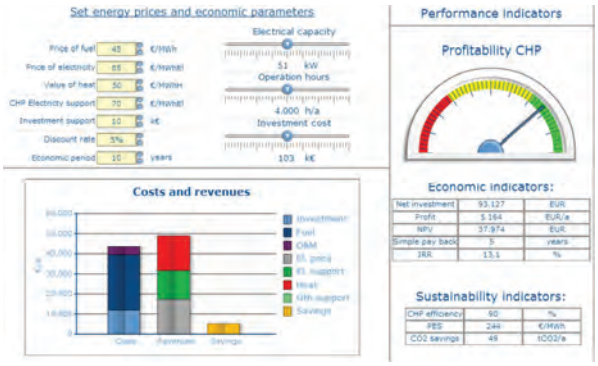

Fig. 8. Case study of a µCHP ROI

4. Conclusion

Lot of examples shown us in Europe, in the USA or in Japan, that µCHP systems can save us energy, money and CO_2 emission as well. If we could merge the µCHP technology with the Smart Grid philosophy, we would have a more useful result with a lot more benefits in Power Network site, and maybe this can be the solution of renewable energy source integration also to the power system.

5. Acknowledgement

I would like to thank for Óbuda University, which provided the conditions required for the preparation of studies and Mr. Imre Fejes and Attila Barlangi who helped us during the measurements. Here we would like to mention the Campus Hungary program, which supported the project and the presentation of the results.

References

[1] http://www.energysolutionscenter.org/gas_solutions/micro_chp_mchp.aspxmicro grid
[2] https://kunaifi.wordpress.com/2008/page/4/
[3] Peter Kadar, Karacsi Mark: Stand-alone island mode operation of microCHP device, IEEE 5th International

Symposium on Exploitation of Renewable Energy Sources, EXPRES 2013, Subotica, Serbia 2013.03.22-23.

[4] Péter Kádár, Mark Karacsi: Requirements of island mode controller for microCHP in microgrid; SISY 2013, 27. Sept., 2013 Subotica, Serbia

[5] Péter Kádár: Low cost microCHP unit; 9th IEEE International Symposium on Intelligent Systems and Informatics, September 8-10, 2011 Subotica, Serbia

[6] http://www.ninessmartgrid.co.uk/our-trials/shetlands-smart-grid/

[7] Basel Tarcheh, Mark Karacsi (2016), Smart-CHP for Urban Energy Production, Kando Conference, 14.09.2016, Budapest, Hungary

[8] http://www.bosch-presse.de/presseforum/details.htm?txtID=6180&tk_id=190

[9] http://saifurrahman.org/sites/default/files/u2/Budapest%20DLP%20Final.pdf

[10] Small Scale Cogeneration Including Automotive Applications, http:// http://me1065.wikidot.com/small-scale-cogeneration-including-automotive-application

[11] Hugo Morais, Péter Kádár, Pedro Faria, Zita A. Vale, H.M. Khodr: Optimal scheduling of a renewable micro-grid in an isolated load area using mixed-integer linear programming Elsevier Editorial System(tm) for Renewable Energy Magazine Volume 35, Issue 1, Pages 151-156; April, 2010

[12] Tiberiu Tudorache, Cristian Roman: The Numerical Modeling of Transient Regimes of Diesel Generator Sets; Acta Polytechnica Hungarica Vol. 7, No. 2, 2010 pp 39 –53

[13] http://www.energysolutionscenter.org/gas_solutions/micro_chp_mchp.aspxmicro grid

[14] Péter Kádár: Making the power system intelligent; ICREPQ'08 International Conference on Renewable Energy and Power Quality; Santander, Spain, March 12-14, 2008

[15] Peter Kadar: Performance measurements of car engine based MicroCHP test device; International Conference on Renewable Energies and Power Quality (ICREPQ'12); Santiago de Compostela (Spain), 28th to 30th March, 2012; Paper No.: 839

[16] An Approach for Distribution Transformer Management with a Multi-Agent System, W. Khamphanchai, M. Pipattanasomporn, Murat Kuzlu, Jinghe Zhang and Saifur Rahman, accepted for publication in IEEE Transactions on Smart Grid, 2014, 11p.

[17] Flywheel Energy Storage Systems for Ride-through Applications in a Facility Microgrid, R. Arghandeh, M. Pipattanasomporn, and S. Rahman, IEEE Transactions on Smart Grid, Vol. 3, No. 4, December 2012, pp. 1955-1962.

[18] Nyers J., Pek Z., 2014, Mathematical Model of Heat Pumps' Coaxial Evaporator with Distributed Parameters. Acta Polytechnica Hungarica, Vol.11, No.10, pp. 41-54.

EXPRES 2018
ISBN: 978-86-919769-3-4

IMPACTS OF THE CLOTHING ON COMFORT PARAMETERS AND HEATING ENERGY REQUIREMENTS

BALÁZS CAKÓ

PhD student
Breuer Marcell Doctorial School, University of Pécs, Faculty of Engineering and Information Technology
Department of Mechanical Engineering
2 Boszorkány u. H-7626 Pécs, Hungary
E-mail: cako.balazs@mik.pte.hu

Reducing the energy consumption of buildings can be achieved not only by energetic upgrading in the narrow sense, but by the correct choice of operating habits, where various forms of awareness-raising play a major role. A considerable part of household energy consumption is used for heating purposes, which is highly influenced by the clothing worn at home. Optimum comfort is often achieved by increasing energy requirements, but, for creating optimal living conditions comfort parameters needs to be satisfied. In the following I present the effects of clothing on comfort parameters and the heating energy demand, as well as the calculation method whereby these effects can be taken into account.

Keywords: *comfort theory, thermal comfort, clothing, heating energy demand, operating habits*

1. Introduction

Human general feeling of well-being is affected by a number of effects, including temperature, humidity, air movement, noise, illumination and various radiations (ionization, sun radiation, vibrations ...). In my research, I examine the effects of temperature, humidity and air movement on human well-being. Human thermal perception, otherwise thermal comfort is described in standard ASHRAE (1981) 55-81 as follows: "... Pleasant thermal perception is a state of mind that expresses satisfaction with the thermal environment. .. " A person's satisfaction concerning thermal environment is determined by heat and material transport between the body and the environment, which is considerably influenced by the activity, the environment and the clothing. Activity greatly influences the heat production, heat release and heat regulation of a human body. Material transition depends largely on air temperature, its spatial, temporal distribution, change, mean radiant temperature of the surrounding surfaces, relative humidity of the air, the partial pressure of air vapor in the air and the air velocity.
Heating energy demand is primarily determined by the temperature in the room concerned to provide the same thermal comfort.

2. Operating temperature

The temperature of the surrounding surfaces, with the convection heat transfer coefficient of the surfaces, has a weighted effect on human thermal perception, which is characterized by the so-called operating temperature (t_o).

$$t_o = \frac{h_r \times t_r + h_i \times t_i}{h_r + h_i} [°C]$$

Where: h_r – Radiant heat transf. coefficient [W/m2K]
h_i – a convective heat transf. coeff.[W/m2K]
t_i – air temperature [°C]
t_r – Mean radiant temperature [°C]

The temperature of the air and the mean radiant temperature of surfaces will affect approximately 50-50% of the operating temperature respectively, that is, one's thermal perception. The mean radiant temperature of the segmenting surfaces can be determined by taking the emissivity coefficient between the vertical surface element placed in the center of gravity of the body and the segmenting surfaces and the absolute temperature of the surrounding segmenting surfaces into account. It is carried out by dividing the test space into 24 parts and determining the emissivity coefficient and the absolute temperature of the surfaces on each surface

element. The value of the emissivity coefficient was determined by *Povl Ole Fanger* by means of measurement, to which he applied a function, thereby, taking the geometric size of the test surface and the position of the body into account, it can be determined by a diagram. In view of this, the mean radiant temperature can be determined as follows.

$$[1.]\quad t_r = \sqrt[4]{\sum_{i=1}^{n} \varphi_{EFi} \times T_{Fi}^4} - 273{,}15[°C]$$

Where:φ_{EFi} – the emissivity coefficient between the vertical surface element the emissivity coefficient between the vertical surface element

T_{Fi}^4 – temperature of the surrounding segmenting surfaces [K]

The temperature of the surrounding segmenting surfaces, depend on the heat transfer coefficient of the structure tested. Building structures are equipped with ever thicker insulation, so their heat transfer coefficient is becoming lower. The lower the heat transfer coefficient is, the higher is the surface temperature and in this case the required internal air temperature can be reduced to reach the same operating temperature.

3. Interior surface temperature

Interior surface temperature (t_s) can be determined by the following formula if heat transfer coefficient (U) is known.

$$[2.]\quad t_s = t_i - \frac{U}{h_i} \times (t_i - t_e)[°C]$$

Where:t_i – indoor air temperature [°C]
t_e – outdoor air temperature [°C]
U – segment heat transfer coefficient [W/m^{2}K]
h_i – internal-side heat transfer coefficient [W/mK]

Interior surface temperature increases significantly due to high heat transfer coefficient requirements at newly built houses, as demonstrated by the following chart:

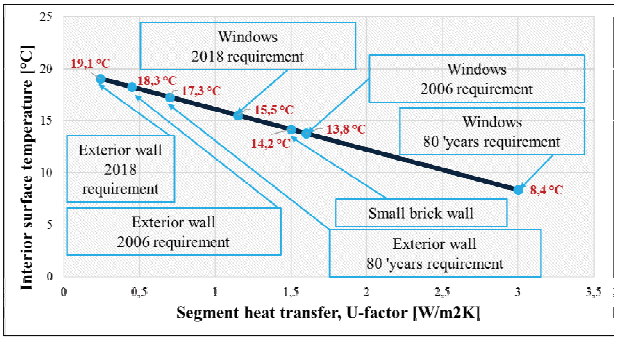

Figure 1.: Effect of the heat transfer factor to the interior surface temperature

The heat transfer coefficient structures of different building periods illustrate the interior surface temperatures taking into account room temperature of 20°C, outdoor dimensioning temperature of -11°C and 8 m^{2}K/W heat transfer coefficient. It is apparent from the chart that the requirements for the segmenting structures have a large effect on the development of the interior surface temperatures. The most striking growth is seen at windows, where it is currently almost one-half times higher as compared to compared to that of the 80s. With the introduction of new requirements, further increase of surface temperatures can be expected. Furthermore, it can be stated that the tightening of the thermal requirements of segmenting structures not only reduces heat losses but also improves the thermal comfort of buildings, as higher interior surface temperatures have a more favorable effect on thermal sensation. In addition, a lower indoor air temperature has to be maintained to achieve the same operating temperature, which reduces heating costs even further.

4. Classification of comfort feeling

The procedure of comfort feeling classification rooms is detailed in standard ASHRAE 55. To perform the relevant calculation, the following initial data are required:

M – metabolic heat production [met]
W – mechanic work [met]
I_{cl} – Insulation of clothing assemble [clo]
t_i – indoor air temperature [°C]
t_r – mean radiant temperature [°C]
φ_i – indoor air relative humidity [%]
v – indoor air velocity [m/s]

Based on these, the velocity threshold can be determined with respect to clothing temperature (t_{cl}) and indoor air temperature (t_i):

$$v_{\max} = \frac{2{,}38 \times (t_{cl} - t_i)^{0,25}}{12{,}1} [m/s]$$

Saturation vapor pressure (p_s) can be determined as a function of the indoor air temperature in Kelvin (T_i). Partial vapor pressure (p_s) can be calculated by multiplying saturation vapor pressure (p_t) and relative humidity (φ_i).

$$p_a = p_s \times \varphi_i [Pa]$$

Clothing conduction resistance (R_{cl}), can be determined from its insulation assemble (I_{cl}).

[3.] $$R_{cl} = 0{,}155 * I_{cl} [m^2 K/W]$$

From this clothing factor (f_{cl}) can be calculated; the way of calculation it is determined by the value of Clothing conduction resistance (R_{cl}). If R_{cl}<0,078, then

$$f_{cl} = 1 + 1{,}29 \times R_{cl}$$

If R_cl≥0,078, then

$$f_{cl} = 1{,}05 + 0{,}645 \times R_{cl}$$

Then the convective heat transfer coefficient of the clothing has to be set, which can be determined by means of an iterative procedure using clothing factor (f_{cl}) and Clothing conduction resistance (R_{cl}), as well as mechanical work (W), metabolic heat production (M) and indoor air temperature (t_i).

Then skin radiant heat loss:

$$H_r = f_{cl} \times 3{,}96 \times 10^{-8} \times (t_{cl}^4 - t_r^4) [W]$$

Skin convective heat loss:

$$H_c = f_{cl} \times h_c \times (t_{cl} - t_i) [W]$$

Skin latent heat loss:

$$H_l = 3{,}05 \times \left[5{,}73 - 0{,}007 \times (M - Work) - \frac{p_a}{1000} \right] [W]$$

Sweat heat loss:

$$H_{sw} = 0{,}42 \times [(M - Work) - 58{,}15] \ [W]$$

Respiratory latent heat loss:

$$H_{rl} = 0{,}0173 \times M \times (5{,}87 - \frac{p_a}{1000}) [W]$$

Respiratory sensible heat loss:

$$H_{rs} = 0{,}0014 \times M \times (34 - t_i) [W]$$

Total heat losses:

$$H = H_r + H_c + H_l + H_{sw} + H_{rl} + H_{rs} [W]$$

Then thermal stress (L) can be calculated as a difference of internal heat production (IHP) and total heat losses (H), where internal heat production (IHP) is given as a difference of metabolic heat production (M) and Work (W).

$$IHP = M - Work \ [W]$$

From this Predicted mean vote (PMV) and Predicted percent dissatisfied (PPD) can be determined.

$$PMV = (0{,}303 \times e^{-0{,}036 \times 58{,}15 \times M} + 0{,}028) \times L$$

$$PPD = 100 - 95 \times e^{-(0.03353 \times PMV^4 + 0{,}2179 \times PMV^2)}$$

According to predicted mean vote (PMV) the space tested can be classifies as Hot, Warm, Mildly warm, Neutral, Mildly Cool and Cool.

5. Insulation of clothing assemble for different items of clothing

The insulation capacity of certain items of clothing is characterized by the so-called clo unit. 1 clo = 0,155 m2K/W. The clo value of certain items of clothing are seen in the following tables.

Table 1.: Insulation of clothing assemble of different items of clothing

Clothing	I_{clo}
Naked	0
Shorts	0,1
Shorts, with open-neck short-sleeve shirt, light socks and sandals	0,3-0,4
Long trousers of light material, with open-neck short-sleeve shirt	0,5
Shorts, wool socks, cotton working shirt and working pants	0,6
Typical businessman garments	1
Typical businessman garments and cotton coat	1,5

Table 2.: Insulation of items of clothing

Items of clothing	I_{clo}	
	light	thick
vest	0,06	
T-shirt	0,09	
underpants	0,05	
Bra and knickers	0,05	
Pants	0,26	0,32
Sweater	0,2	0,37
Jacket	0,22	0,49
Blouse	0,2	0,29
Fabric pants	0,26	0,32
Sweater	0,17	0,37
jacket	0,17	0,37
	short	**long**
camisole	0,13	0,19
Shirt	0,14	0,22
Sandals	0,02	
shoes	0,04	
Boots	0,08	

6. Sample calculation

The calculations were made for a typical room of a building built in the 80's, with a floor area of 29.5 m^2. The room is bordered by three outer walls, two of which are glazed, but the proportion of glazing is less than 50%. During the calculations I took two conditions into account in terms of the thermal engineering aspect: one of with structures used at the time of construction and the other is with structures typically used in Hungary in 2018. The latter is in line with the Hungarian requirements applicable in 2018 (Decree No. 7/2006 TNM). Besides, the calculations were also performed on three different garments. Assuming lightweight wearing (I_{clo} = 0.61), then wearing normal clothing (I_{clo} = 1), and assuming warm clothing (I_{clo} = 1.5). I made the calculations for the same comfort feeling. Comfort feeling and the annual net heating energy demand are in correlation with the activity; this calculation applies to normal activity.

Table 3.: Calculation summary

	Room without thermal insulation			**Insulated room**		
clo	0,61	1	1,5	0,61	1	1,5
t_i [°C]	28,5	26,7	23,8	27,3	25,0	22,4
t_{ks} [°C]	22,7	21,2	18,8	25,4	23,6	21,5
Q [W]	6765	6429	5924	2582	2390	2169
G [hK]	148930	132180	107780	134970	114330	92737
Z [h]	8562	8211	7332	7631	6853	5952
Q_F [MWh/a]	17,59	15,52	12,57	4,57	3,81	3,04
E_F [kWh/m^2a]	596	526	426	155	129	103
PMV	-0,06	0,06	0,04	0,05	0,04	0,07
PPD	5%	5%	5%	5%	5%	5%
Comfort feeling	**Neutral**	**Neutral**	**Neutral**	**Neutral**	**Neutral**	**Neutral**

Q – Heat loss [W], G – heating degree-days [hK], Z – Length of heating season [h],
Q_F – Annual net heating energy demand [MWh/a]

The table shows that in order to achieve the same comfort feeling, a considerably lower indoor air temperature is required in case of warmer clothing. It can be seen that this reduces the annual net heating energy demand proportionately. For insulated structures, assuming the same clothing, the required air temperature is significantly lower. With warmer clothing (Iclo = 1.5), depending on the heat insulation of the building, up to 29-33% energy savings can be achieved as compared to light clothing (I_{clo} = 0.61) in terms of heating energy. But even in the case of normal (I_{clo} = 1) clothing, 12-17% savings can be achieved as compared to light clothing (I_{clo} = 0.61). Dressing habits have changed considerably over the past decades. During the period when the typical heating mode was decentralized, i.e. fireplace, home wear was often warmer, I_{clo} = 1.5 was at home, while today it is considered too much and uncomfortable. Due to the low level of energy prices and the spread of central heating systems, the homogeneous development of the temperature distribution within the building and the premises has changed the user habits and I_{clo} = 1 was a common wear. But it is not uncommon that people wear light clothes at home for comfort reasons. Representative examples of this are the panel block of flats, where heating temperature typically cannot be controlled or only by opening the windows, and in these homes often air temperatures of 26-29 ° C prevail, which can only be tolerated in light clothing. It is also characteristic that users of previously unregulated and high-temperature homes became accustomed to the wasteful way of life and operate their controllable heating systems at unreasonably high temperatures as they are used to light clothing.

7. Conclusion

Significant heating energy savings can be achieved not only by thermal insulation of segmenting structures or by the correct selection of the traditional operating parameters of heating systems (e.g. time-programmed operation), but also by choosing the right home wear while at the same time providing the same comfort. Although different energetic analyzes

(e.g. compulsory audits for large companies) pay attention to changing operating patterns, but, in my view, it is insufficient. However, the industry has no such obligation to the population. In my opinion, awareness-raising measures can greatly reduce global energy use compared to the opportunities currently being exploited.

8. Summary

The tightening of energy requirements improves the quality of buildings, not only in terms of thermal engineering but also from the point of view of comfort. In addition, achieving optimal comfort often leads to increased energy demand, but, for creating optimal living conditions comfort parameters needs to be satisfied. If energy and comfort upgrades are carried out simultaneously, investment cost savings can be achieved as early as during the design phase, since unnecessary oversizing can be avoided.

References

[1] ASHRAE Standard 55-2010 Thermal Environmental Conditions for Human Occupancy, Refrigerating and Air-Conditioning Engineers, Inc.

[2] Magyar Z., Révai T., 2014, Thermal Insulation of the Clothing 2nd Royal Hungarian Army in Winter Campaign in the Light of Thermal Manikin Measurements, ACTA POLYTECHNICA HUNGARICA 11:(7) pp. 197-207.

[3] Bánhidi L., Kajtár L., 2000, Komfortelmélet, Műegyetemi kiadó, Budapest.

[4] Nyers J., Pek Z., 2014, Mathematical Model of Heat Pumps' Coaxial Evaporator with Distributed Parameters. Acta Polytechnica Hungarica, Vol.11, No.10, pp. 41-54.

[5] Odry A., Kecskés I., Burku E., Odry, P., 2017, Protective Fuzzy Control of a Two-Wheeled Mobile Pendulum Robot: Design and Optimization, WSEAS transactions on systems and control 12:(#32) pp. 297-306.

[6] Kassai M., Kajtar L., Nyers J. (2017), Experimental optimization of energy consumption for DC refrigerator by PID controller tuning and comparison with On-Off refrigerator. Thermal Science. DOI: 10.2298_TSCI170504188K.

[7] Kajtár L., Kassai M., 2010, A new calculation procedure to analyse the energy consumption of air handling units, Periodica polytechnica-mechanical engineering 54:(1) pp. 21-26.

[8] Takács J., 2015, Enhance of the efficiency of exploitation of geothermal energy, International symposium, Subotica, Serbia, Proceedings EXPRES 2015, pp. 46-49.

[9] Živner L., Niková, I., Füri B., 2016, Efficiency of the Heat Pump System for Domestic Hot Water Preparation in The Winter Season. In Magyar Épületgépészet. Vol. 65, no. 7-8 (2016), pp. 12-15. ISSN 1215-9913.

[10] Skalík L., 2016, Variation of Solar Energy System Components According to its Efficiency. Proceedings EXPRES 2016, Symposium Subotica, Serbia, 31. 3. - 2. 4. 2016, Subotica : CD-ROM, pp. 119-122. ISBN 978-86-919769-0-3.

[11] Kurčová M., The effect of thermal insulation of an apartment building on the thermo-hydraulic stability of its heating system. In Slovak Journal of Civil Engineering. Vol. 23, no. 4 (2015), s. 8-18. ISSN 1210-3896. Database WOS: 000217748500002

[12] Kurčová M., Ehrenwald P., 2016, Possibility Cooperation of Space Heating System with Heat Pump. Proceedings EXPRES 2016 Symposium, Subotica, Serbia, 31. 3. - 2. 4. 2016, CD-ROM, pp. 52-54. ISBN 978-86-919769-0-3.

[13] Kalmár F. (2016), Interrelation between glazing and summer operative temperature in buildings, International Review of Applied Sciences and Engineering, 1, 51-60.

[14] POÓS T.; ÖRVÖS M.; LEGEZA, L.: Development and thermal modeling of a new construction biomass dryer. Drying Technology 31 (16), 2013, 1919-1929.

[15] Kadar P., Karacsi M., Stand-alone island mode operation of microCHP device, IEEE 5th International Symposium on Exploitation of Renewable Energy Sources, EXPRES 2013, Subotica, Serbia 2013.03.22-23.

[16] Nyers J., 2016, COP and Economic Analysis of the Heat Recovery from Waste Water using Heat Pumps, International J. Acta Polytechnica Hungarica Vol. 13, No. 5, pp. 135-154.

EXPRES 2018
ISBN: 978-86-919769-3-4

GREEN ROOF TEMPERATURE DISTRIBUTION MONITORING SYSTEM

LASZLO LENKOVICS[a]

Faculty of Engineering and Information Technology, University of Pécs
H-7624 Pécs, Boszorkány u. 2, Hungary
[a]E-mail: lenkovics@mik.pte.hu

Abstract

The paper presents the green roof construction and monitoring project at the faculty of engineering, University of Pécs, Hungary, and the research goals concerned. The green roofs, their testing methods, thermal, solar radiation intensity and water balance in terms of measurement. The data collected will be used to examine the difference in heat transfer coefficient, and the thermal and energetic effects of the soil on the roof surface. The surface will be tested with direct and reflected solar radiation. The amount of absorbed and reflected radiation as well as its energetic effect is also being examined. This paper deals with issues about designing and implementing green roofs, presents the faculty's test system used to measure temperature, solar radiation intensity, water flow. Based on earlier calculations, the possibility and importance of developing the used equipment will be presented as well as the setup of the data collecting system, parts of the system and data collecting methods. The paper introduces the measurement of energetics and its changing factors in all seasons. The goal of my research is to offer a comprehensive study of the aggregated annual data, and to have a standard framework about the thermal intensity and energetics of green roofs. I would like to use the results to specify calculation in standards and decrees, as well as for calculations in energetics and thermal intensity of buildings. The current Hungarian literature available is more about architectural, construction and implementation directives, and is less about effects energetics and water balance. My work would like to help this situation.

Keywords*: green roof, intensity of solar radiation, thermal engineering, water management, energetics*

1. Introduction

Big cities at the beginning of the 21th century are characterized by population concentrated in the small area, huge construction projects, ever-growing artificially built surfaces, accumulation of untreated solid and liquid waste. Nearly 3/4 of Europe's population lives in urban areas, and current trends show that people still happy to move to cities, thus this proportion is likely to increase further on. With the expansion of cities, the landscape is transformed. Roofs and clad surfaces conquest space from green areas. Urbanization and development should not be stopped, in fact, it even has to be encouraged. With modern, environmentally-friendly architecture and engineering, the balance can be maintained, and the former built-in areas can be partially converted back to nature. In the concreted, asphalted, built-up areas rainwater cannot make its way into ground. In these areas the plants, insects disappear, the biological balance is turned upside down. Green spaces are decreasing with current architectural concepts, no new green spots can be created at ground level of existing densely populated areas. An effective solution to this issue can be the development of green roofs in our cities, which have not only energy, comfort, water management, aesthetic effect, but offer positive environmental and ecological impact as well.

2. Construction of the Test Circuit

An extensive green roof and two control roofs have been developed on the top of the building engineering laboratories of building "C" building of the Faculty of Technology and Informatics at the University of Pécs. This is an extensive green roof of approximately 45 m2 areas, which was placed next to two control roofs of the same size.

The current structure of layers of roof is a straight layered, one-shelled warm roof. The waterproofing is made of Sika PVC. There is no data available on thermal insulation, but the lowest compressive strength (AT-N 100) heat insulation which still can be used is suitable for bearing the load of an extensive green roof.

When constructing the "Control roof", were built the following structure of layers were applied on the existing waterproofing:

- special top soil - 10 cm - 98 kg/m2 wet weight
- DIADEM VLF 300 filter layer
- DIADEM Dia-Drain leaking and water retention layer, thickness 2.5 cm
- DIADEM VLU 500 mechanical protective layer
- existing waterproofing SIKA PLAN PVC

A plastic control shaft was placed above the confluence was replacing the foliage, too. A 20-cm-wide washed river gravel separating layer was placed around the confluence in the full thickness of the topsoil. Along the attic wall 20-cm-wide washed river gravel dividing strip was also installed. Among the river gravel and the topsoil aluminum edge elements were installed.

Plants were planted by planting a mixture of Sedum cuttings (containing 5 varieties). The plants do not require irrigation, nutrient supply, except for a longer (1-month long or more) summer drought, when it is recommended to water the green roof once.

In addition to these, a "Control Roof2" was built, a 10 cm Roofmate XPS thermal insulation foam and a mechanical protective layer were added to the existing Roof Layer. Thermal conductivity coefficient of thermal insulation λ=0,035 (W/m2K).

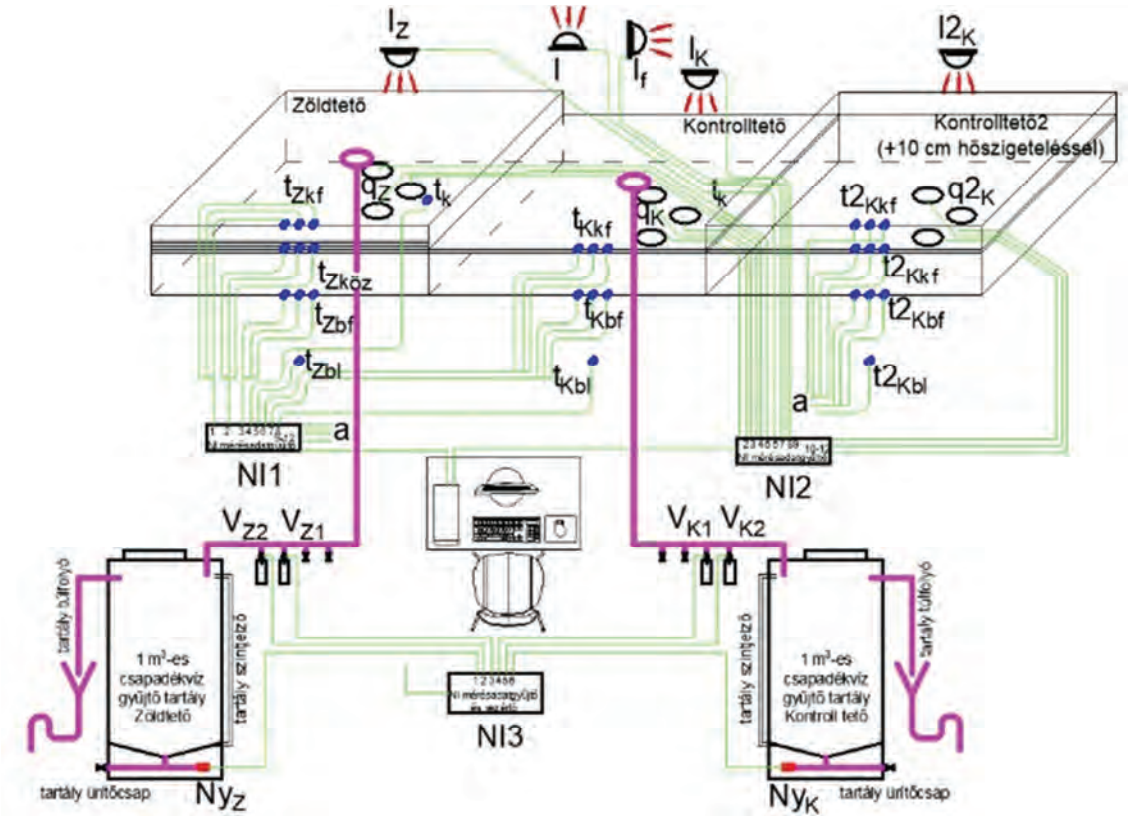

Fig.1 Construction of the testing system

- **Measuring the temperature**
  - t_K: Outdoor air temperature
  - **Green roof**
    - tZkf: Green roof external surface temperature
    - tZköz: Green roof intermediate surface temperature
    - tZbf: Green roof interior surface temperature
    - tZbl: Green roof interior air temperature
  - **Control roof**
    - tKkf: Control roof external surface temperature
    - tKbf: Control roof interior surface temperature
    - tKbl: Control roof interior air temperature
  - **Control roof2 (+10 cm-thick thermal insulation)**
    - t2Kkf: Control roof external surface temperature
    - t2Kbf: Control roof interior surface temperature
    - t2Kbl: Control roof interior air temperature
- **Measuring Solar radiation**
  - I: Measuring global horizontal solar radiation intensity
  - If: Measuring global vertical solar radiation intensity
  - IZ: Measuring green roof reflected radiation intensity
  - IK: Measuring control roof reflected radiation intensity
  - I2K: Measuring control roof reflected radiation intensity
- **Measuring rainwater**
  - VZ1: Water sampling on the Green roof at the beginning of rain
  - VZ2: Water sampling on the Green roof in the second phase of raining
  - NyZ: Pressure transmitter on the Green roof to measure water level
  - VK1: Water sampling on the Control roofn at the beginning of rain
  - VK2: Water sampling on the Control roof in the second phase of raining
  - NyK: Pressure transmitter on the Control roof to measure water level

- **Measuring heat transfer density**
  - qZ: 3 pcs Green roof heat transfer densitometer (under purchase)
  - qK: Control roof 3 pcs heat transfer densitometer (under purchase)
  - q2K: Control roof2 3 pcs heat transfer densitometer (under purchase)

- **Test-data collectors**
  - NI1: Temperature, heat transfer density, solar radiation data collector
  - NI2: Temperature, heat transfer density, solar radiation data collector
  - NI3: Rainwater data collector and controller

3. Testing system

A testing system has been developed with three test-data collectors.

- **Measuring temperature**

In the temperature-measuring system, 28 pcs thermometer have been installed. In the testing circle of the Green roof, the external surface temperature (tZkf) of the Green roof is measured by 3 pcs self-adhesive Pt-100, placed 25 cm from each other. Between the Green roof and the existing roof layer, (tZköz) 3 pcs self-adhesive Pt-100, was placed, too, 25 cm from each other again, while for measuring interior surface temperature (tZbf) 3 pcs self-adhesive Pt-100, was placed, too, 25 cm from each other again. In the internal space, under the measuring spots, 1 air temperature meter has been installed (tZbl). The measuring spots are located in the same plane.
The control roof is also measured on the outer surface (tKkf) by 3 pcs self-adhesive Pt 100 25 cm apart. Also 3 pcs (tKbf) self-adhesive Pt 100 placed 25 cm apart were installed for measuring the interior surface temperature of the control roof. In the internal space, under the measuring spots, 1 air temperature meter has been installed (tKbl). The measuring spots are also located in one plane.
Outside, 1 pcs outdoor temperature sensor was placed.
Measurement of controlroof2 is also done on an external surface (t2Kkf) by 3 pcs self-adhesive Pt 100 installed 25 cm apart. Also 3 pcs (t2Kbf) self-adhesive Pt 100 placed 25 cm apart were installed for measuring the interior surface temperature of the control roof. In the internal space, under the measuring spots, 1 air temperature meter has been installed (t2Kbl). The measuring spots are also located in one plane.

- **Measuring Solar radiation**

For solar radiation measurements, 5 pcs solar radiation intensity meters were added to the test circuit, 1 pcs (IZ, IK and I2K) over each of the three roof surfaces facing the roof surfaces. Their task is to measure the reflected radiation emitted from the roof surfaces. In addition, 1 pcs horizontally positioned solar radiation intensity meter (I) and 1 pcs vertically positioned solar radiation intensity meter (If) have also been installed. By subtracting the value of the

reflected radiation from the horizontal solar radiation intensity on the roof surfaces, the values of absorbed radiation on the roof surfaces are obtained, thus its effect on the roof surface and on the building can be investigated.

❖ **Measuring Rainwater**

For water balance measurement, 2 independent systems have been developed, which are completely identical. The main part of the measuring unit is one a 1-m3 container for each one, this is where the water from the Green roof and the control roof are drained. The roof water drainage is led into a room under the roofs by a DN 110 KG-PVC pipe that enters the rainwater reservoir. The tanks have overflows and drainage outlet pipes. The 1-m3 rainwater collecting tanks are mounted on legs so that a pressure transmitter (NyZ, NyK) could be installed at the lowest point of each tank. The pressure transmitters have a precision of 1 mm. During the planned measurements, the tanks receive every rain in an empty state, but the pressure transmitter tube is not drained so it would constantly measure a basic hydrostatic pressure above which it already knows the required precision. The pressure transmitters signals are recorded by a computer. There is also a sampling tap 10 cm above the bottom of the tank.
The drainage of rainwater into both tanks has a horizontal (0.5% slope) section, with 4 side pipes (branches) on each, within this section. 2 branches on each belong to 1 solenoid valve (VZ1, VZ2 and VK1, VK2) drain rainwater to a 1-liter screw-in sampling vessel. 1 branch on each is a manual sampling tap, while the fourth tap on each system is a reserve for later expansion. The solenoid valves are controlled from a computer.

❖ **Measuring heat transfer density**

3 heat transfer densitometers (qZ, qK, q2K) is going to be installed for each surface in the near future. The designed type is PHFS-09e Large Surface Area Heat Flux Sensor with large surface sensor and minimal film thickness. The measuring devices are going to be installed in the plaster on the inner ceiling on the surfaces to be measured.

4. Test-collector, controller

Data recording and control tasks are provided by 3 existing measuring instruments. They are National Instrument built-in freely programmable data collector and control system that are ideal for testing larger systems such as thermal engineering testing of boiler houses, auditing and receiving multiple sensors' signals. The device is capable of network communication, providing remote access over a local LAN network, even data retrieval and intervention can be performed through the device. Devices can collect data on their own memory or on a computer that can access the LAN network. The device has its own memory and can be used for stand-alone operation, in which case it is not necessary to connect a separate PC to the device.

The main elements of 2 NI FieldPoint system (NI1, NI2) for temperature, heat transfer density and solar radiation intensity data collection:
Each system has 1 cFP-2220 - Ethernet and communication module with 256 MB RAM internal memory, but in this case, for the sake of simplicity and security, the measurement is done over a network, and a measuring PC collects the data.

To measure the temperature 2 cFP-RTD-124 - 8-channel 16-bit RTD module (RTD, Ohms) are used on each system. It converts the analogue signals from the Pt100 Resistance Thermal Sensor to a digital signal, through an adapter card specifically designed for this purpose.
To measure solar radiation intensity 1 cFP-AI-112 - 8-channel 16-bit Analog Input Module (mA, mV, V) are used for each system. It transforms the analog signals (mV) of the 5 Kipp & Zonen CMP3 solar radiation intensity detector into a digital signals.

The main elements of the third NI FieldPoint system (NI3) are to control the sampling valves and to receive the pressure transducer signals to perform the level measurement:
1 cFP-2200 - Ethernet and communication module with 128 MB RAM internal memory, but in this case for simplicity and security reasons the measurement is performed over a network; a PC collects the data.

1 cFP-DIO-550 – 8-Channel Digital Output / Input Module.
The Green roof and the reference roof control 2 sampling valves each independently. The thermal drives of the valves are of Danfoss TWA-V NC (230V / 2W, IP41) type. Due to voltage differences, control is performed by inserting a total of 4 auxiliary retractors (230 / 24V). Valves must have 2 positions for sampling: open and closed states.
The level detection of the measuring tanks of the Green roof and reference roof, the analog signals (mA) of a Wika P-30 pressure transmitters on each is received whereby the water volume of the tank can be determined.

5. Measuring program

The measuring and data collecting program is made by means of LabView software released by National Instruments, which enables graphical programming. During the programming, a separate application was

made for temperature, heat transfer density and solar radiation intensity for data collection as well as for water balance measurement and for the control data collector.

Fig 2. A screenshot of a program used for measuring thermal engineering and solar radiation data.

The device and the software are the products of the same manufacturer; they are absolutely universal high-precision devices, so their programming is quite complicated. The software was originally designed for engineers and includes pre-programmed graphical interface modules, so you do not have to start programming completely from the beginning. The graphical programming interface is not the usual text programming, the individual parameters are contained in a graphical block, which are linked by lines to additional prefabricated function blocks Basically, the program is displayed in 2 main windows, one for the user interface and the programmer's graphic interface, here one can find the prefabricated * .vi-s or blocks and blocks of input parameters and their relationship.

Measuring temperature is continuous, 28 programmed temperature are measured 24 hours a day, 365 days a year. At the beginning of measurement, the sampling interval can be set. I set the sampling time during the measurement for 5 minutes to be able to keep track of possible changes from the data. The outdoor temperature, the intermediate and the internal temperatures do not change or change only slightly in 5 minutes, the surface temperature can significantly change during the 5 minute as weather conditions change.

Rainwater sampling takes place in 2 periods on each tank. The first sampling is required at the beginning of the rainfall. This made in a way that, when increase is detected by the tank level sensor, the first valve opens and then closes after a specified time. The second sampling is necessary during the rainfall when the topsoil agent has completely wet. It would be ideal to perform the thirds sampling at the end of the rain, in the last phase. This could be quite difficult to accomplish as it is not possible to predict exactly when the rainfall will finish. We have found a possible method for indicating the end of the rainfall. A decrease in the volume flow of water coming down the drain signals the end of the rain, which can be deduced from the rising tendency of the reservoir level. If the increase of the level of the reservoir shows down compared to the previous one, it opens the second sampling valve.

5. Summary

The measuring system for my research has been completed.

This article deals with the design and construction issues of Green roofs. I present the test circles installed at the faculty, the testing and measuring sytems of temperatures, heat, solar radiation intensity and water quantity. The structure of the data collector system, the methods of data collecting and measuring. The purpose of my research is to study the aggregate annual energy balance comprehensibly, and to incorporate the thermal and energetic properties of Green roof layers into a standardized framework. I would like to use the results to make the standards more accurate for calculating the relevant regulations and to calculate energy and thermal engineering data for buildings

The first data of measurement are available and I have already started analyzing them.

References

[1] Szlivka F. D. (2016), Zöldtetők vizsgálata energia megtakarítás, valamint a környezeti terhelés csökkentése érdekében – Doctorial (PhD) thesis.

[2] Horváthné Pintér J. (2011). ZÖLDTETŐK tervezési és kivitelezési irányelvei. Budapest: ÉMSZ.

[3] Gerzson L. (2003). Növények a kertépítészetben. (S. Gábor, Szerk.) Budapest: Mezőgazda Kiadó.

[4] Dunett N., Kingsbury N. (2004). Planting Green Roofs and Living Walls. Portland,Oregon: Timber Press.

[5] Eördöghné Miklós M. (2013): A település szerkezet és a vezetékes víz fogyasztás nagyságának összefüggései. In: Dövényi Zoltán – Donka Attila (ed..): A geográfia változó arcai. IDResearch Kft./Publikon Kiadó Pécs, ISBN 978-615-5001-88-8, HU ISSN 1789-0527, pp. 65-78

[6] Eördöghné Miklós M. (2018): Az erővíz-gazdálkodás ökologikus eszköze: a Zöldtető – Magyar Installateur

[7] ZEOSZ: Zöldtető rétegrendje, 2012

[8] Szőke A. (2015): Extenzív Zöldtetők, és azokon alkalmazott egyes Sedum fajok komplex értékelése (PhD) értekezés

[9] Kurčová M., The effect of thermal insulation of an apartment building on the thermo-hydraulic stability of its heating system. In Slovak Journal of Civil Engineering. Vol. 23, no. 4 (2015), s. 8-18. ISSN 1210-3896. Database WOS: 000217748500002

[10]Nyers J., Kajtar L., Slavica T., Nyers, A. (2014) Investment-savings Method for Energy-economic Optimization of External Wall Thermal Insulation Thickness, Energy and Buildings, 86, 268-274.

EXPRES 2018
ISBN: 978-86-919769-3-4

APPLICATION OF THERMOPILE TECHNOLOGY

I. FARKAS [a], *A. SZENTE*[b], *P. ODRY*[c]

University of Dunaújváros/Computer Engineering, Dunaújváros, Hungary
Paks Nuklear Power Plant, Paks, Hungary
Polytechnic of Subotica/Electrical Engineering, Szabadka, Serbia
[a]imka26@gmail.com,
[b]szentea@npp.hu,
[c]odry@appl-dsp.com

Thermopile technology enables us to convert the waste heat to useful electricity. This article is going to deal with two applications of the thermoelectric generators. Firstly we are going to overview the current state in the field of battery charging using the heat from the exhaust pipe in automobiles and to choose the right TEG module to ensuring the energy supply for the cooling system of nuclear plants in a case of natural disaster, or any system failure. It has been shown in recent years that there is a great need for additional security measures to be taken in high security systems in case of occurrence of unanticipated events. A Nuclear Power Plant is exactly such kind of a sophisticated system. Thou, before we begin to work on improving the overall security of a system, we must familiarize ourselves with the type of event that causes the issue during an unanticipated event. For this we need a well-constructed simulation. The fortification of the removal of decay heat following the subcritical stage of a reactor shutdown forms a significant portion of the workings of a nuclear power plant. The lack of such a measure could lead to a catastrophic meltdown (Fukushima 2011). The necessary electrical energy for this process under normal conditions is supplied by the primary (national and home power grids) and secondary (diesel generators) electrical supply systems. One of the key factors of the insurance of higher plant safety could be the application of a third diverse decay heat removal ensuring system.

Keywords: *Thermopile, TEG module, thermoelectric generator, Nuclear Power Plant.*

1. Thermoelectric generator

Thermoelectric generators (TEG) could be used in the near future in many industrial applications ranging from solar energy applications and automotive industry to nuclear power production and several other fields of engineering. Application of thermoelectric generators to recover wasted heat from the exhaust system of an automobile could be a promising utilization of the thermoelectric technology to improve the efficiency of an internal combustion engine. Currently this area is a rapidly evolving segment of the application of TEG technology.

On the other hand the safety applications of the thermoelectric generators is huge. In case of a natural disaster the nuclear plant shuts down, but the decay heat continues to elevate the temperature in the plant. Without the cooling system the plant is going to explode. It is possible to build a safety net with TEG modules to keep the temperature under a critical value for a few days for the help to arrive.

Thermoelectric generators (TEGs) allow direct conversion of heat energy to electricity without any moving parts and have advantages such as durability and maintenance-free and noiseless operation.

The thermoelectric generator is a semiconductor device which is governed by the following physical effects that describe the heat flow inside a thermoelectric generator. These are the Seebeck effect, Fourier effect, Joule effect and the Thomson effect. Generally the simplest mathematical description of the energy conservation of a TEG element can be modeled by one dimensional heat transfer and electrical current flow process.

Zorbas et al. [1] developed a model for the evaluation of the performance of a thermoelectric generator. The developed model takes into account the thermal contact resistant effect and also the thermal resistance of the applied ceramic plates of the TEG. The model has been applied to describe the behavior of a commercial TEG which has been tested in an exhaust system of a gasoline engine. Carmo et al. [2] presents a characterization of thermoelectric generators by measuring the load dependent behavior. The investigation has been carried out for modest temperature differences (□T<=51). Waste heat recovery of a low cost thermoelectric generator for a stove investigated by Nuwayhid et al. [3]. They have studied an alternative electric power supply from a wood or petroleum heated stove in regions where

the constant electric power supply cannot be achieved. F. Meng et al. [4] developed a complete numerical model with inner and external multi-irreversibilities of commercial thermoelectric generator in which physical properties, geometric dimensions, and flow parameters are all considered. It has been concluded that the main loss among the losses caused by inner effects is the Fourier heat leakage. The impact of the Thomson effect has been investigated by Chen et al. [5]. The thermal behavior and cooling power of three different TECMs have been investigated numerically with the aim to recognize the performance of miniature TEC in the presence\absence of Thomson effect.

Currently the following semiconductor material pairs have been investigated most widely, these are the BiTe, PbTe and SiGe semiconductor materials which can be operated efficiently in different temperature range. Higher the temperature more efficient the TEG device to produce electricity but there is an upper temperature limit where the materials melt. Table I. contains the approximate upper limit temperature and the thermal efficiency of the semiconductor material pairs by Schaevitz [10].

Table 1. Temperature upper limit and the thermal efficiency of the semiconductor material pairs

Material pair	Temperature limit [^{o}C]	Efficiency [%]
BiTe	300	6
PbTe	600	9
SiGe	1100	11.5

D.

In addition to this the approximate temperature distribution of an exhaust system of automobiles are needed to calculate a good estimation of the electrical power harvested by thermoelectric generators.

The aim of this study is to present a comparison of the efficiency of different commercially available TEG modules applying in the exhaust system of different diesel or gasoline engine automobile.

E.

Table 1 contains the studied thermoelectric modules all of them commercially available. The table shows the geometric dimension of the TEG modules, the maximum tested temperature differences between the cold and hot side of the TEG, and the produced maximum electrical power.

Table 1. Thermoelectric modules of them commercial use

Module name	Dimensions	ΔT [^{o}C]	P_{max} [W]
TEC1-12707	40 mm x 40 mm	51	0.5
TEC1-12708	40 mm x 40 mm	68	0.85
Melcor HT9-3-25 Bi2Te3 N=31	25 mm x 25 mm	190	2.5
		61	0.4
Melcor HT6-12-40 Bi2Te3	40 mm x 40 mm	68	0.75

F.

G.

2. The simulation of the cooling

To be able to analyze the task, in the first step let's see how large this energy is [1,5]. The codes that use numerical methods to estimate the remnant heat (decay heat) (Melcor, Relap 1-2-3, Trac, Origen) are capable to model the state with a precision of 3-5%.

a. The simulation of remnant heat

Using MATLAB R2013a with numerical methods we simulated (figure 5.), a T=335days constantly operational P_0 = 1485MWt („Megawatt thermal") heat energy producing reactor, it's remnant heat 10 days following it's shutdown (864000s) is shown on figure6. This value even after ten days is more than 3MWt.

The algorithm used [M. Ragheb, 3/22/2011]: [2]

$$P(t) = 6.48x10^{-3}\, P_0\, [t^{-0.2} - (t+T_0)^{-0.2}]\ [MWt] \qquad (1)$$

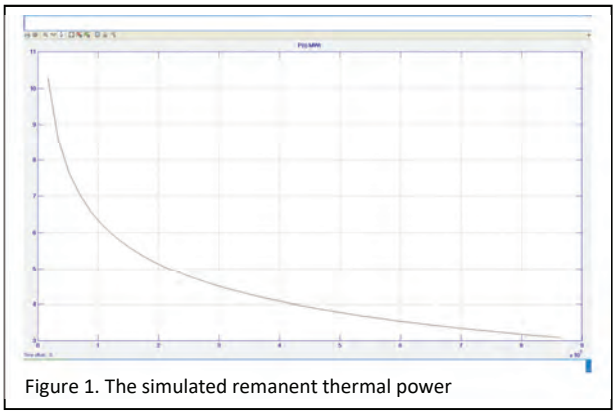

Figure 1. The simulated remanent thermal power

b. The emergency stop and the addition of thermal mass in the system after shutdown

Hereinafter, we excited the SCRAM (emergency stop) signal shutdown reactor and associated metal work combined transfer function with the current heat output signal (Figure 1.).

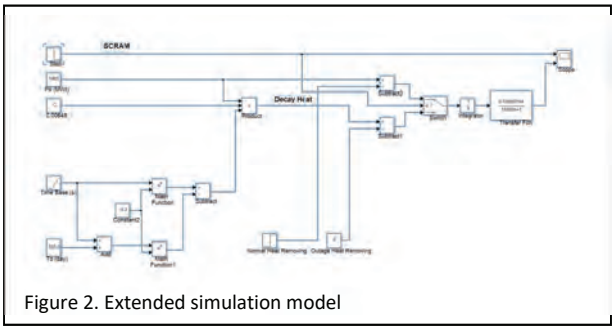

Figure 2. Extended simulation model

The transfer function was determined by a single proportional storage member (PT1) function, determined because of water and metal mass, considering the reactor, fuel, main water circuit lines, primary coolant masses and specific heat values. Without forced circulation or additional heat removal, using an account

with very high heat storage capacity, the output function scaled in average temperatures even after ten days shows a monotonic character (Figure 2.). Assuming continuously available (fixed) emergency stop heat extracting system and power, the about 4MWt heat removal reverses its trend on the seventh day, at a temperature of 300° C (figure 3, the third chart).

It should be noted, a lesser value is also capable of reversing the trend, that is to cause cooling, since the thermal decomposition function decreases monotonically, the question is when and how long will it allow the average temperature to climb up. In the case of our operating systems protection signals are formed at - 305°C and 310°C values, it is not appropriate to allow a higher value for a standing block either. An obvious question is whether the huge, metal and water - weight stored heat energy should be directly converted in to electrical energy by an electrical (TEG) converter and used for powering the residual heat removal as a "third kind" diverse authoritarian type supply.

Main equipment otherwise covered with insulation if you cover them with TEG –considering characteristics of temperature and ventilation of the area (the box) will continue, - it is required due to cold-side heat removal by the TEG–to generate approximately 2.5 - 3.0 MW of electricity, if we assume current TEG efficiencies [4].

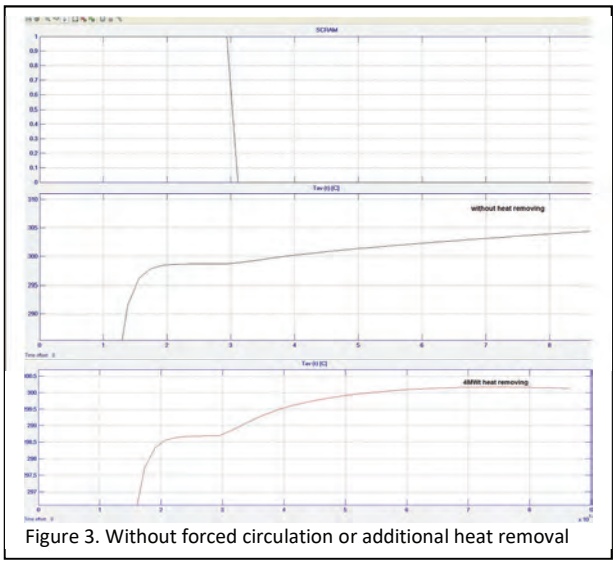

Figure 3. Without forced circulation or additional heat removal

c. The installation of TEG as a residual heat-absorber

A system thus formed from a thermal perspective is a negative feedback system, which guarantees safety (9) for protection against over temperature. The thermoelectric generator in the feedback path can also be modeled as a PT1 member, however, it's time constant is much smaller than the pre-coupling loop, the time constant of the technology.

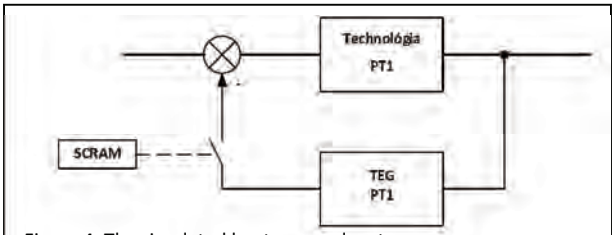

Figure 4. The simulated heat removal system

The thus constructed MATLAB model can be seen on figure 2., while the cooling curves are shown on figure 3. The "minima" function that does not allow the temperature to climb above 300 °C, should have at least $aY = \frac{0.0015}{700S+0.1}$ transfer function. Increasing the time constant does not affect the shape of the curve, it determines the availability of electric power that can be extracted from the TEG, while the proportional transfer component has effect on the slope of the cooling.

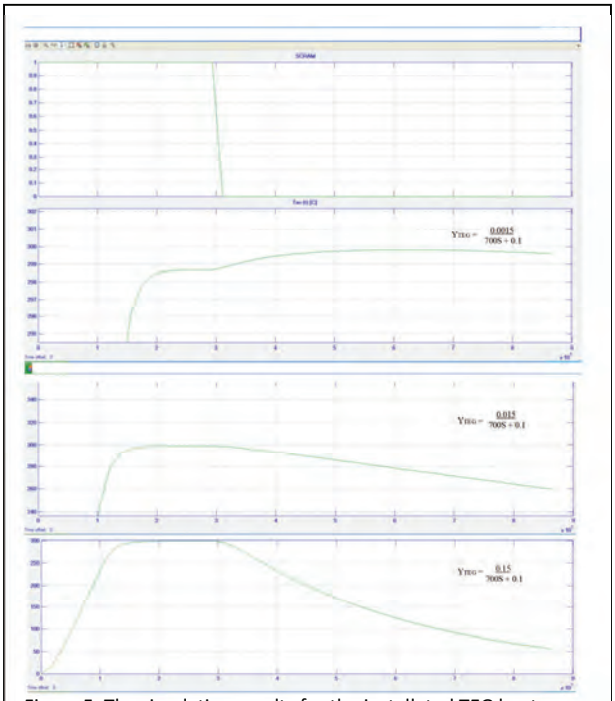

Figure 5. The simulation results for the installated TEG heat removal

d. TEG as a residual heat-absorber

The increase of storage capacity can be resolved by the storage of electricity generated by the TEG's in batteries (Figure 6).

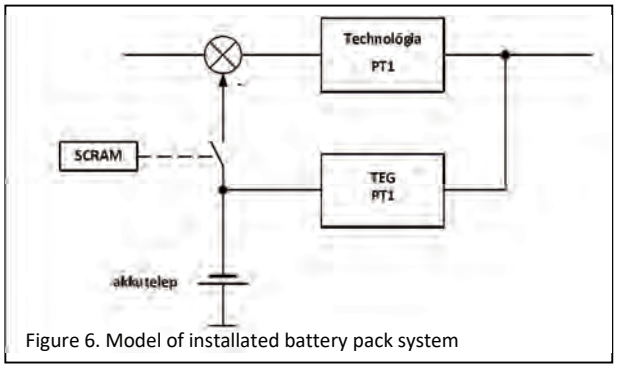

Figure 6. Model of installated battery pack system

During the campaign, the heat produced is continuously "there" in a time after SCRAM as well in the form of stored heat, so during the residual heat removal's critical stage of 2-3 days the multiple amount of charger (conditioning)power could be removed from the batteries to maintain the circulation. Each plant has a battery-supported DC rail (220V or 24V), so building that will not be an additional cost.

3. Analysis of a nuclear power plant from the usage perspective of a TEG

The thermopile technology is turning out to be an interesting application in the field of nuclear power plants. It has been successfully used for some time now in outer space electric power generation [3]. It holds additional capabilities in high-energy nuclear systems. Continued, we explore these application possibilities in this article.

Nuclear power plants are essentially thermal power plants fueled by nuclear fission reactions. Instead of the conventional burning of fuels like in the furnaces of thermal power plants, nuclear reactions in the reactor are generating the energy. However, using the hot water coming out the reactor, only relatively low pressure (40-60bar) saturated steam can be produced, so the cycle's parameters are rather moderate. This is the cause of the relatively low efficiency of nuclear power plants (η = 30 - 40%). The following table shows the thermal characteristics of the main types of thermal reactors:

4. Approximation of the extractable power with the TEG

An assessment of the potential primary circuit surfaces: in the situation with six main water conduits, their coverable length with TEG in total is 120m, accounted for a hot and cold branch of 10-10 m. Obviously, the treatment, operation equipment, nozzles, valves, thermometer bag places cannot be affected with the TEG covering. With a 560mm diameter, main water conduit, on most the pipe surfaces we can have access to a usable surface of 210 m^2, with 270°C average temperature. This means that on the cold end 250 °C, on the hot end 280°C temperatures can heat the placed TEG's. Calculating with six, 10m long, 4 m diameter steam generators we get a surface of 754 m^2, at 220°C which is coverable. A major piece of equipment surface is the pressurizer where the coverable area is 52 m^2, but the temperature of the surface is 280°C. The similar exploration of the secondary circuit: a 135 m long, 465 mm diameter main steam pipe means a surface of 197 m^2, at 220 °C. Calculating with a water supply system average temperature of 180 °C, with a 426mm diameter on 120m length, we get a similar surface of 160m^2. The major secondary containers, low - and high-pressure preheater lines, supply containers usable surfaces relative to the block are: 395m^2, 100°C average temperature preheater, 480m^2, 200°C average temperature high pressure preheater, two 105m^2, 150°C temperature supply tanks. The above are the major places for energy retrieval, leaving out the auxiliary systems and small unusable surfaces. The room temperatures, „cold side temperatures" are between 30°C - 50°C.

Thanks to Thomson, Seebeck and Peltier's research, we use thermocouples for measurement purposes for a long time now. However, the phenomenon of using it as an energy source application is made possible through experimenting with new materials. One of the best types of such thermoelectric modules (TEG's) with the best thermoelectric properties is the bismuth-telluride (Bi_2TE_3) based pseudo-binary group of alloys. Figure 7. shows some of the more important TEG material pairs efficiency as a function of temperature.

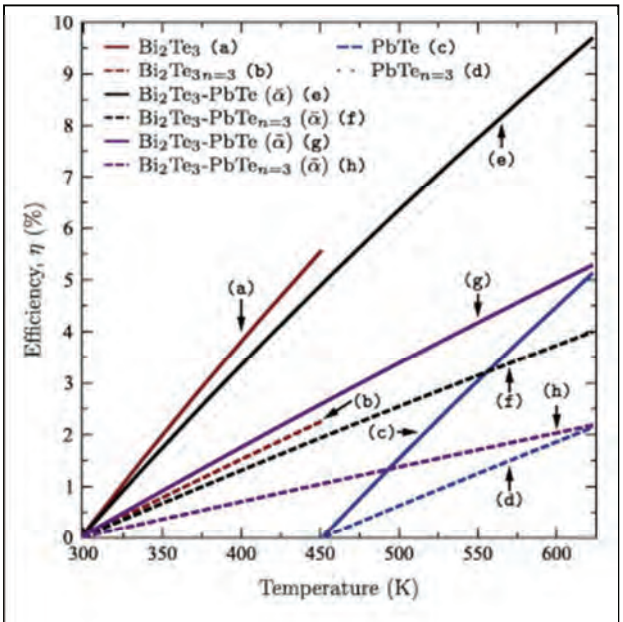

Figure 7. TEG material pair efficieny

Hot side

Cool side

Heat source temperature:	500 °C
Hot side temperature	480 °C
Cool side temperature:	45 °C
Open circuit voltage:	19.45 V
Output voltage:	9.75 V
Load current:	1.13 A
Output power:	11.0 W
Surface:	0.004 m^2

Figure 8. CMO-32-62S CASCADE TEG module

1. Summary

In this paper, we have tried to show how is it possible to simulate processes taking place in an abandoned nuclear power plant. As you can see this can be resolved perfectly using MATLAB. We have outlined the theoretical possibility of usage of residual heat removal using a third, diverse way method. In further studies, we try to put more emphasis on the fine tuning of the simulated system and to clarify the physical realization of the possibilities.

During the study, it can be concluded that, yes, there is justification in using the TEG in nuclear power plants. We may have to wait a few years so that TEG's with such parameters hit the market that enable greater power generation (and thus enabling the operation of stronger motors with them), but the results outlined here are said to be promising. If we only consider that the resulting 2.68 MW, the daily consumption of a small town, can be covered by it, or it can supply the mentioned measuring and signaling devices current needs, we should look at it as it is worth it. In any case, its usage is worth further consideration when critical outages or emergencies occur.

References

[1] K. T. Zorbas, E. Hatzikraniotis, K. M. Paraskevopoulos, Power and efficiency calculation in commercial TEG and application in wasted heat recovery in automobile.

[2] J.P. Carmo, J. Antunes, M.F. Silva, J.F. Riberio, L.M. Goncalves, J.H. Correia, Characterization of thermoelectric generators by measuring the load-dependence behavior, *Measurement* 44, (2011), 2194-2199.

[3] R.Y. Nuwayhid, D.M. Rowe, G. Min, Low cost stove-top thermoelectric generator for regions with unreliable electricity supply, Renewable Energy 28, (2003), 205-222.

[4] Fankai Meng, Lingen Chen, Fengrui Sun, Numerical model and comparative investigation of a thermoelectric generator with multi-irreversibilities, *Energy*, 36, (2011) 3513-3522.

[5] Wei-Hsin Chen, Chen-Yeh Liao, Chen-I Hung, A numerical study on the performance of miniature thermoelectric cooler affected by Thomson effect, Applied Energy, 89, (2012) 464-473.

[6] Laszlo Kajtar, Jozsef Nyers, Janos Szabo: Dynamic thermal dimensioning of underground spaces; Volume 87, 1 July 2015, Pages 361–368

[7] M. Ragheb: Decay heat generation in fission reactors, 3/22/2011

[8] A. Szente, I. Farkas and P. Odry: *The application of Thermopile Technology in high Energy Nuclear Power Plants*, Expres 2014 http://www.tecteg.com/

[9] M. Ragheb (22 March 2011). *"Decay Heat Generation in Fission Reactors"*. University of Illinois at Urbana-Champaign. *Retrieved 26 January 2013*

[10] Nyers J., Kajtar L., Tomic S., Nyers A., 2014, Investment-savings Method for Energy-economic Optimization of External Wall Thermal Insulation Thickness, ENERGY AND BUILDINGS 86: pp. 268-274.

EXPRES 2018
ISBN: 978-86-919769-3-4

A SURVEY OF FACTORS AFFECTING HEAT DELIVERY AND HEAT BALANCE

L GARBAI[a] *, A JASPER*[b]*,*

Department of Building Service and Process Engineering,
Budapest University of Technology and Economics, Hungary

[a]garbai@epgep.bme.hu
[b]jasper@epgep.bme.hu

Abstract - Our study examines the issue of how the heat balance and the heat delivery capacity of district heating systems is affected by system component properties and the heat delivery parameters set, including, in particular, primary and secondary forward hot water temperature, and primary and secondary circulated hot water flow. In an earlier study of ours [1], a calculation model was provided on the heat balance of the district heating system in case of diverse operating parameters – such as primary and circulated secondary mass flow, and primary and secondary forward water temperatures –, and the internal temperatures developing in buildings under given external meteorological conditions. In the course of our investigations, a so-called heat output convection coefficient or heat delivery capacity was introduced, which is a new calculation formula, and can be used for determining the amount of heat output convection from the heat source to the indoor air of buildings by setting the factors mentioned, wherefrom it naturally exits through delimiting walls in the form of loss. This study surveys the sensitivity and interaction of the factors affecting heat delivery capacity. An example is provided for heat balance calculation.

NOMENCLATURE

$\dot{Q}$	heat power,
k	heat transmission coefficient,
A	surface,
$\dot{m}$	mass flow,
t	temperature,
t_i	indoor air temperature,
t_e	external temperature,
ϕ	Bosnjakovic coefficient,
$\dot{W}$	heat capacity flow rate.

Subscripts:

hexch	heat exchanger,
flat	flat,
rad	radiator,
1	primary system,
2	secondary system.

1. Introduction

District heating plays a very important role in meeting heat demands both in Europe and in Hungary, enabling the implementation of heat and electricity cogeneration, and providing ideal conditions for the use of renewables and for implementing EU energy policy directives. In Hungary, 650,000 homes are supplied by district heating.

A problem of major practical importance in the operation of district heating systems is to calculate the heat balance of the district heating system by taking variable operating parameters into consideration. Therefore our study presents, by relying on an earlier study of ours [1], [2], [3] the interaction of factors affecting heat delivery capacity and heat balance. Interaction is demonstrated through the derivatives of affecting factors. This model is termed as a sensitivity test. The heat delivery capacity, respectively, of the primary and secondary systems of the district heating system is presented separately, to be followed by the heat balance of the interconnected primary and secondary systems. With similar problems are dealt Nyers J. et al. [4], [5], Szánthó Z. [6] and Kajtár L. [7], [8], [9] at al. in the works.

2. Examination of the sensitivity of factors affecting heat delivery capacity.

Heat delivery by secondary system

$$\dot{Q} = \frac{1}{\frac{1}{2\dot{m}_2 c} + \frac{1}{(kA)_{rad}} + \frac{1}{(kA)_{flat}}}(t_2' - t_e) \tag{1}$$

Sensitivity of heat delivery capacity in function of secondary forward temperature

$$\frac{\partial \dot{Q}}{\partial t_2'} = \frac{1}{\frac{1}{2\dot{m}_2 c} + \frac{1}{(kA)_{rad}} + \frac{1}{(kA)_{flat}}},$$

$$\dot{m}_2 = const., t_e = const. \tag{2}$$

Sensitivity of heat delivery capacity in function of secondary circulated mass flow

$$\frac{\partial \dot{Q}}{\partial \dot{m}_2} = -(t_2' - t_e) \cdot \frac{1}{\left(\frac{1}{2\dot{m}_2 c} + \frac{1}{(kA)_{rad}} + \frac{1}{(kA)_{flat}}\right)^2}(2\dot{m}_2 c)^{-2} 2c$$

$$t_2' = const., t_K = const. \tag{3}$$

Interaction of factors affecting heat delivery: cross-derivatives

Secondary forward water temperature

$$t_2' = \dot{Q}\left(\frac{1}{2\dot{m}_2 c} + \frac{1}{(kA)_{rad}} + \frac{1}{(kA)_{flat}}\right) + t_e \tag{4}$$

Sensitivity of secondary forward water temperature to secondary circulated water quantity

$$\frac{\partial t_2'}{\partial \dot{m}_2} = 2\dot{Q}(2\dot{m}_2 c)^{-2} c \quad \dot{Q} = const. \tag{5}$$

Heat delivery capacity in the primary system

$$\dot{Q} = \frac{1}{\frac{1}{2\dot{m}_1 c} + \frac{1}{(kA)_{hexch}} + \frac{1}{2\dot{m}_2 c}}(t_1' - t_2'') \tag{6}$$

Factors affecting heat delivery in the primary system

$$\frac{\partial \dot{Q}}{\partial t_1'} = \frac{1}{\frac{1}{2\dot{m}_1 c} + \frac{1}{(kA)_{hexch}} + \frac{1}{2\dot{m}_2 c}},$$

$$t_2'' = const. \tag{7}$$

$$\frac{\partial \dot{Q}}{\partial \dot{m}_1} = \frac{1}{\left(\frac{1}{2\dot{m}_1 c} + \frac{1}{(kA)_{hexch}} + \frac{1}{2\dot{m}_2 c}\right)^2}(2\dot{m}_1 c)^{-2} 2c$$

$$t_1', t_2'' = const., \dot{m}_2 = const. \tag{8}$$

$$\frac{\partial \dot{Q}}{\partial \dot{m}_2} = \frac{1}{\left(\frac{1}{2\dot{m}_1 c} + \frac{1}{(kA)_{hexch}} + \frac{1}{2\dot{m}_2 c}\right)^2}(2\dot{m}_2 c)^{-2} 2c$$

$$t_1', t_2'' = const., \dot{m}_1 = const. \tag{9}$$

$$\frac{\partial \dot{Q}}{\partial t_2''} = -\frac{1}{\frac{1}{2\dot{m}_1 c} + \frac{1}{(kA)_{hexch}} + \frac{1}{2\dot{m}_2 c}},$$

$$t_1' = const. \tag{10}$$

Interconnection of the primary and secondary systems

Aggregate heat delivery capacity

$$\dot{Q} = \frac{1}{\frac{1}{(kA)_{rad}} + \frac{1}{(kA)_{flat}} + \frac{1}{\dot{m}_1 c\phi} - \frac{1}{2\dot{m}_2 c}} \cdot (t_1' - t_K) \tag{11}$$

Factors affecting heat delivery in the unified system

$$\frac{\partial \dot{Q}}{\partial t_1'} = \frac{1}{\frac{1}{(kA)_{rad}} + \frac{1}{(kA)_{flat}} + \frac{1}{\dot{m}_1 c\phi} - \frac{1}{2\dot{m}_2 c}} \tag{12}$$

$$\frac{\partial \dot{Q}}{\partial \dot{m}_1} = (t_1' - t_e) \cdot \frac{1}{\left(\frac{1}{2\dot{m}_1 c} + \frac{1}{(kA)_{hexch}} + \frac{1}{2\dot{m}_2 c}\right)^2} (\dot{m}_1 c\phi)^{-2} \frac{\partial}{\partial \dot{m}_1} \dot{m}_1 \phi \tag{13}$$

$$\dot{m}_1 = const., \dot{m}_2 = const.$$
$$\dot{W}_1 = const., \dot{W}_2 = const.$$
$$\phi = const., t_K = const.$$
$$t_b \neq const.$$

$$\frac{\partial \dot{Q}}{\partial \dot{m}_2} = (t_1' - t_K) \cdot \frac{1}{\left(\frac{1}{2\dot{m}_1 c} + \frac{1}{(kA)_{hexch}} + \frac{1}{2\dot{m}_2 c}\right)^2} \cdot \left[(\dot{m}_1 c\phi)^{-2} \frac{\partial}{\partial \dot{m}_1} \dot{m}_1 \phi - (2\dot{m}_2 c)^{-2} 2c\right] \tag{14}$$

$$\dot{m}_1 = const., \quad t_1' = const., \quad t_K = const.$$

Cross-derivatives of the factors affecting heat delivery in the unified system

$$t_1' = \dot{Q} \cdot \left(\frac{1}{(kA)_{rad}} + \frac{1}{(kA)_{flat}} + \frac{1}{\dot{m}_1 c\phi} - \frac{1}{2\dot{m}_2 c}\right) + t_e \tag{15}$$

$$\frac{\partial t_1'}{\partial \dot{m}_1} = \dot{Q}(\dot{m}_1 c\phi)^{-2} \frac{\partial}{\partial \dot{m}_1} (\dot{m}_1 c\phi) \tag{16}$$

$$\frac{\partial t_1'}{\partial \dot{m}_2} = \dot{Q}(\dot{m}_1 c\phi)^{-2} \frac{\partial}{\partial \dot{m}_2} (\dot{m}_1 c\phi) - \dot{Q}(2\dot{m}_2 c)^{-2} 2c \tag{17}$$

$$\frac{\partial \dot{m}_1}{\partial \dot{m}_2} \tag{18}$$

3. Example

There is an average district heated apartment where the dates are the following:

Q_{flat} [W]	5000
t_e [°C]	-15
t_{in} [°C]	20
t1' [°C]	130
t1" [°C]	80
t2' [°C]	90
t2" [°C]	70
$\dot{m}_1 c_1$ [J/sK]	100
$(kA)_{hexch}$ [W/K]	200
$(kA)_{rad}$ [W/K]	83,33333
$(kA)_{flat}$ [W/K]	142,8571

Changing of the indoor air temperature as a function of the primary forward temperature:

t_1' [°C]	Q [W]	t_i [°C]
130	5000	20
129	4 965,52	19,76
128	4 931,03	19,52
127	4 896,55	19,28
126	4 862,07	19,03
125	4 827,59	18,79
124	4 793,10	18,55
123	4 758,62	18,31
122	4 724,14	18,07
121	4 689,66	17,83
120	4 655,17	17,59
119	4 620,69	17,34
118	4 586,21	17,10
117	4 551,72	16,86
116	4 517,24	16,62
115	4 482,76	16,38
114	4 448,28	16,14
113	4 413,79	15,90
112	4 379,31	15,66
111	4 344,83	15,41

4. Summary

As mentioned in the introduction, this study examined the impact of factors affecting the heat balance of the district heating system on heat delivery capacity, in reliance on our earlier investigations. An example for the sensitivity of affecting factors was provided. The cross-derivatives of factors were presented. It was analyzed through an example what mass flow correction can compensate for the reduction of forward hot water temperatures in each load state. The temperature reduction impact of the absence of compensation was shown.

References

[1] Garbai, L.: District heating (in hungarian), 2012. ISBN: 978-963-279-739-7

[2] Jasper, A.: Optimization of district heating system design and operation (in hungarian), PhD dissertation, 2017.

[3] Garbai L, Jasper A: Analysis of steady states in district heating systems. In: Nyers József (szerk.) Internationale symposium "EXPRES 2016" Subotica: 8th International Symposium of Renewable Energy Sources and Effectiveness. Konferencia helye, ideje: Szabadka, Szerbia, 2016.03.31-2016.04.02. Szabadka: Visoka Technicka skola strukovnih studija u Subotici, 2016. pp. 81-83. (ISBN:978-86-85409-96-7)

[4] Nyers J., Nyers A.: “Hydraulic Analysis of Heat Pump's Heating Circuit using Mathematical Model”. 9rd ICCC International Conference” Proceedings-USB, ISBN 978-1-4799-0061-9 pp 349-353, Tihany, Hungary. 04-08. 07. 2013.

[5] Nyers J.: "COP and Economic Analysis of the Heat Recovery from Waste Water using Heat Pumps".International J. Acta Polytechnica Hungarica Vol. 13, No. 5, 2016, pp. 135-154. DOI:10.12700/APH.13.5.2016.5.8.

[6] Szánthó Z: Determining the optimal schedule of district heating, Periodica Politechnica Ser. Mech. Eng. VOL.44 No. 2. Pp.285-300. (2000.)

[7] Dr. Erdősi István, Dr. Kajtár László Távhőszolgáltatás változó tömegáramú hőhordozóval (in hungarian) ÉPÜLETGÉPÉSZET 1985:(2) pp. 49-55. (1985)

[8] Kajtár László, Erdősi István, Barna Lajos: A kombinált szabályozás alkalmazási lehetőségei forróvíz távhőrendszerekben, 11. Távhő Konferencia: 5. Távhőrendszerek. 155 p. Konferencia helye, ideje: Hajdúszoboszló, Magyarország, 1985.09.25-1985.09.27. Budapest: ÉTE, 1985. pp. 101-114. (ISBN:963-8041-67-6)

[9] Kajtár László, Erdősi István: Távhőrendszer mennyiségi és minőségi szabályozása, számítógépi program, 11. Távhő Konferencia. Konferencia helye, ideje: Hajdúszoboszló, Magyarország, 1985.09.25-1985.09.27. Budapest: Energiagazdálkodási Tudományos Egyesület, 1985. pp. 50-51. (ISBN:963-8041-61-7)

EXPRES 2018 **In technical co-sponsors**

- **The main sponsor is ELZETT Subotica**
- **Government** of Subotica
- **BME** University, Budapest
- **Tera Term** doo, Subotica,
- **Óbuda** University, Budapest Hungary
- **Annus Auto Saloon and Service,** Subotica
- **AKE-Đantar doo,** B. Topola
- **Mini Pani,** Subotica
- **Suboticagas**